NAVAL POSTGRADUATE SCHOOL
Monterey, California

THESIS

TRANSMITTING BEAM PATTERNS OF THE ATLANTIC BOTTLENOSE DOLPHIN (*TURSIOPS TRUNCATUS*): INVESTIGATIONS IN THE EXISTENCE AND USE OF HIGH FREQUENCY COMPONENTS FOUND IN ECHOLOCATION SIGNALS

by

Tobias J. Lemerande

June 2002

Thesis Advisor: Thomas G. Muir
Co-Advisors: Steven R. Baker
Samuel H. Ridgway

THIS PAGE INTENTIONALLY LEFT BLANK

REPORT DOCUMENTATION PAGE

Form Approved OMB No. 0704-0188

1. AGENCY USE ONLY ***(Leave blank)***	**2. REPORT DATE** June 2002	**3. REPORT TYPE AND DATES COVERED** Master's Thesis

4. TITLE AND SUBTITLE Transmitting Beam Patterns of the Atlantic Bottlenose Dolphin (*Tursiops Truncatus*): Investigations in the Existence and Use of High Frequency Components Found in Echolocation Signals.

5. FUNDING NUMBERS RPXW5

6. AUTHOR (S) Tobias J. Lemerande

7. PERFORMING ORGANIZATION NAME(S) AND ADDRESS(ES)
Naval Postgraduate School
Monterey, CA 93943-5000

8. PERFORMING ORGANIZATION REPORT NUMBER

9. SPONSORING / MONITORING AGENCY NAME(S) AND ADDRESS(ES)
Space and Naval Warfare Systems Command, San Diego

10. SPONSORING/MONITORING AGENCY REPORT NUMBER

11. SUPPLEMENTARY NOTES The views expressed in this thesis are those of the author and do not reflect the official policy or position of the U.S. Department of Defense or the U.S. Government.

12a. DISTRIBUTION / AVAILABILITY STATEMENT
Approved for public release; distribution is unlimited.

12b. DISTRIBUTION CODE

13. ABSTRACT ***(maximum 200 words)*** In January 2002, time synchronized underwater pictures and echolocation signals of a free-swimming bottlenose dolphin were recorded. More than 80 experimental trial runs were recorded at the Space and Naval Warfare Center's Marine Mammal Facility in San Diego, California. The apparatus recorded 30 underwater images per second and sonar signals up to 400 kHz. Data analysis shows wide transmitting beam patterns at frequencies lower than 135 kHz contain a majority of the energy in the echolocation signal, agreeing with previously documented work. However, further analysis shows significant energy at higher frequencies. Early in the experiment, the dolphin steered narrow high frequency signals and adjusted the energy content in those different frequencies while scanning the target. To emit these high frequency components, the dolphin changed the wave shape of the emitted sound pulse. As the experiment progressed, the animal's task became routine and the high frequency signals were noticeably absent until low frequency noise was projected into the water, at which time the high frequencies were again present in the emitted sound pulses. Resultant transmitting beam patterns provide excellent evidence of the presence of high frequency sound emissions, and also indicate how these signals are used during echolocation tasks.

14. SUBJECT TERMS Biosonar, *Tursiops Truncatus*, bottlenose dolphin, mine detection	**15. NUMBER OF PAGES** 148
	16. PRICE CODE

17. SECURITY CLASSIFICATION OF REPORT	**18. SECURITY CLASSIFICATION OF THIS PAGE**	**19. SECURITY CLASSIFICATION OF ABSTRACT**	**20. LIMITATION OF ABSTRACT**
Unclassified	Unclassified	Unclassified	UL

NSN 7540-01-280-5500 **Standard Form 298 (Rev. 2-89)**
Prescribed by ANSI Std. 239-18

THIS PAGE INTENTIONALLY LEFT BLANK

Approved for public release; distribution is unlimited.

TRANSMITTING BEAM PATTERNS OF THE ATLANTIC BOTTLENOSE DOLPHIN (*TURSIOPS TRUNCATUS*): INVESTIGATIONS IN THE EXISTENCE AND USE OF HIGH FREQUENCY COMPONENTS FOUND IN ECHOLOCATION SIGNALS

Tobias J. Lemerande
Lieutenant, United States Navy
B.S., United States Naval Academy, 1996

Submitted in partial fulfillment of the
requirements for the degree of

MASTER OF SCIENCE IN APPLIED PHYSICS

from the

NAVAL POSTGRADUATE SCHOOL
June 2002

Author: Tobias J. Lemerande

Approved by: Thomas G. Muir, Thesis Advisor

Steven R. Baker, Co-Advisor

Samuel H. Ridgway, Co-Advisor
Space and Naval Warfare Systems Center
San Diego

William B. Maier II, Chairman
Department of Physics

THIS PAGE INTENTIONALLY LEFT BLANK

ABSTRACT

In January 2002, time synchronized underwater pictures and echolocation signals of a free-swimming bottlenose dolphin were recorded. More than 80 experimental trial runs were recorded at the Space and Naval Warfare Center's Marine Mammal Facility in San Diego, California. The apparatus recorded 30 underwater images per second and sonar signals up to 390 kHz. Data analysis shows wide transmitting beam patterns at frequencies lower than 135 kHz contain a majority of the energy in the echolocation signal, agreeing with previously documented work. However, further analysis shows significant energy at higher frequencies. Early in the experiment, the dolphin steered narrow high frequency signals and adjusted the energy content in those different frequencies while scanning the target. To emit these high frequency components, the dolphin changed the wave shape of the emitted sound pulse. As the experiment progressed, the animal's task became routine and the high frequency signals were noticeably absent until low frequency noise was projected into the water, at which time the high frequencies were again present in the emitted sound pulses. Resultant transmitting beam patterns provide excellent evidence of the presence of high frequency sound emissions, and also indicate how these signals are used during echolocation tasks.

THIS PAGE INTENTIONALLY LEFT BLANK

TABLE OF CONTENTS

LIST OF FIGURES

ACKNOWLEDGEMENTS

I would like to thank the many people who helped guide and assist me throughout the eighteen months over which this research was conducted.

From the Naval Postgraduate School, special thanks go to my thesis advisors, Professor Tom Muir and Professor Steve Baker, and to Major Don Carrier, USMC, who assisted greatly during the experiment portion of this thesis. Also from NPS, special thanks go to Mary Redmond, George Jaksha, Bill Gavlick and Sam Barone for their technical assistance and expertise.

Space and Naval Warfare Systems Center-San Diego provided the research fellowship and grant that funded this project. Without the people from SSC-San Diego, this thesis would not have been possible. Specifically, I would like to recognize the “Dolphin Doctor”, Sam Ridgway, Don Carder and the Temporary Threshold Shift (TTS) training team whose expertise, professionalism and patience made the ensured the experiment was a success and proceeded with little or no problems. From the TTS training team, I want to recognize specifically Patricia Kamolnick, Jennifer Jeffress, Nicole Trushenski, Kevin St. John and Sean Drake. And, lastly from SSC-SD, the two U. S. Navy Atlantic bottlenose dolphins, “Nemo” and “Wenatchee”, who made the experiment an overwhelming success.

Finally, I wish to thank my wife Saskia. When frustration set-in and got the best of me, she encouraged me to persevere. Without her support, this entire project would have been neither possible nor enjoyable.

THIS PAGE INTENTIONALLY LEFT BLANK

I. INTRODUCTION

In the past forty years, scientists have conducted extensive research to gain knowledge about marine mammal sonar. Tremendous effort has been specifically focused on bottlenose dolphins' (*Tursiops Truncatus)* abilities to use biological sonar (biosonar) to detect objects underwater and buried in ocean sediment. Experiments conducted in the 1980s did not record significant dolphin sound emissions above 150 kHz.[Ref. 1] In the last five years, however, scientists identified and confirmed the existence of higher frequencies in dolphin echolocation signals.[Ref. 2] Further investigations into these high frequency components are currently being conducted by the Naval Postgraduate School and the Space and Naval Warfare Systems Center in San Diego, California (SSC-SD). This thesis presents the results of analyses of echolocation transmitting beam patterns of the bottlenose dolphin, including the recently discovered high frequency components.

A. BACKGROUND

Au compiled composite transmitting beam patterns using results from several experiments conducted with three different bottlenose dolphins.[Ref. 1] These plots show the dolphins' maximum frequencies extending no higher than 122 kHz. In 1997, researchers recorded *Tursiops Truncatus* sounds containing frequencies as high as 500 kHz.[Ref. 2] The following year, additional experiments confirmed the existence of these high frequencies.[Ref. 3] Further

studies again recorded and analyzed these high frequency emissions.[Ref. 4] In addition to these three experiments, sounds reaching 305 kHz have been recorded from wild white beaked dolphins.[Ref. 5] These high frequencies may help explain how marine mammals employ biosonar.

B. RESEARCH MOTIVATION

Captive dolphins have experimentally shown the ability to successfully discriminate between two cylindrical targets that differ in wall thickness by less than 0.3 mm.[Ref. 6] The method *Tursiops Truncatus* uses to achieve such high resolution remains unknown; the recently discovered high frequencies may play a part in understanding how these animals' sonar operates. Scientists at SSC-SD are currently attempting to engineer a biomimetic sonar system that duplicates the dolphins' high resolution sonar.[Ref. 7] However, prior to producing a dolphin-like sonar, a greater understanding of dolphin echolocation must be achieved. The results contained in Chapter IV provide new transmitting beam patterns that show the spatial representation of energy at frequencies not previously examined.

C. EXPERIMENT OBJECTIVES

The transmitting beam pattern experiments reported by Au *et al* in Ref. 8 collected echolocation signals and underwater video images of a bottlenose dolphin stationed on a bite bar. No definite time correlation between the recorded images and sound signals existed. In the present

study, the author and Dr. Thomas Muir, of the Naval Postgraduate School, conducted experiments in January 2002 at SSC-SD, in which transmitting beam patterns of two Atlantic bottlenose dolphins were measured. During these experiments, for the first time in dolphin research, echolocation sound signals were digitally time synchronized with underwater pictures of a free-swimming bottlenose dolphin taken using a submerged video camera.

D. THESIS OUTLINE

This chapter introduced the topic of biosonar, previous *Tursiops Truncatus* transmitting beam patterns, and the discovery of high frequency components in dolphin echolocation signals. The next chapter describes what is presently known about the dolphin echolocation system, its functionality, and the use of marine mammals in the U. S. Navy. Chapter III details the present experiment configuration and procedure. Chapter IV discusses the raw data, signal processing techniques used to analyze the selected raw data and graphical representations of *Tursiops Truncatus'* transmitting beam patterns, including commentary on how the dolphin steers high frequency emissions and adjusts the energy content at specific frequencies to scan a target. The final chapter discusses conclusions obtained from this research and provides insight for future experiments.

THIS PAGE INTENTIONALLY LEFT BLANK

II. DOLPHIN ECHOLOCATION

A. THE DOLPHIN ECHOLOCATION SYSTEM

Marine mammals use sound for many purposes. The research described in this thesis is concerned only with sound signals used for echolocation. During echolocation, dolphins emit and receive sound waves, called “clicks”, in a manner that allows the animal to "chart" the surrounding environment out to a distance of approximately 100 meters.[Ref. 9] A graphical representation of an actual click, emitted by a U. S. Navy dolphin in San Diego, California, is shown in Figure 1.

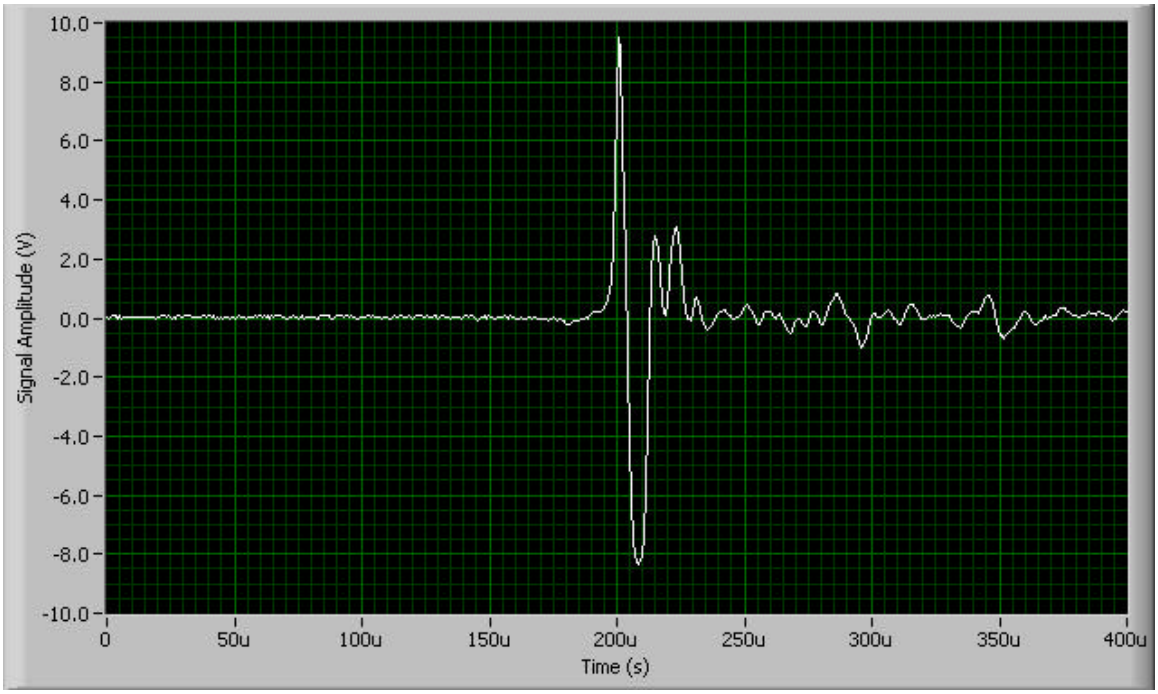

Figure 1. Graphical representation of a single click dolphins use to echolocate objects.

Dolphins most commonly emit groups of successive clicks, commonly called “click trains”, an example of which is shown in Figure 2.

It is thought that dolphins produce sound by actively controlling the action in the nasal plugs. The sound emissions are a result of acoustic transients as air passes

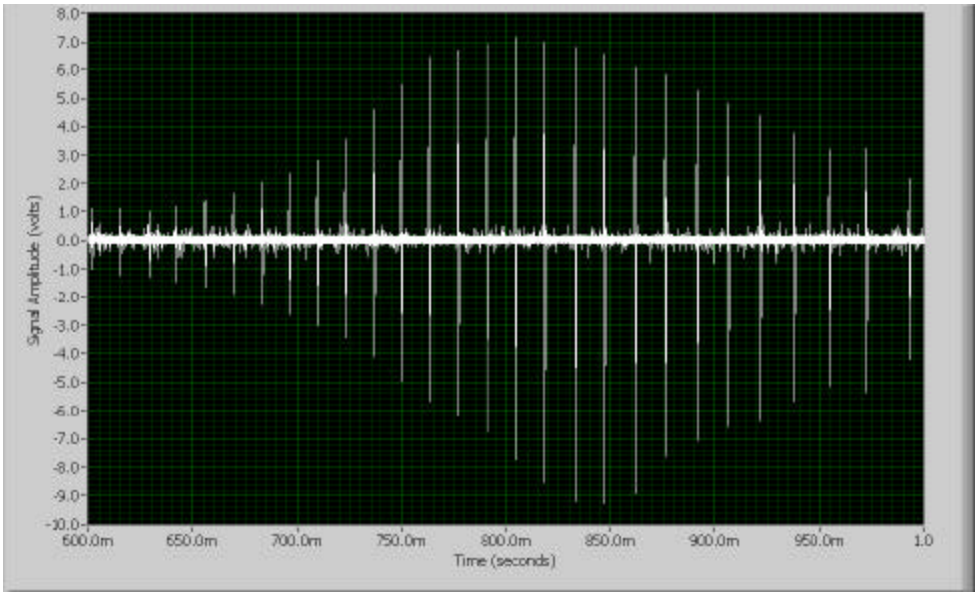

Figure 2. A click train is a group of clicks emitted in “rapid-fire” succession.

between the nasal plugs and walls of the nasal cavity [Ref. 10]. The sound is projected into the water after passing through the melon (see Figure 3), wherein the emitted sound can be steered to point at a target.[Ref. 11] The tissue in the melon and head act as a sonar “window”, easily coupling the projected sound from the animal directly into the water. Research indicates the panbone, within the lower jaw, plays a significant part in the dolphin's ability to receive sound signals.[Ref. 12]

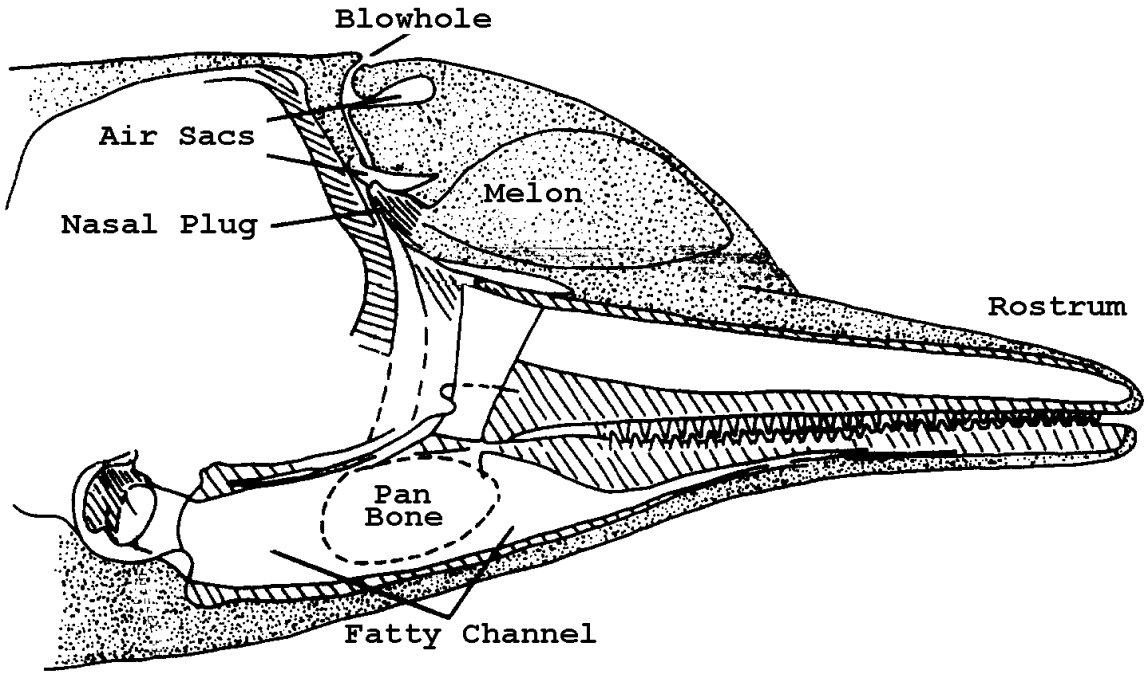

Figure 3. The basic anatomy of a dolphin used in echolocation. (After Ref. 13)

B. U. S. NAVY MARINE MAMMAL PROGRAM

The U.S. Navy's Marine Mammal Program incorporates specially trained Atlantic and Pacific bottlenose dolphins for defense against combat swimmers, for mine detection and neutralization, as pictured in Figure 4, for the recovery of exercise mines and torpedoes, and for sundry other duties. These animals are “born and bred” in the U. S. Navy. Currently, the U.S. Navy is the only military service in the world that actively employs marine mammals.

The species *Tursiops Truncatus* has a very reliable and accurate sonar system for detecting mines buried in ocean sediments, although beluga (white) whales are equally

Figure 4. A member of the U. S. Navy Marine Mammal System's MK 7 team marks a target mine on the ocean bottom in San Diego Bay. (From Ref. 14)

competent. Dolphins are used because of their exceptional biological sonar that is unmatched by man-made sonar in detecting objects in the water column, on the ocean bottom, and buried in ocean sediment.[Ref 14] However, these animals are expensive to train and keep healthy. While marine mammals have tremendous capabilities, limiting factors such as environmental conditions and logistics can hinder their military deployment and effectiveness. Although the Navy's marine mammals are very effective mine-hunters, operational commanders desire area search rates that would surpass the capabilities of dolphins. Additionally, the dolphins, being mammals, become fatigued and must of course be fed and cared for by highly specialized veterinarians and trainers. They are also

susceptible to harsh environmental conditions that can hinder their effectiveness.

A U. S. Navy goal is to employ a sonar system that mimics the dolphin’s ability and produces comparable results. In littoral warfare, the Navy and Marine Corps need a mobile mine-hunting sonar system that can be deployed in coastal waters, anywhere in the world. Such a system would enable American forces to better conduct amphibious operations in the projection of naval power ashore.

THIS PAGE INTENTIONALLY LEFT BLANK

III. EXPERIMENT CONFIGURATION

A. ACQUISITION SYSTEM

1. Hydrophone and Camera Apparatus

Seven hydrophones and a small underwater camera, pictured below, were used to collect data during the experiment.

Figure 5. ITC-1089D hydrophone and underwater camera.

All seven hydrophones were omni-directional ITC-1089D transducers that had an active 0.25” (diam.) spherical lead zirconate titanate (PZT) sensing element, schematically represented in Figure 6. The receiving response characteristics for each hydrophone range from 1 kHz to 390 kHz and are provided in Appendix A. Due to low light conditions in the dolphin’s pen in San Diego, a small, underwater infrared camera was used to capture video images. The seven hydrophones were arranged along a line formation, separated by 9.0 ± 0.2 cm. To ensure proper orientation throughout the experiment, each hydrophone was secured firmly in grooved mounting brackets.

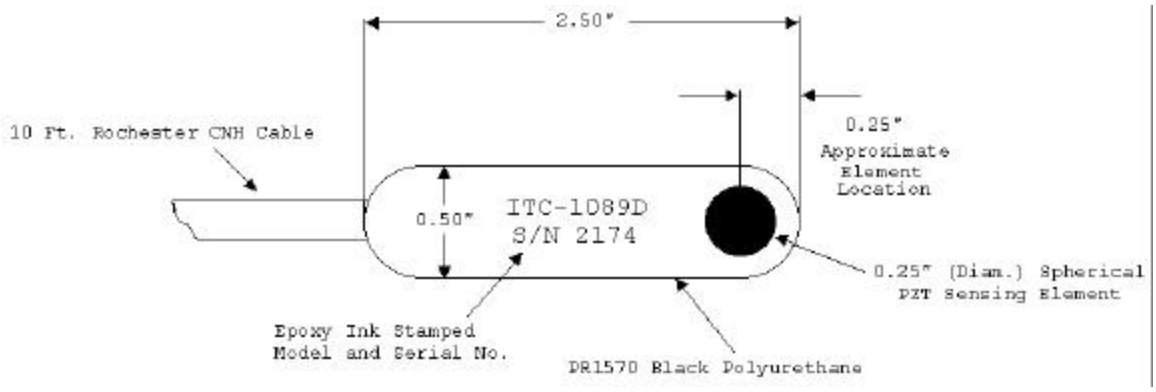

Figure 6. Schematic showing the construction of ITC-1089D hydrophone.

The hydrophone assembly was attached to a poly-vinyl chloride (PVC) bracket which was clamped around the cylindrical camera housing. The apparatus could be configured for measurements in either the horizontal plane, as shown in Figure 7, or rotated 90° for a vertical arrangement, as illustrated in Figure 8.

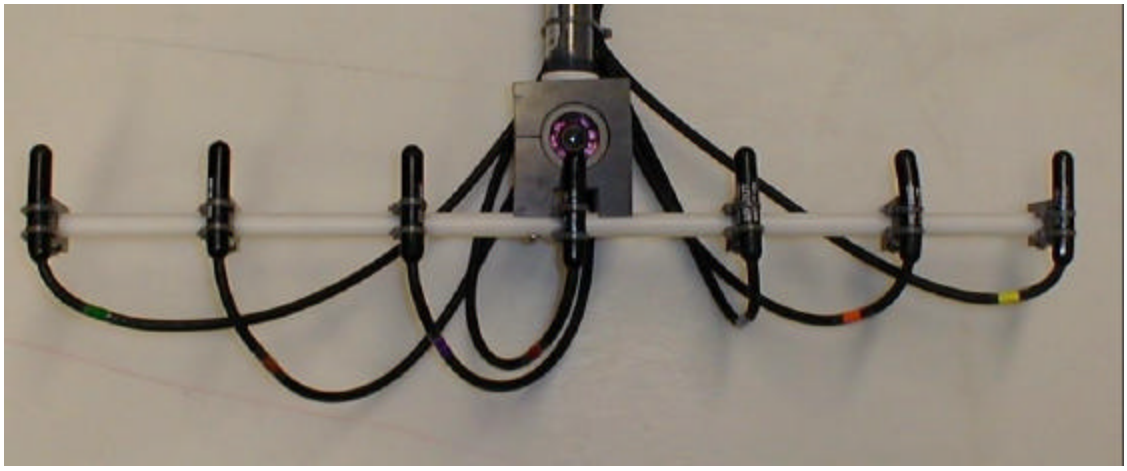

Figure 7. Hydrophone and camera apparatus configured for measurements in the horizontal plane.

Figure 8. Hydrophone and camera apparatus configured for measurements in the vertical plane.

Lengths of PVC pipe were attached to the camera housing, enabling the entire assembly to be submerged to a depth of two meters. When below the surface, the hollow PVC pipes filled with water.

When arranged in the horizontal plane, the central on-axis hydrophone was set just below the camera's aperture; in the vertical plane, the on-axis hydrophone was just a couple millimeters to the left of the aperture, as one looked through the camera. In both configurations, the tip

of the on-axis hydrophone is slightly visible but did not distort any acquired images.

2. Data and Image Acquisition System

Analog signals generated by the hydrophones were electronically filtered and amplified. 8-pole Bessel filters, set for a high-pass configuration, passed all frequencies above 5 kHz. This setting blocked much of the ambient noise present in San Diego bay. Signals exiting the filters fed directly into two National Instruments (NI) BNC-2110 Desktop Adapters. Each BNC-2110 unit communicated directly with a NI PCI-6110E Data Acquisition (DAQ) board via a 68-pin input/output (I/O) connector. The PCI-6110E DAQ board used a 12-bit analog to digital converter (ADC) for each of the four simultaneously sampled analog inputs.[Ref. 15] The camera's video signal went through a closed circuit television (CCTV), providing a live video feed during the experiment, to a NI PCI-1409 Image Acquisition (IMAQ) board. The PCI-1409 IMAQ board is a high-accuracy, monochrome board that acquires images in real time.[Ref. 16] The hardware configuration is schematically represented in Figure 9. The two DAQ boards and the IMAQ board were configured using software instrument drivers and Measurement and Automation Explorer (MAX) provided by NI. The software programs, LabVIEW 6i (Full Development System) and IMAQ Vision, controlled the DAQ and IMAQ boards.

LabVIEW is a graphical programming language that uses icons instead of lines of text to create applications and

uses dataflow programming, where data determine execution. LabVIEW is fully integrated for communication with the DAQ and IMAQ boards. A LabVIEW program is called a Virtual Instrument (VI) because its appearance and operation imitates physical instruments, such as oscilloscopes, multi-meters and spectrum analyzers.[Ref. 17]

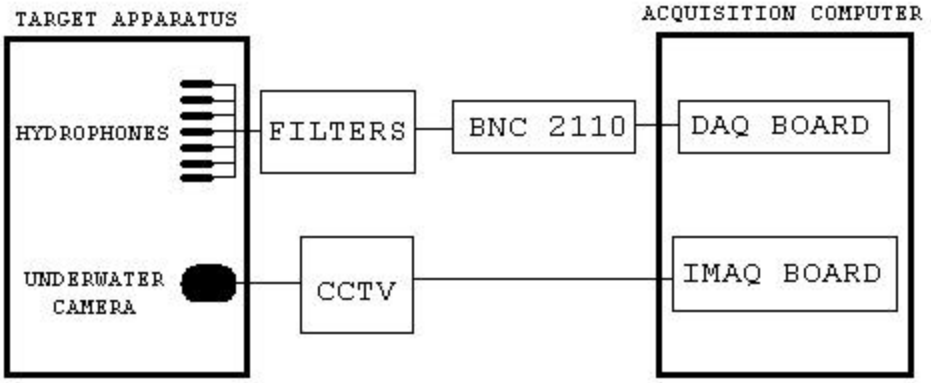

Figure 9. Schematic diagram showing the acquisition hardware configuration used to record time synchronized biosonar signals and underwater images.

In this experiment, the acquired sonar signals directly correlated to the captured underwater images of the dolphin as the animal echolocated on the target. The three boards were synchronized for simultaneous triggering by transistor-to-transistor logic (TTL) on the common Real-Time System Integration (RTSI) bus shared by all three boards. The triggering and time synchronization was verified in the laboratory prior to conducting the experiment. The VI used to control the data and image acquisition during the experiment is provided in Appendix B.

In order to detect and record frequencies extending up to 390 kHz, the data sampling frequency (F_s) was set at 1.25 MHz. This sampling rate met the Nyquist criteria, which states that the maximum detectable frequency (f_{max}) equals half the sampling rate. The IMAQ board recorded 30 images per second (ips).

B. EXPERIMENT PROCEDURE

Two different U. S. Navy Atlantic bottlenose dolphins, named “Wenatchee” and “Nemo”, were used in this experiment. The dolphins were required to echolocate a submerged “target”, the hydrophone and camera apparatus, using biosonar. A training target was used to train each dolphin prior to conducting the actual experiment, at which time the hydrophone and camera apparatus was substituted for the training target. Each dolphin was trained to swim from the trainer, positioned at the starting location, to the target location, touch the target with the tip of their rostrum and return to the trainer. Upon touching the target, the trainer used an underwater buzzer to signal, or “bridge”, the animal to return to the starting location. The fundamental goal of the experiment was for the dolphin to locate the target using only its echolocating capabilities.

Several training runs were conducted to familiarize the dolphin with the required task. A standard training target, an aluminum pole with a styrofoam sphere on one end, was initially used to prevent any confusion on the dolphin’s part. The dolphin swam two initial runs with no

visual constraints. Once the animal had successfully found the target pole, a soft rubber cone or “eyecup” was placed over one eye and two more runs were conducted. After successfully finding and touching the target pole, another eyecup was placed over the second eye, as seen in Figure 10. The dolphin then swam a fifth run; with both eyes completely covered, the animal echolocated the target.

Figure 10. During the experiment, soft rubber eyecups prevented U. S. Navy dolphin “Nemo” from seeing the target, compelling him to echolocate the target with his sonar.

Upon each return to the trainer, the dolphin received a fish reward, shown in Figure 11.

Figure 11. Temporary Threshold Shift trainer, Nicole Trushenski, rewards “Nemo” with fish after completing a successful echolocation task.

For the experiment, the hydrophone and camera apparatus replaced the target pole; it was intended that the dolphin would echolocate primarily on the largest portion of the target which was the camera housing and PVC clamping bracket. When the trainer sent the dolphin on an experimental run, the apparatus was submerged in the water. The sound of the apparatus entering the water gave the dolphin a general direction in which to "ping". Just as rehearsed in the training runs, the dolphin left the starting location, echolocated the apparatus, touched it and returned to the trainer for a fish reward. This was the standard routine for the experiment. The hydrophone and camera assembly was often repositioned around the

dolphin pen in order to encourage the dolphin to echolocate the target in a new or different sector.

On the fourth day of the experiment, ”white noise” (broadband) signals were passed through a 135 kHz low pass filter to a transmitting hydrophone that projected the sound into the dolphin's pen. The sound source (transmitter) was another ITC-1089D hydrophone, mounted approximately one meter above the camera, on the same pole as the other seven hydrophones and camera. The results of this portion of the experiment will be discussed in the next chapter.

For each echolocation run, four seconds of data were recorded and stored on hard disk. Each measured “trial run” yielded 5×10^6 samples per hydrophone, for a total of 3.5×10^7 samples and 120 images. Over the course of four days, more than 80 trial runs were recorded.

C. HYDROPHONE AND CAMERA APPARATUS TARGET STRENGTH

Following the highly successful dolphin echolocation experiment, an additional experiment was conducted at the Naval Postgraduate School to estimate the hydrophone and camera apparatus’ Target Strength (TS); TS is the measured ratio of the sound pressure of the scattered (reflected) pulse referred to a range of one meter, to the sound pressure of the incident pulse at the target. The same hydrophone and camera apparatus used during the dolphin echolocation experiment served as the target, and was set in the horizontal configuration. The schematic

representation shown in Figure 12 illustrates the TS experimental set up.

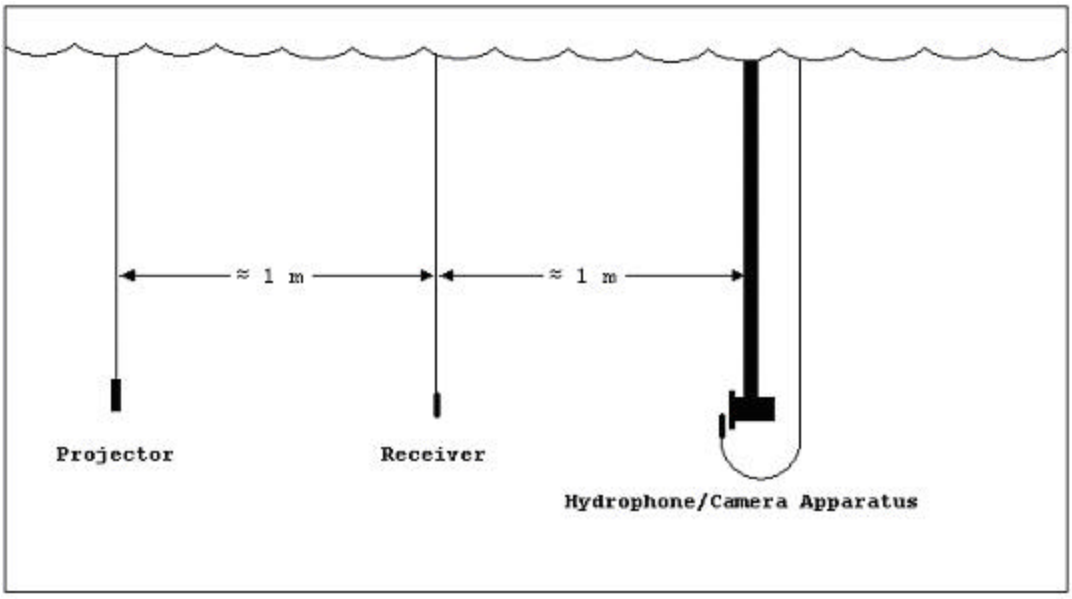

Figure 12. Experiment set up used to determine the hydrophone and camera apparatus' Target Strength.

Submerged in a 2m x 3m x 6m anechoic test tank, a standard U. S. Navy E27 hydrophone (projector) was positioned approximately two meters in front of the target. An ITC-1089D hydrophone (receiver) was positioned approximately midway between the target and the projector. For the experiment, the projector emitted a single cycle pulse aimed at the target. The receiver sensed the projector's emitted pulse and the signal reflected off the target. Measurements were made at 100 kHz, 200 kHz, 300 kHz and 400 kHz. Figure 13 is a graphical representation of the emitted 100 kHz signal and the reflected signal measured by the receiving hydrophone.

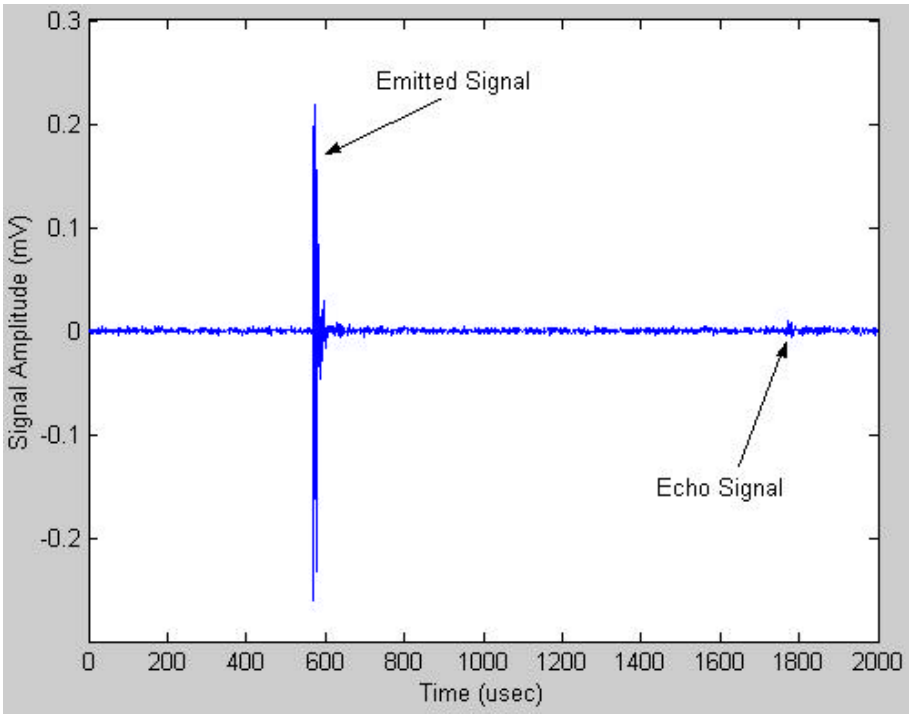

Figure 13. Waveform trace of the emitted and reflected pulses. The ratio of the emitted signal to the echo signal provided a crude approximation of the hydrophone and camera apparatus' Target Strength.

The echo signal was received approximately 1.3 ms later, the time for a sound wave to travel two meters in water. For the four sampled frequencies, the reflected pressure at a range of one meter was found to be approximately 8 to 10 percent (-22 to –20 dB) of the pressure incident on the target (hydrophone and camera apparatus). These rudimentary results will be revisited in the next chapter as they apply to data acquired when low frequency noise was injected into the dolphin's pen.

THIS PAGE INTENTIONALLY LEFT BLANK

IV. EXPERIMENTAL RESULTS

A. RAW DATA

This experiment recorded time synchronized echolocation signals and underwater images of a dolphin swimming directly toward the hydrophone array and camera apparatus. Over the course of this experiment, it was readily apparent that the dolphin's acquired experience (self training) significantly affected the outcome of each trial run. For this reason, an extensive amount of data were collected, the most representative of which are presented in this chapter. In each of the data sets selected for analysis, photographic images are accompanied by time synchronized echolocation click trains. Prior to presenting experimental results, a brief discussion concerning data acquisition is given.

B. SIGNAL PROCESSING

1. Echolocation Clicks

a. Signal Composition

Unfortunately, despite years of naval research, considerable unresolved questions exist regarding the composition of an echolocation click. Signal processing techniques used in this thesis analyzed the main portion of the click, as highlighted in Figure 14. The analysis did not include reverberation contained in the signal's trailing section, considered by some including Professor Kamminga [Ref. 18] and the present author, to be skeletal echoes and perhaps resonances inside the dolphin's head.

They are not part of the active echolocation click and probably do not contribute significantly to the animal's ability to effectively echolocate.

Figure 14. The highlighted portion of the echolocation click contains most of the emitted pulse's energy. The click's "tail" most likely results from skeletal resonances and echoes within the dolphin's head.

b. Reflections Seen by On-Axis Hydrophone

The raw data collected by the on-axis (0°) hydrophone shows interference that distorted the waveform. The camera housing lens acted as a rigid boundary, which inverted the phase of the incident wave upon reflection. The reflection is easily seen by the second large amplitude negative peak, circled in Figure 15.

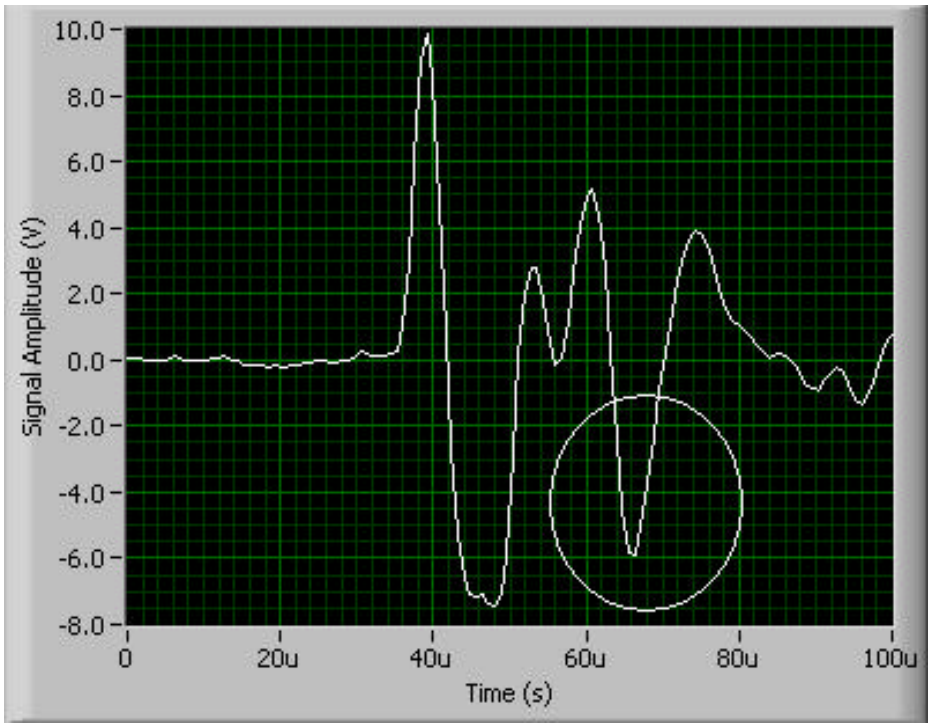

Figure 15. The signal collected by on-axis (0^{o}) hydrophone had a large second negative peak due to the incident wave reflecting off the camera lens and destructively interfering with the incident sound wave.

Based on the hydrophone's geometry and distance from the camera lens (1.1 ± 0.3 cm) the reflected wave destructively interfered with the incoming wave after approximately 21 μs. None of the signals received by the other six hydrophones exhibit this wave shape. This interference most likely accounts for many of the inconsistencies observed at 0° in the resulting transmitting beam pattern plots. Specific instances where this applies will be pointed out in the analysis portion of this chapter.

c. Temporal-Spectral Conversion

The DAQ boards digitized the analog signals generated by each hydrophone. The dolphin's echolocation transmissions were now represented as discrete time sequence signals. A 1.25 MHz sampling rate yielded one data point every 0.8 μs. The discrete digital time domain signals were all converted to frequency spectra using LabVIEW VIs. The *Scaled Time Domain Window VI* applied a Hanning Window to the time domain signal. The *Zero Pad VI* added zeroes to the signal to make the discrete time signal a 64-point time sequence, in order to employ a Discrete Fourier Transform (DFT) routine (a DFT requires an input sequence with 2^n points). The *Auto Power Spectrum VI* used DFT algorithms to compute the single-sided, scaled auto power spectrum (V^2_{rms}) of a given time domain signal.[Ref. 19] The *Spectrum Unit Conversion VI* converted the power spectrum to power spectral density (V^2_{rms}/Hz). A schematic diagram showing this process is shown in Figure 16.

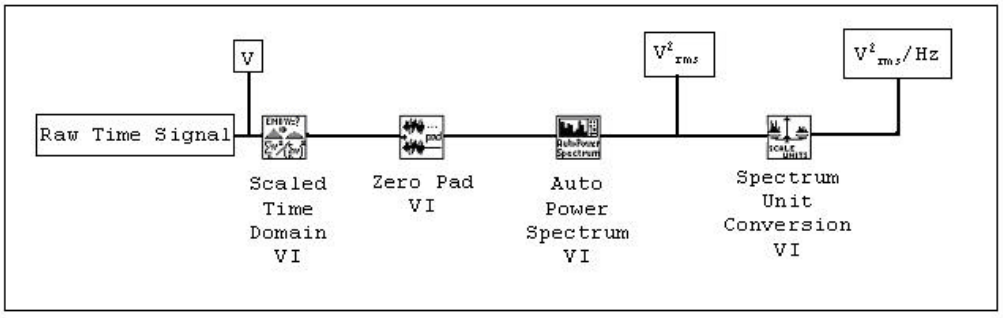

Figure 16. Schematic representation showing how LabVIEW VIs were employed to convert dolphin sonar signals, recorded in the time domain, to the frequency spectrum.

The resultant frequency spectrum yielded discrete data points every 19,531.25 Hz apart in 1 Hertz bins. Amplifier gain, hydrophone sensitivity, and range corrections were then applied to yield the sound pressure spectrum ($\mu Pa^2/Hz$). In this thesis, processed sound signals represent the dolphin's emitted "Energy Flux Spectral Density" (EFSD) given by

$$\left(\frac{\mu Pa^2}{Hz}\right)\left(T_{signal}\right)\left(\frac{1}{r_o c}\right)=\left(\frac{pJ}{m^2 \cdot Hz}\right)$$

where T_{signal} is the time record length of the signal in seconds and $\rho_o c$ is the characteristic impedance of water ($Pa \cdot s/m$). In underwater acoustics, measurements are commonly given in "levels", which have units of decibels (dB). The plotted transmitting beam patterns show the recorded echolocation clicks' "Energy Flux Spectral Density Levels" (EFSDL).

2. Underwater Images

It was difficult to clearly see the dolphin beyond a range of 2.5 meters; *Tursiops Truncatus* blends well with its watery environment. The trainer painted a zinc oxide cross on the dolphin's melon, as shown in Figure 17, in an effort to make the dolphin's head more easily seen underwater. In some instances, the zinc oxide contrasted well with the dolphin's skin in the images. However, in many cases, sunlight scattered off the dolphin's melon and blanked the zinc oxide stripes. The dolphin's eyecups

proved to be the most prominent and easily recognizable visible features.

Figure 17. U. S. Navy dolphin “Wenatchee” approaches the hydrophone and camera apparatus. In this photograph, the dolphin is about 0.5 m from the camera and the zinc-oxide stripes are clearly visible.

While the trainer held the dolphin still, calibration pictures were taken at fixed ranges of one and two meters. During the actual experiments, the dolphin's range was estimated by comparing the number of pixels between eyecups in the calibration pictures with those selected for analysis. This range, combined with the known distance between adjacent hydrophones, was used to determine the proper azimuthal extent for transmitting beam pattern plots.

C. TRANSMITTING BEAM PATTERNS

In this section, the temporal and spectral attributes of echolocation click trains from six different trial runs

are shown. The spectral plots will clearly illustrate *Tursiops Truncatus*' transmitting beam patterns, with special emphasis on the high frequency components. The plotted transmitting beam patterns show each click's EFSDLs, referenced to that click's maximum EFSDL. Moreover, a subsequent examination of individual clicks' waveforms will reveal the existence of the high frequency components.

1. Horizontal Plane

a. Trial Run 1-3

Trial Run 1-3 is comprised of six pictures and 13 echolocation clicks. This data set was the third trial run on the first day of the experiment and was also the third trial run with the hydrophone and camera apparatus in the horizontal configuration. The selected click train segment is graphically shown in Figure 18; the acquired underwater images are shown in Figure 19. In all six images, the sunlight scattered off Nemo's melon and blanked the painted zinc oxide stripes, but his eyecups are very distinct. In these images, the dolphin is completing a turn toward the target; Nemo made a wide angled approach while echolocating the target. The resulting beam patterns are plotted in Figures 20 to 22. In the first six clicks there is no distinct peak above 160 kHz at the center hydrophone. This is most likely due to the destructive interference caused by the camera lens, as discussed earlier in the chapter.

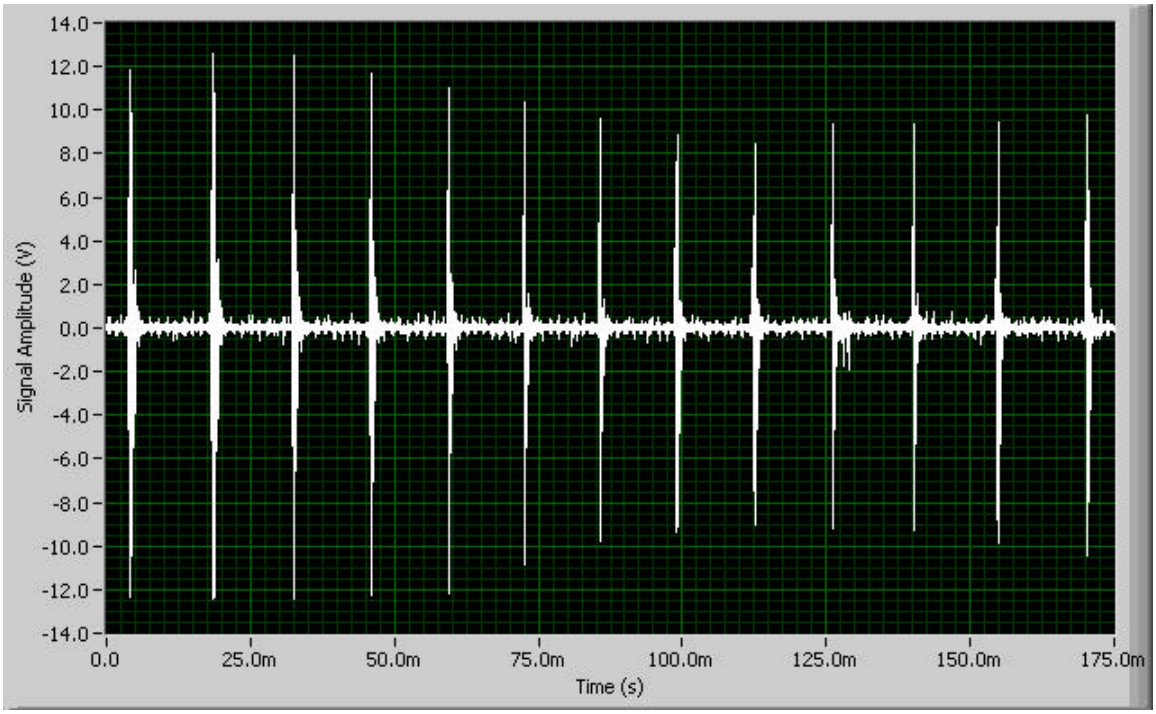

Figure 18. Trial Run 1-3 click train.

Throughout these 13 clicks, the frequency with the maximum EFSDL is unmistakably 78 kHz. However, significant energy, contained in focused beams, is present in frequencies as high as 293 kHz. In Click 7, the 293 kHz beam is centered on the -2.6° hydrophone. Subsequent clicks show the dolphin shifted the 293 kHz beam to the -5.1° hydrophone. By Click 10, the 156 kHz, 195 kHz and 254 kHz beams all centered on the -5.1° hydrophone. By Click 11, all five plotted frequencies have peaks at the -5.1° hydrophone and have become noticeably narrower than those same frequencies' beams in Click 1. In Clicks 12 and 13, the 293 kHz beam is 18 dB lower than the maximum EFSDL.

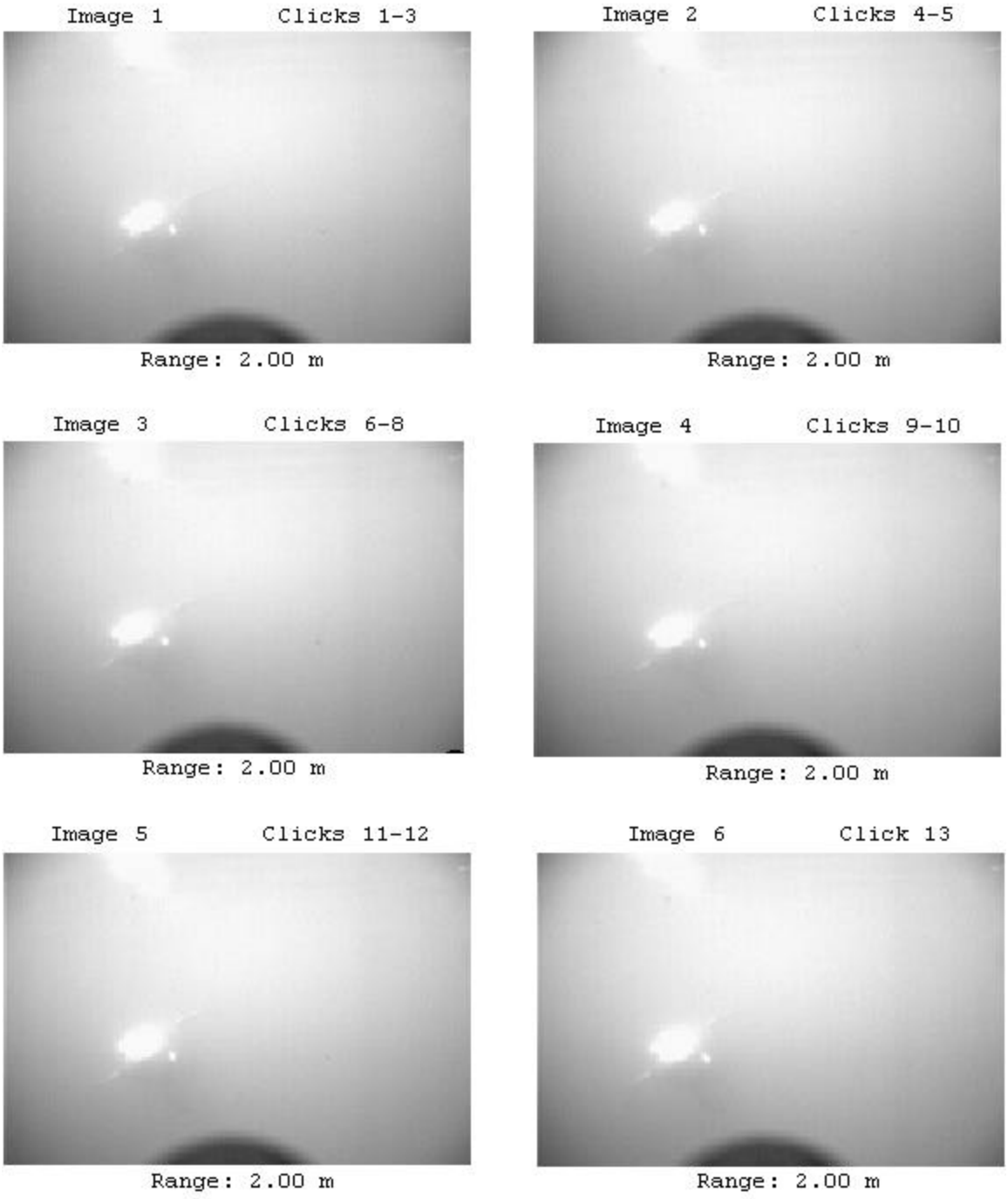

Figure 19. Trial Run 1-3 images 1 through 6.

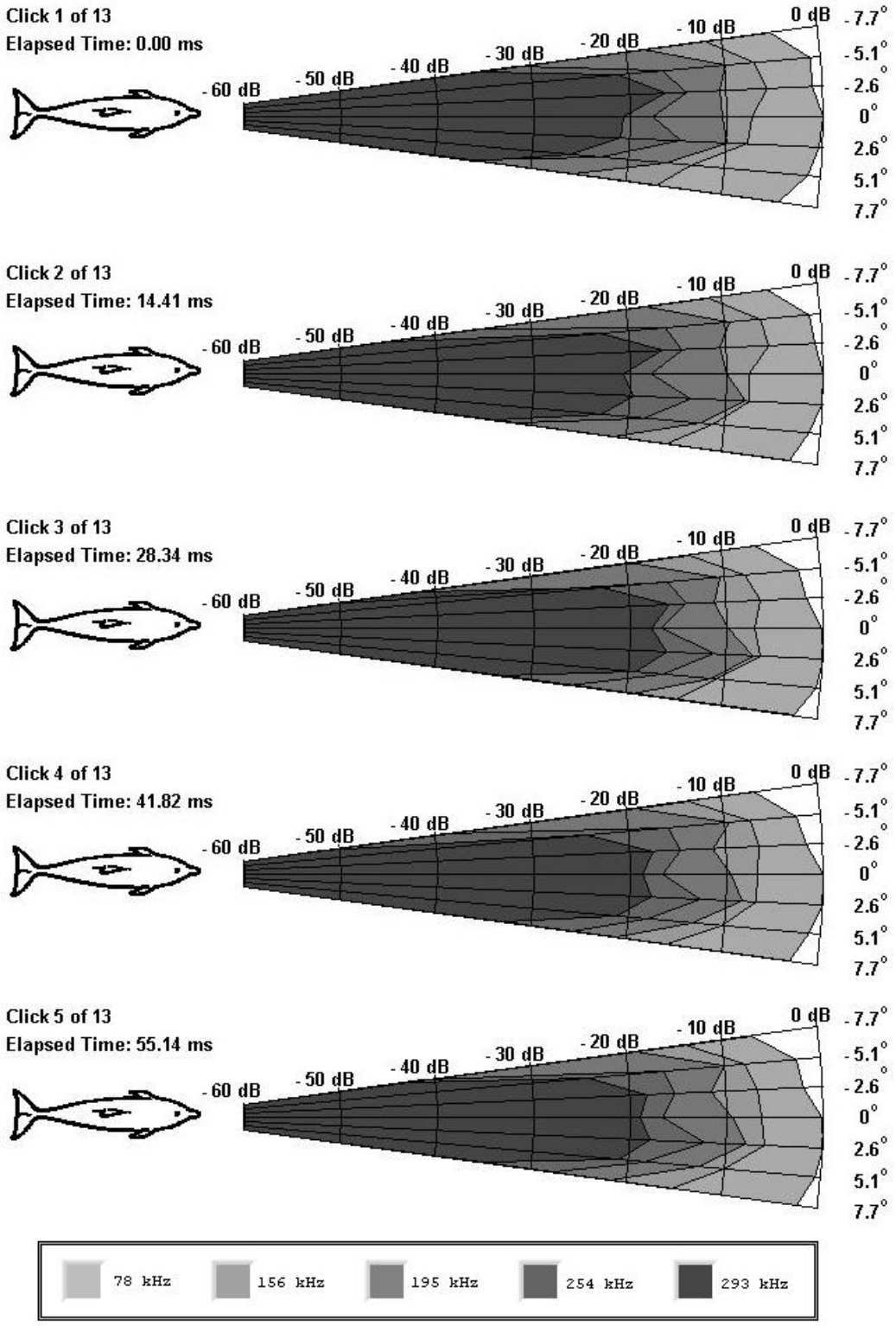

Figure 20. Trial Run 1-3 Clicks 1 through 5.

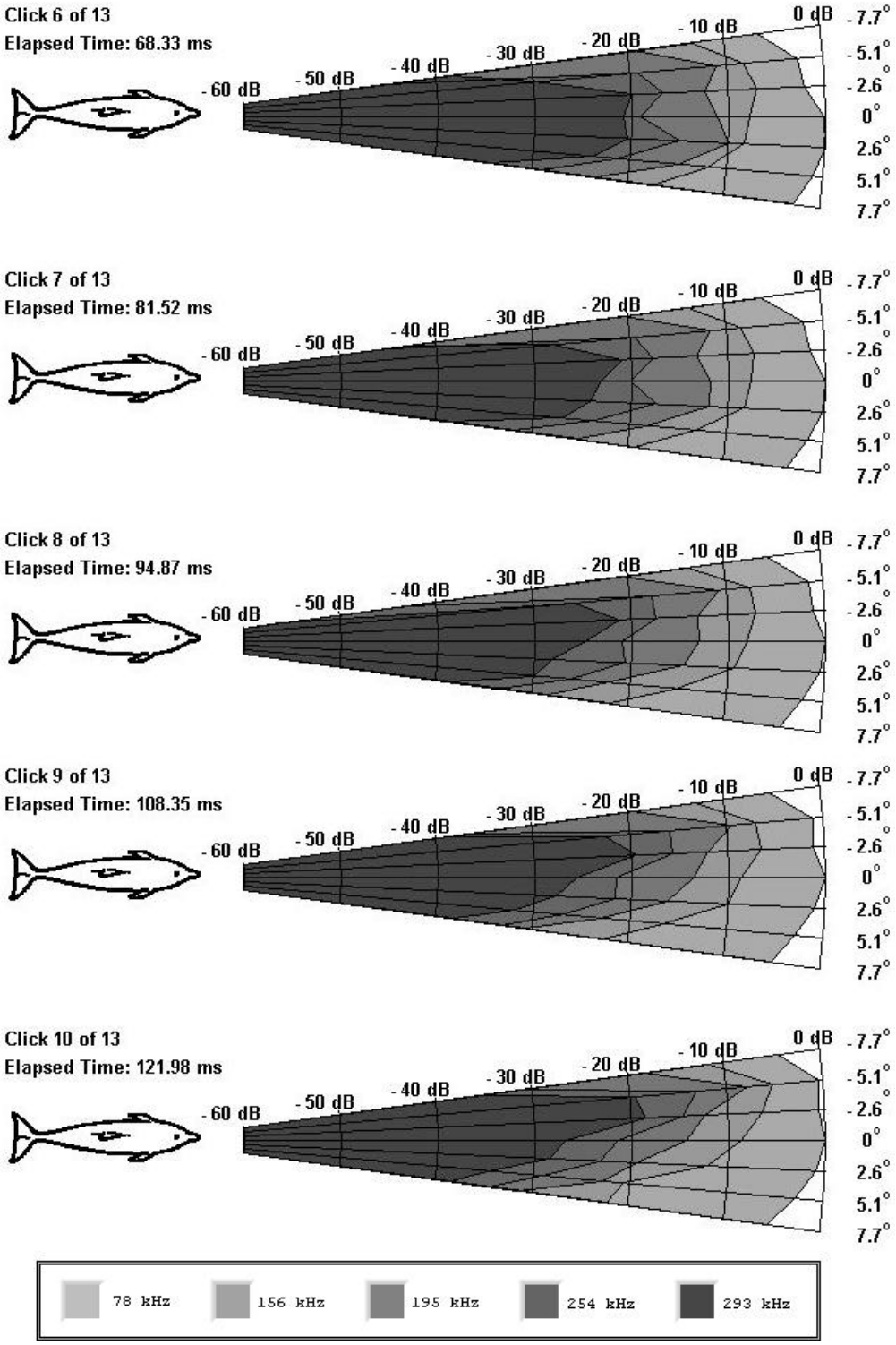

Figure 21. Trial Run 1-3 Clicks 6 through 10.

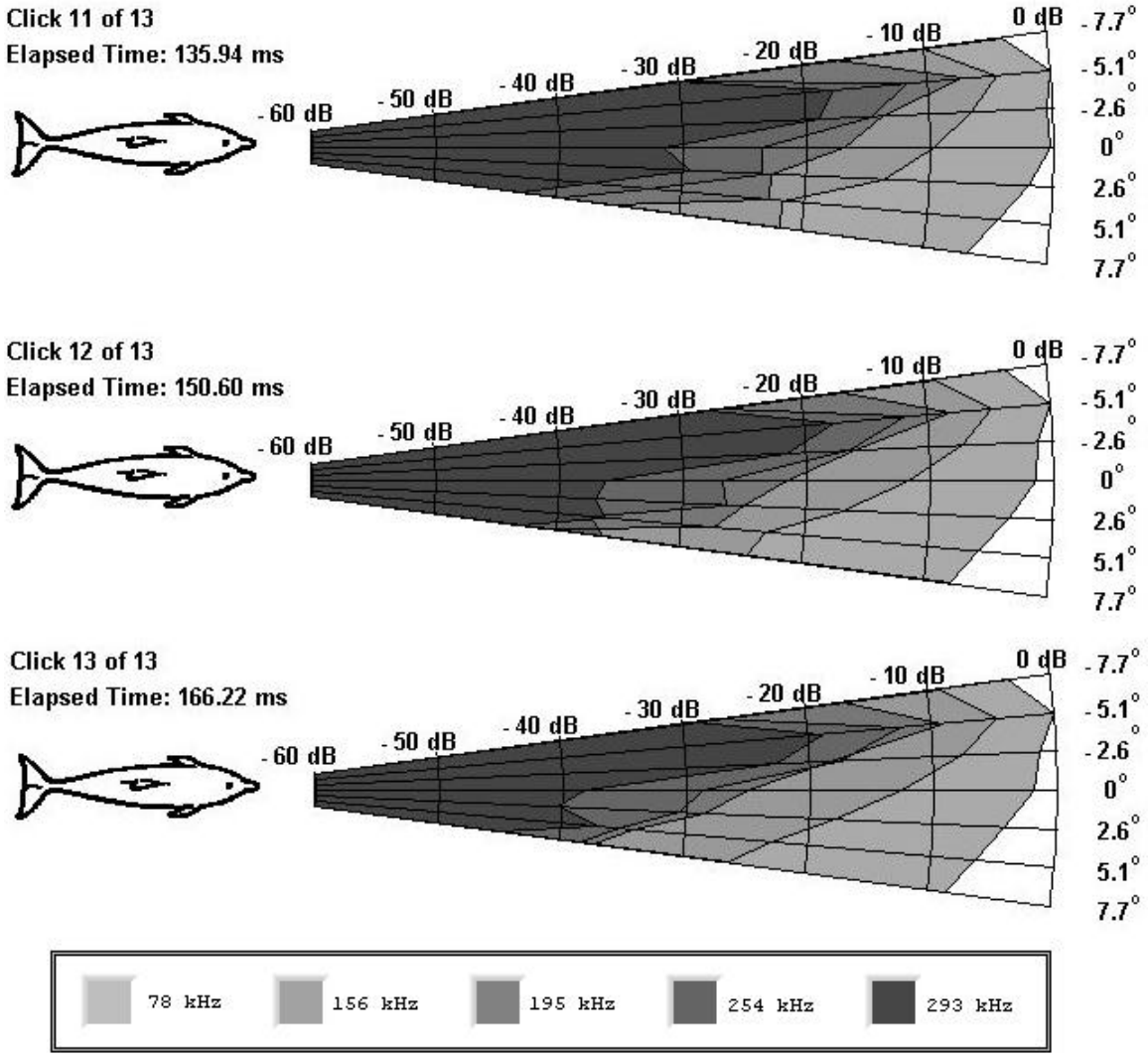

Figure 22. Trial Run 1-3 Clicks 11 through 13.

Figure 23 shows the waveform differences in Click 13 as it was received at the 5.1° hydrophone, where the high frequencies had significantly lower EFSDLs than other frequencies received at –5.1°, where high frequency components had maximum EFSDLs.

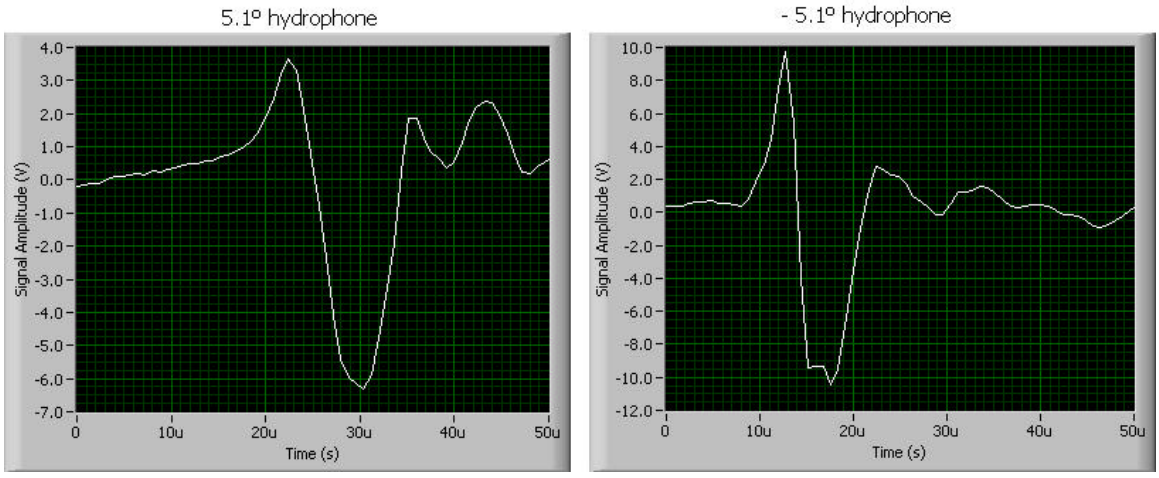

Figure 23. Click 13 received at two different hydrophones during Trial Run 1-3.

b. Trial Run 3-23

Trial Run 3-23 was conducted late in the afternoon on day three of the experiment; the click train accompanying these images spans slightly more than 195 ms and is displayed in Figure 24. The dolphin's zinc oxide stripe is plainly visible in the six images presented in Figure 25. During his approach, “Nemo” rolled slightly over to one side. By day three, “Nemo” had completed more than 40 trial runs before conducting this one. When compared to the signals shown in Trial Run 1-3, the plotted high frequency EFSDLs (Figures 26 to 35) are noticeably lower than those seen in Trial Run 1-3. In this click train, the dolphin did not use the high frequencies while echolocating.

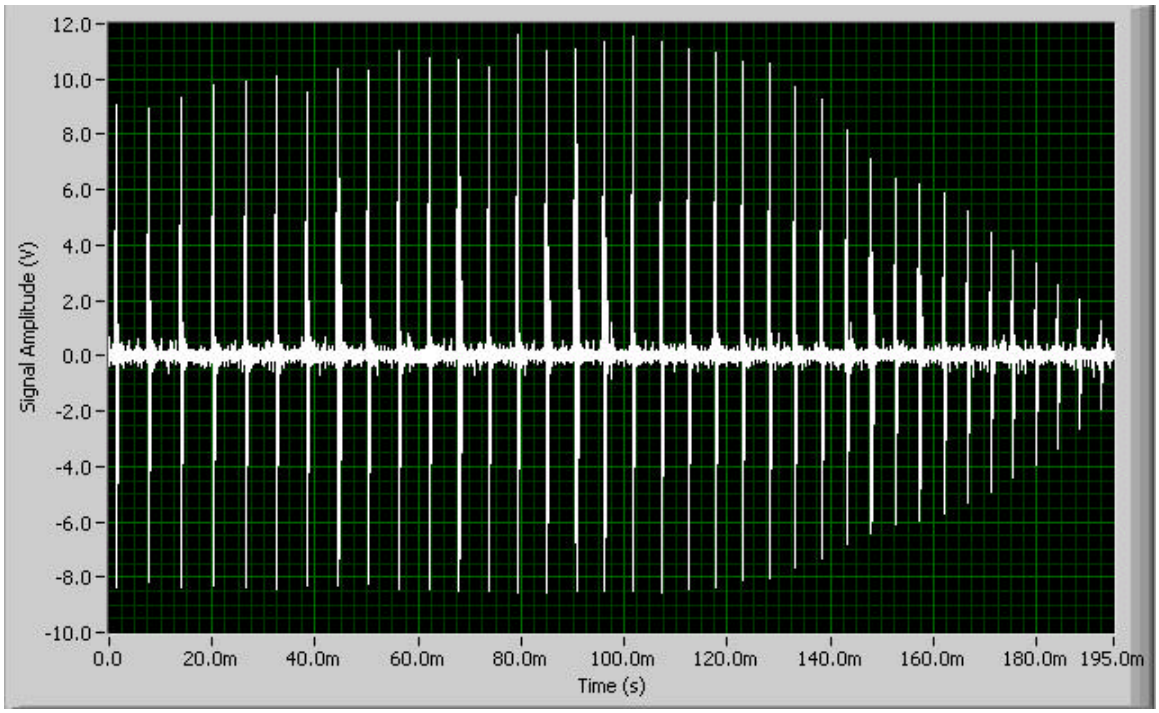

Figure 24. Trial Run 3-23 click train.

Although some of the high frequencies have narrow transmitting beams they have low EFSDLs throughout the click train; by click 37, nearly all of the energy is contained in frequencies below 156 kHz. The plotted frequencies above 156 kHz have 25 dB differences from the click's maximum EFSDL at 58 kHz. In Trial Run 1-3, the maximum EFSDL at 293 kHz was 18 dB lower than the peak EFSDL; in the trial run examined here, Trial Run 3-23, the maximum EFSDL at 293 kHz is approximately 35 dB lower.

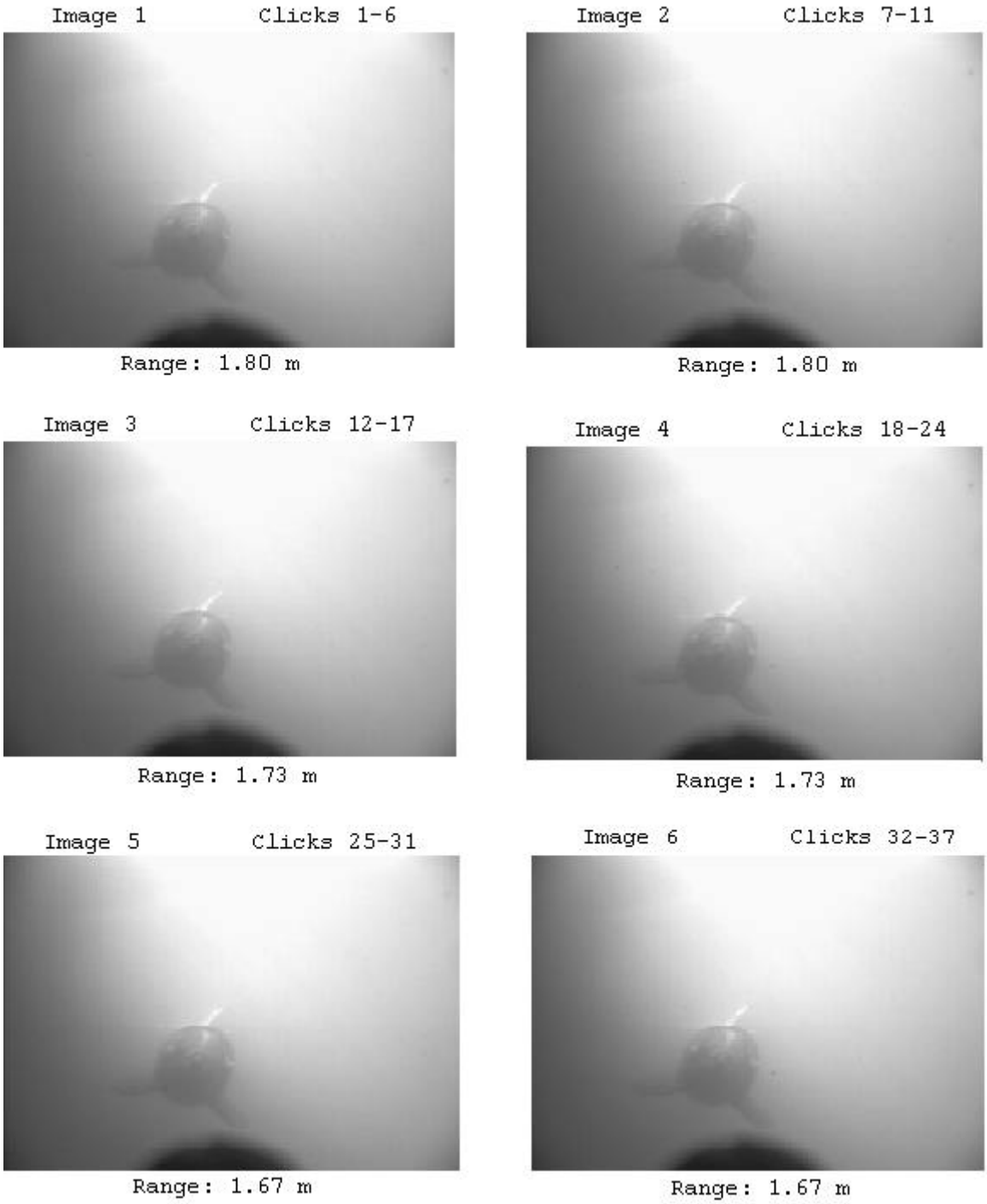

Figure 25. Trial Run 3-23 images 1 through 6.

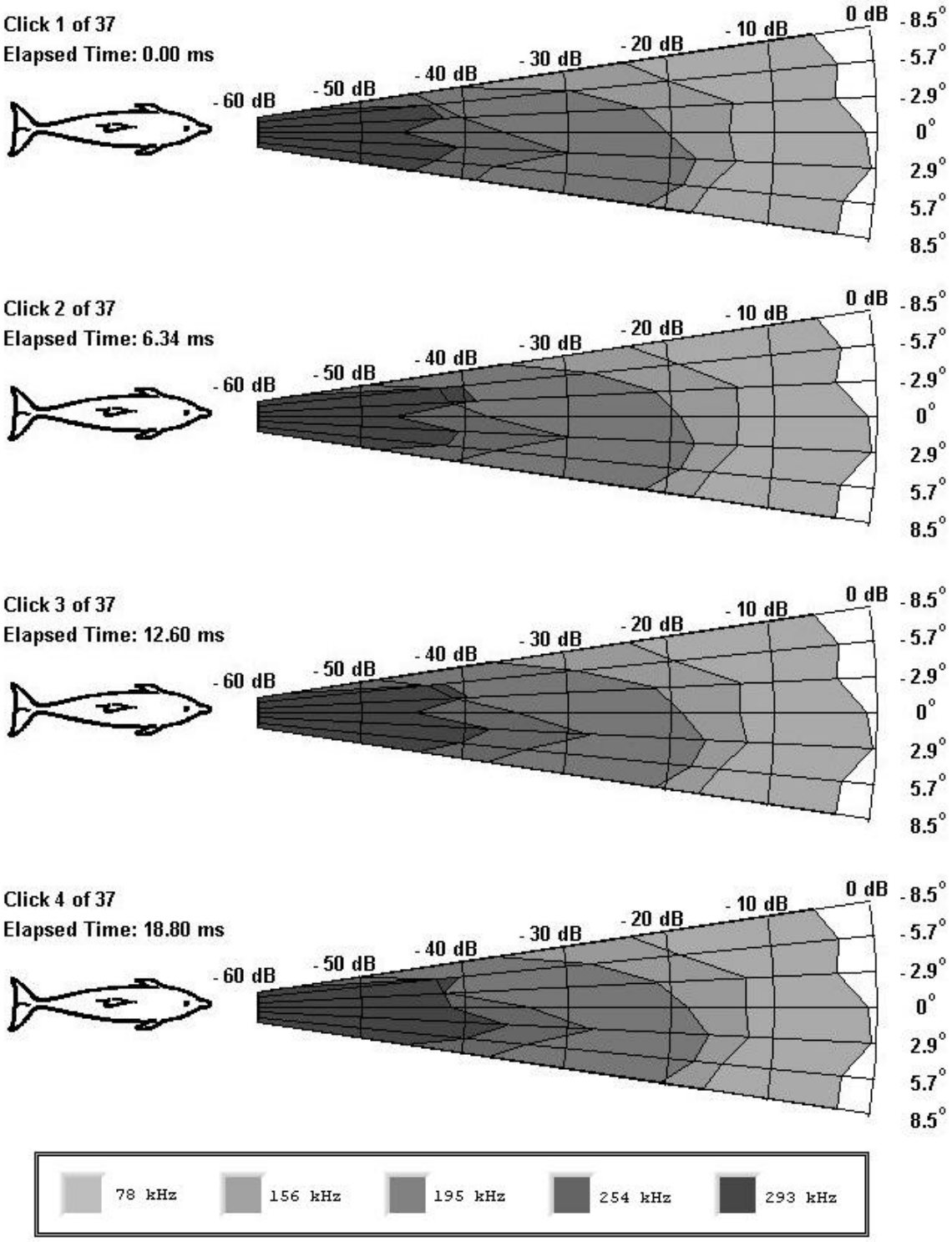

Figure 26. Trial Run 3-23 Clicks 1 through 4.

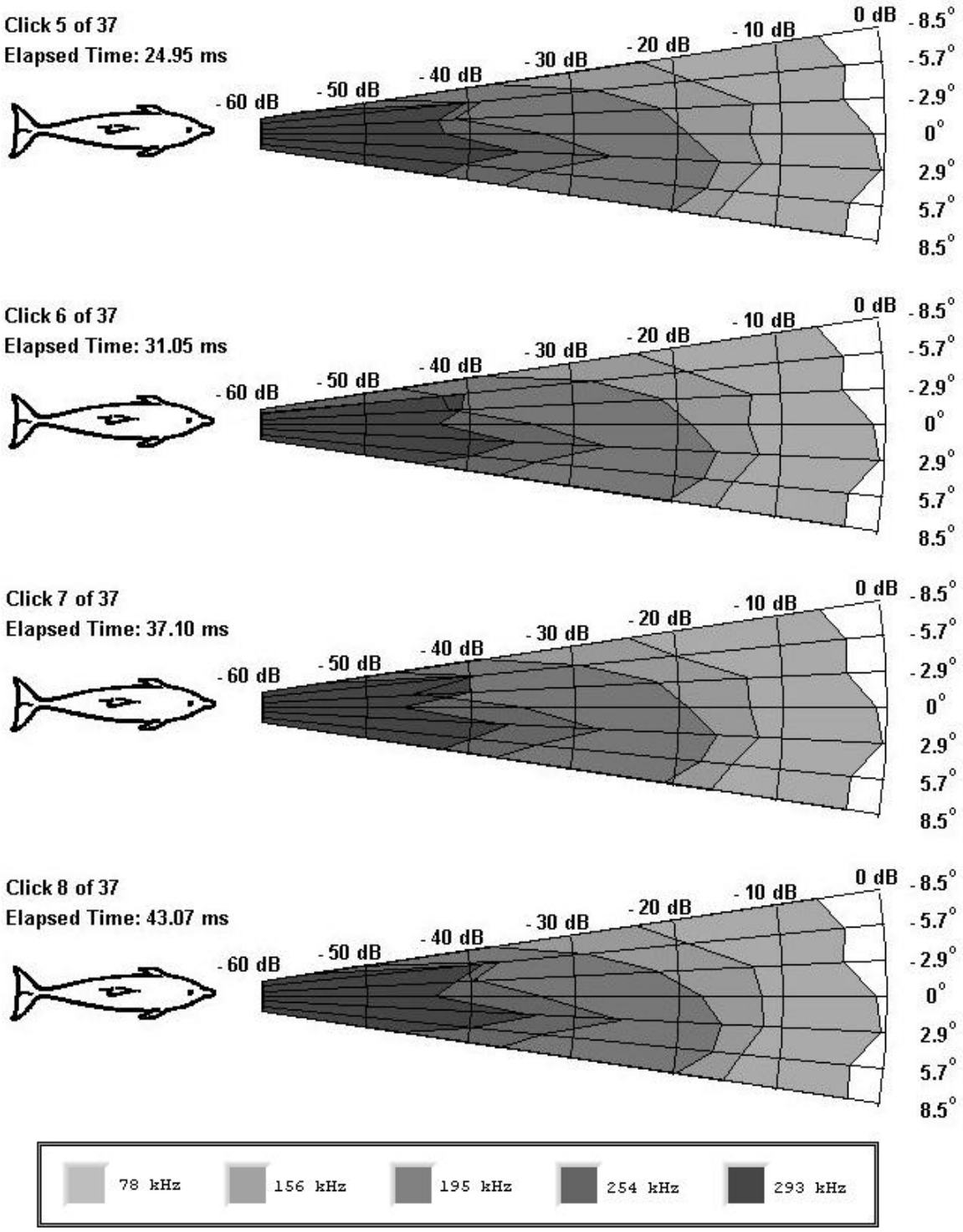

Figure 27. Trial Run 3-23 Clicks 5 through 8.

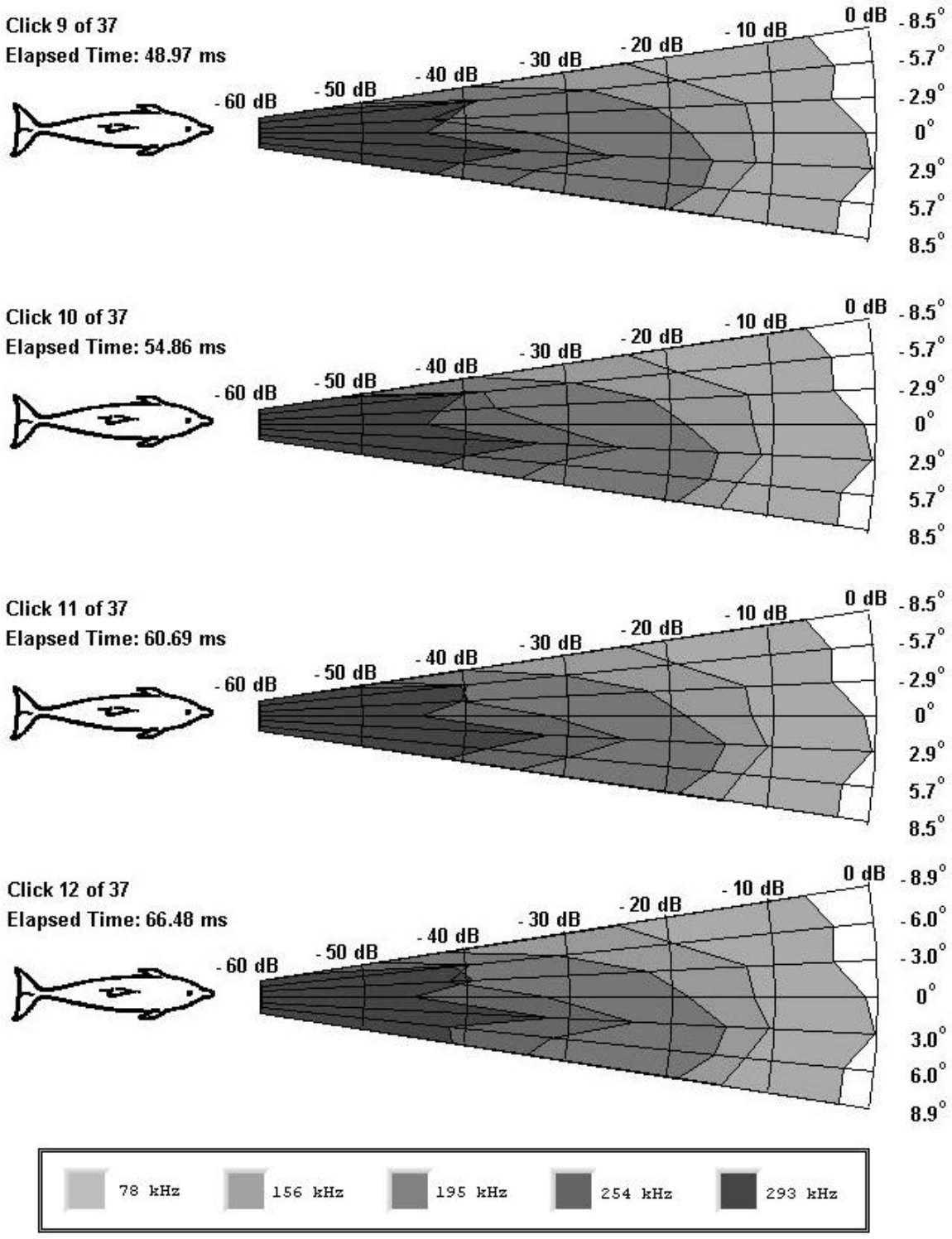

Figure 28. Trial Run 3-23 Clicks 9 through 12.

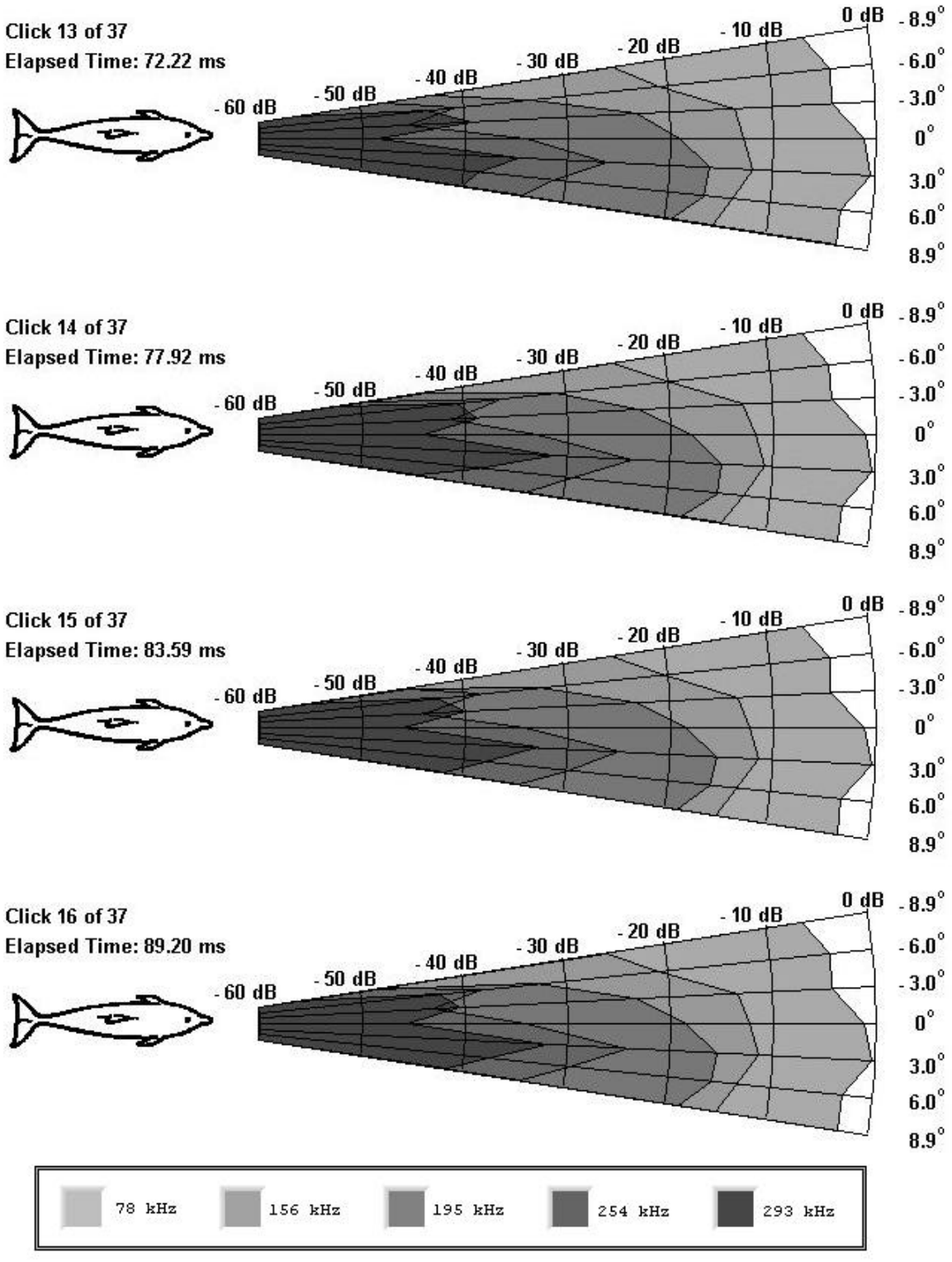

Figure 29. Trial Run 3-23 Clicks 13 through 16.

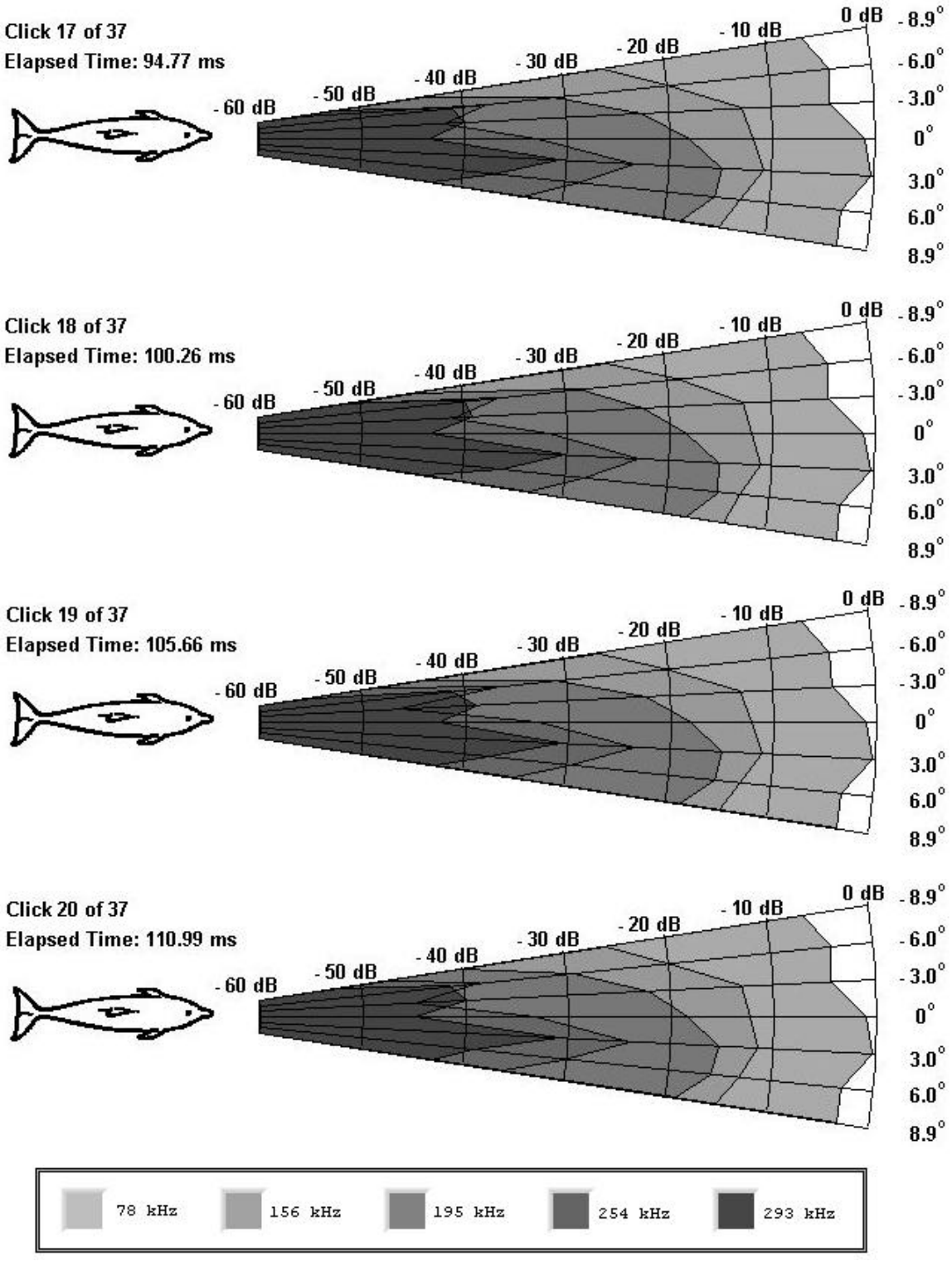

Figure 30. Trial Run 3-23 Clicks 17 through 20.

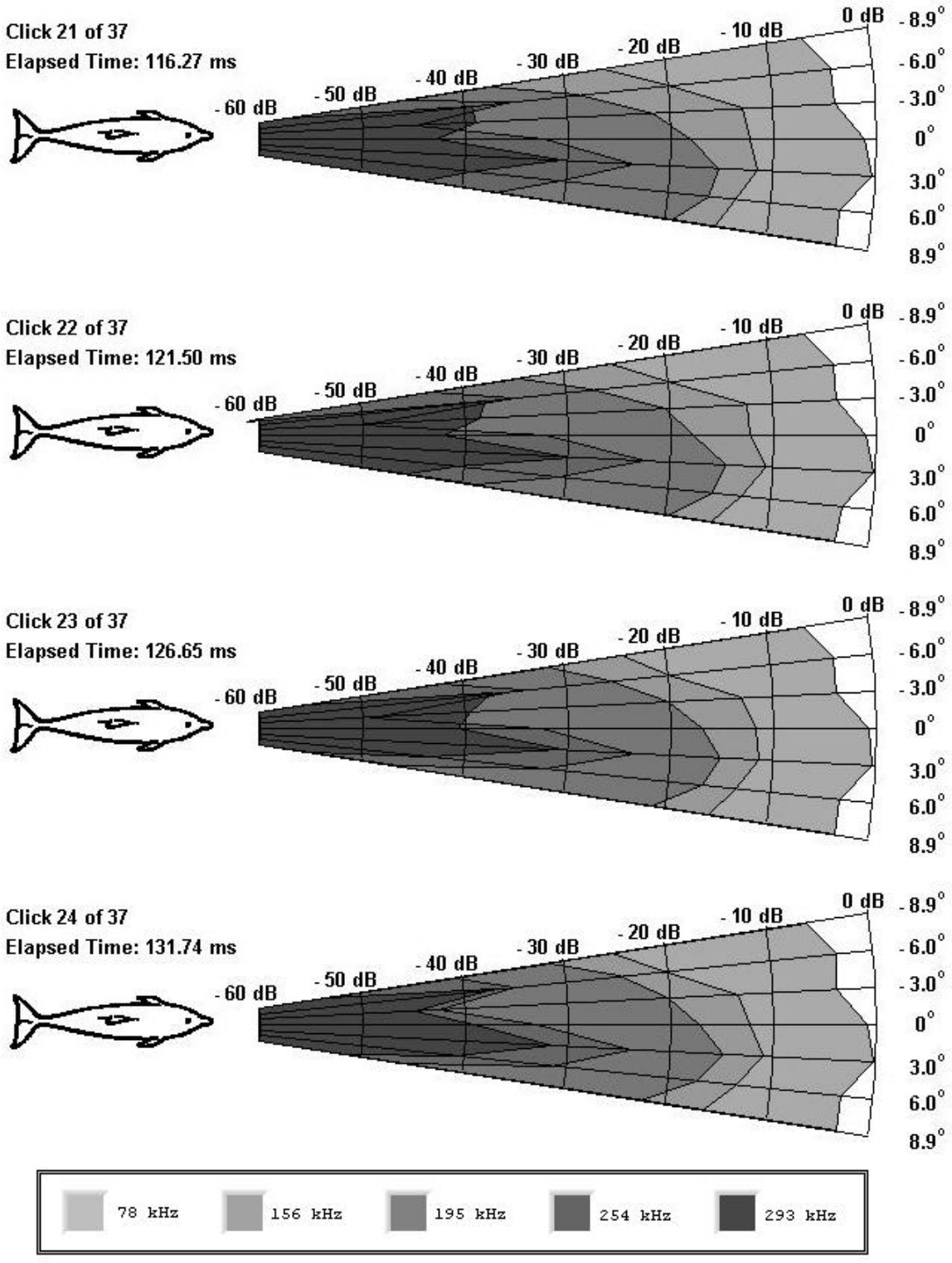

Figure 31. Trial Run 3-23 Clicks 21 through 24.

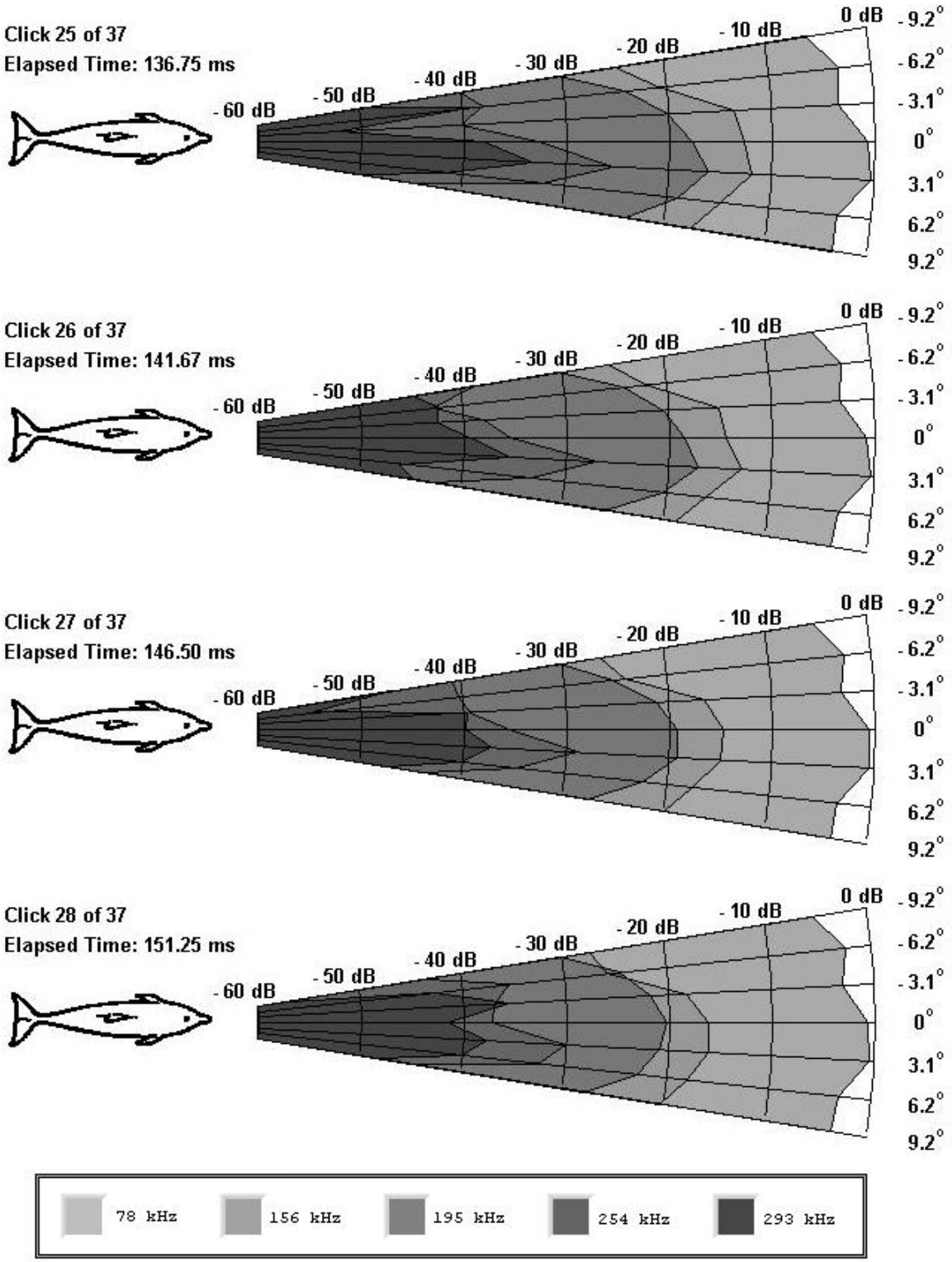

Figure 32. Trial Run 3-23 Clicks 25 through 28.

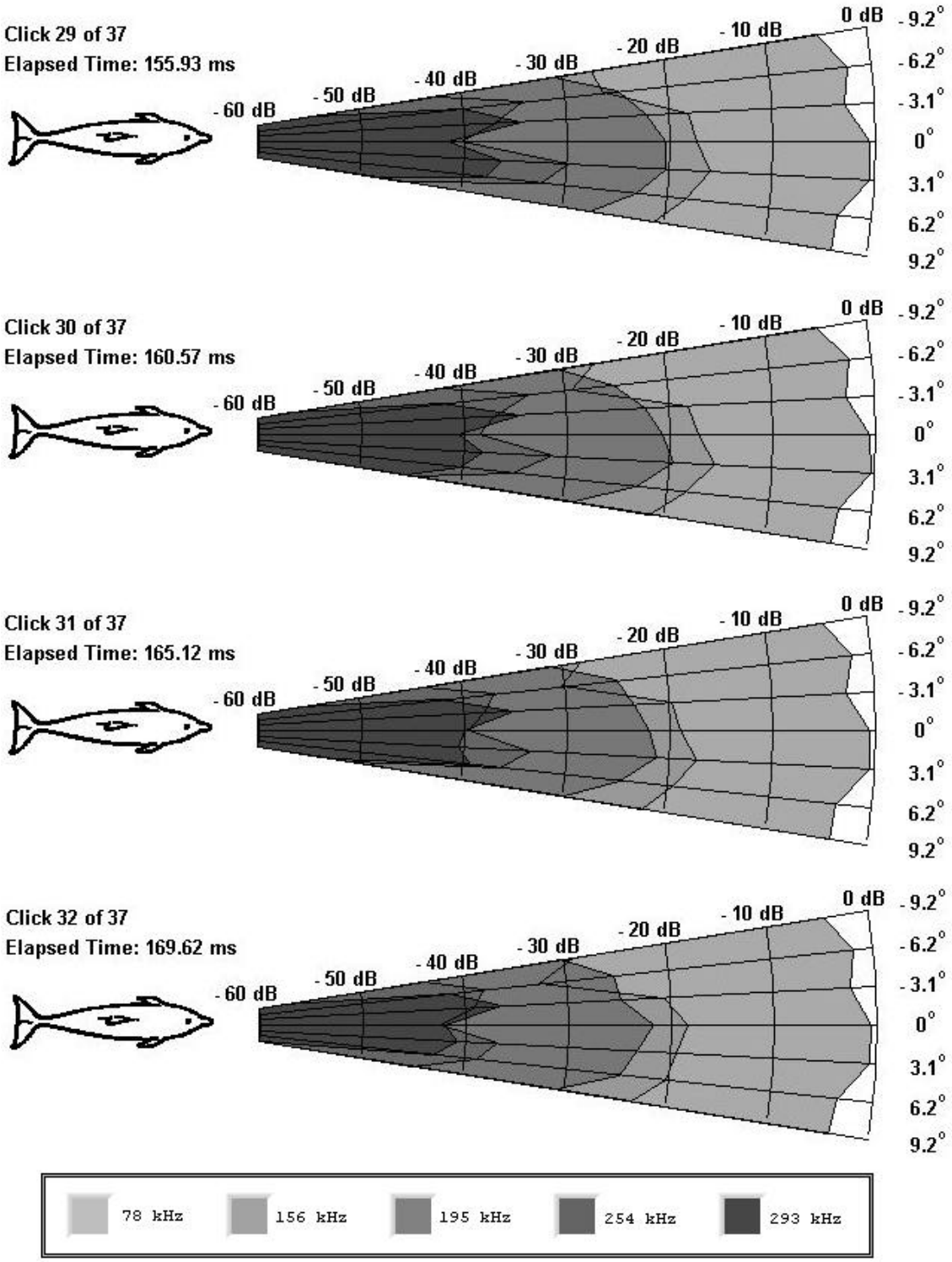

Figure 33. Trial Run 3-23 Clicks 29 through 32.

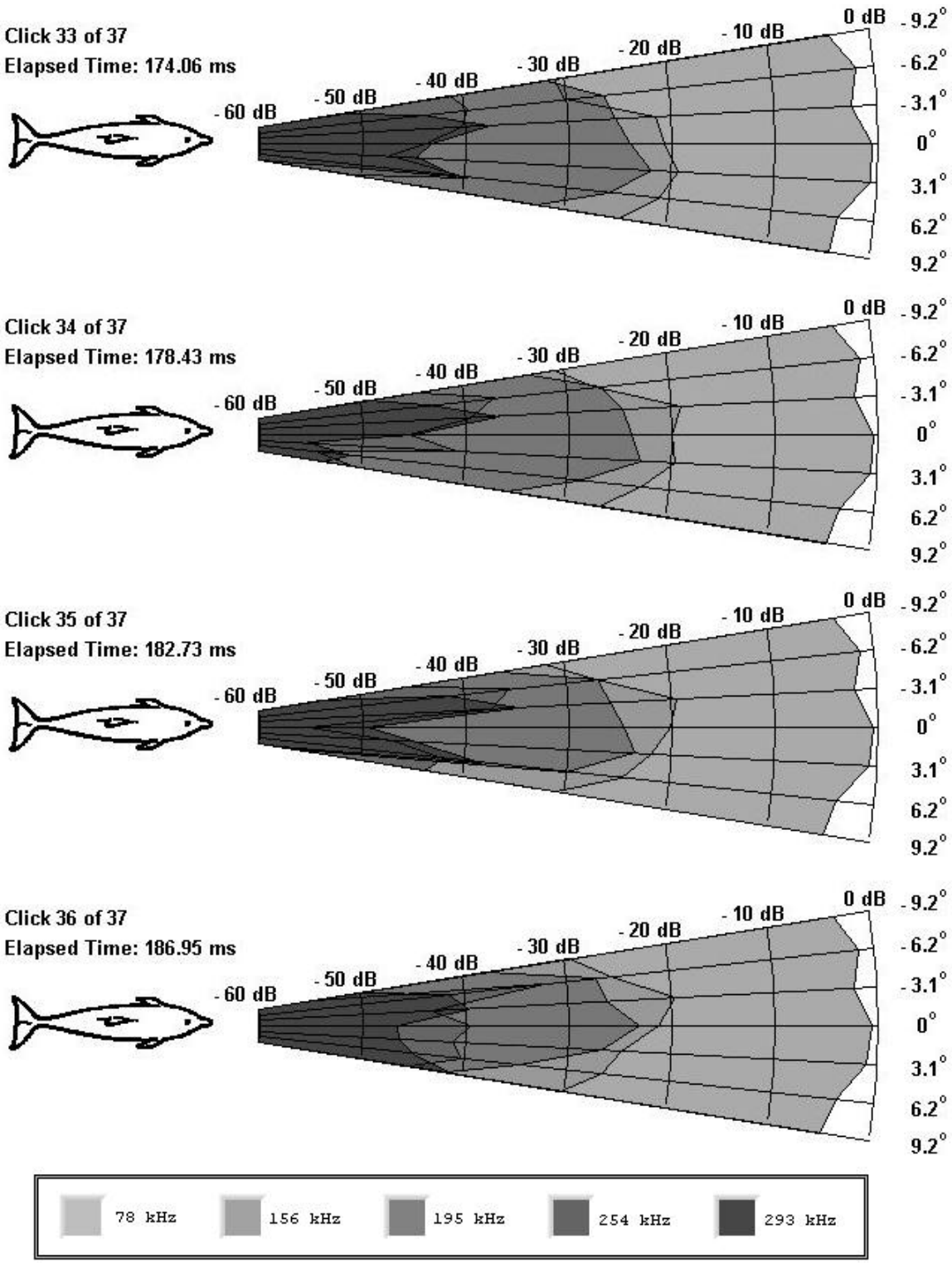

Figure 34. Trial Run 3-23 Clicks 33 through 36.

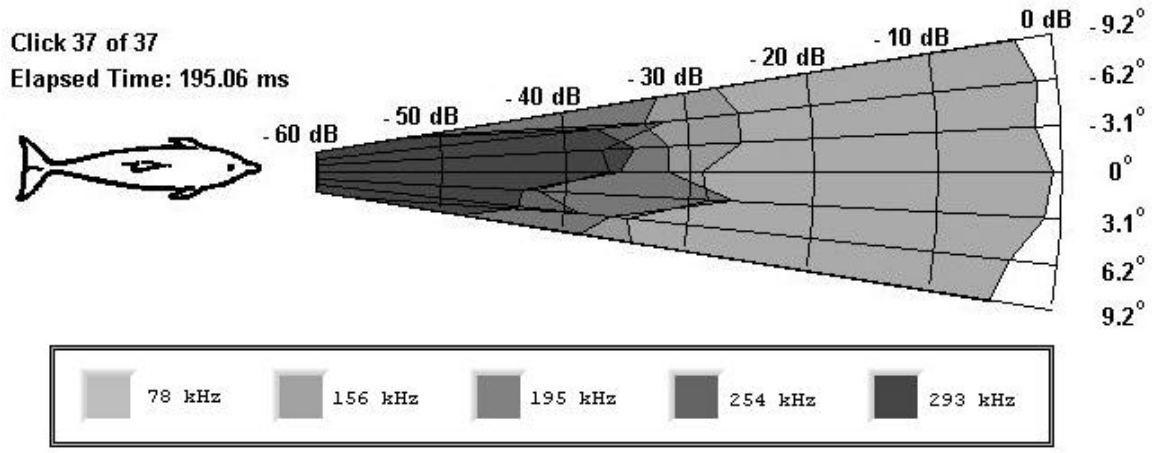

Figure 35. Trial Run 3-23 Click 37.

Figure 36 shows Click 4 received at the -2.9° and 2.9° hydrophones. Even though the peak frequency centered on the 2.9° hydrophone, the high frequency EFSDLs are rather insignificant. The difference in these two waveform shapes is not nearly as drastic as the difference seen in Figure 23.

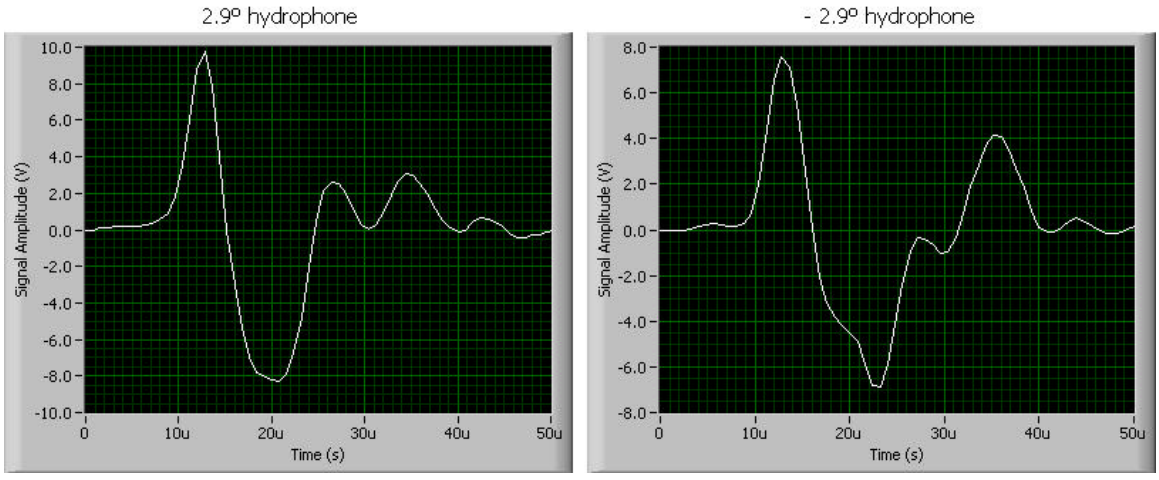

Figure 36. Click 4 received at two different hydrophones during Trial Run 3-23.

c. Trial Run 3-26

Trial Run 3-26 was recorded shortly after Trial Run 3-23. The 23 clicks collected in this data set are depicted in Figure 37. An extra click appears amidst this click train; this click came from a dolphin in the neighboring pen. The vertical zinc oxide stripe is clearly

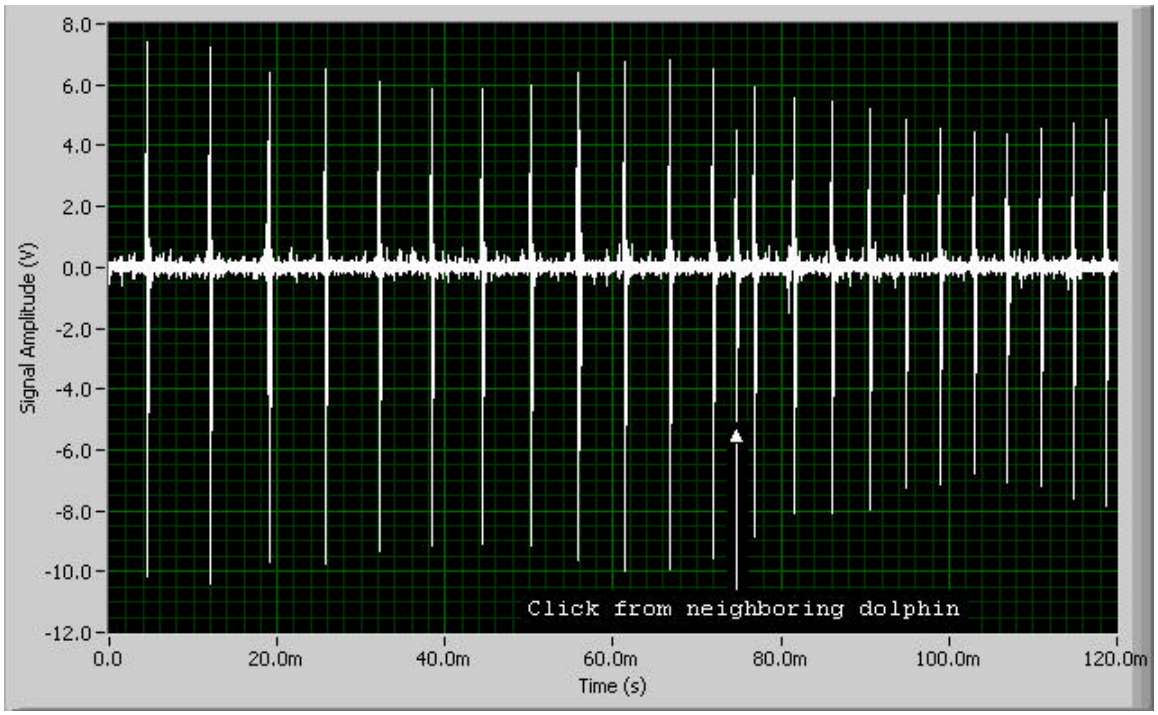

Figure 37. Trial Run 3-26 click train.

visible in the four underwater images presented in Figure 38. Just as in Trial Run 3-23, the plots shown in Figures 39 to 46 show that high frequency components do not contribute greatly to the echolocation signal.

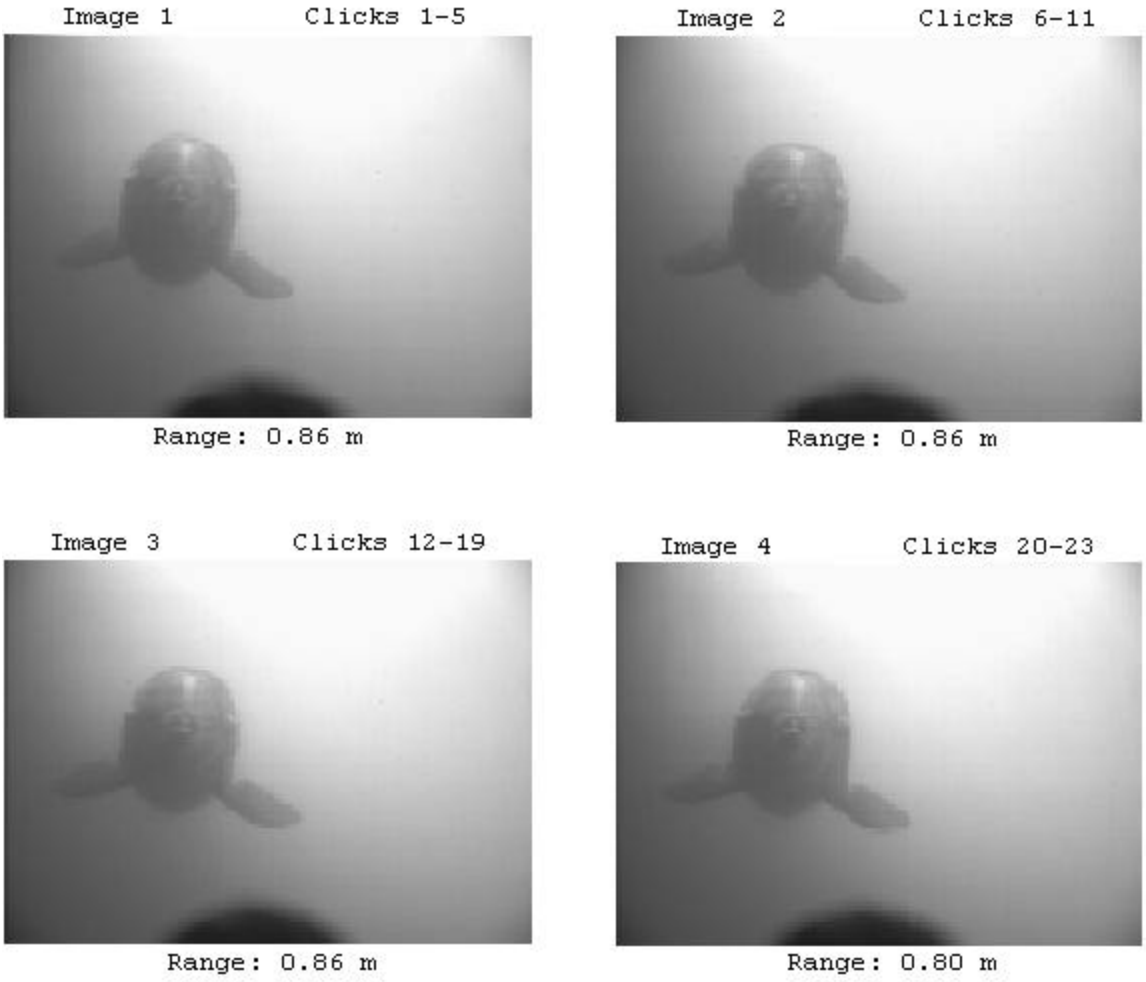

Figure 38. Trial Run 3-26 images 1 through 4.

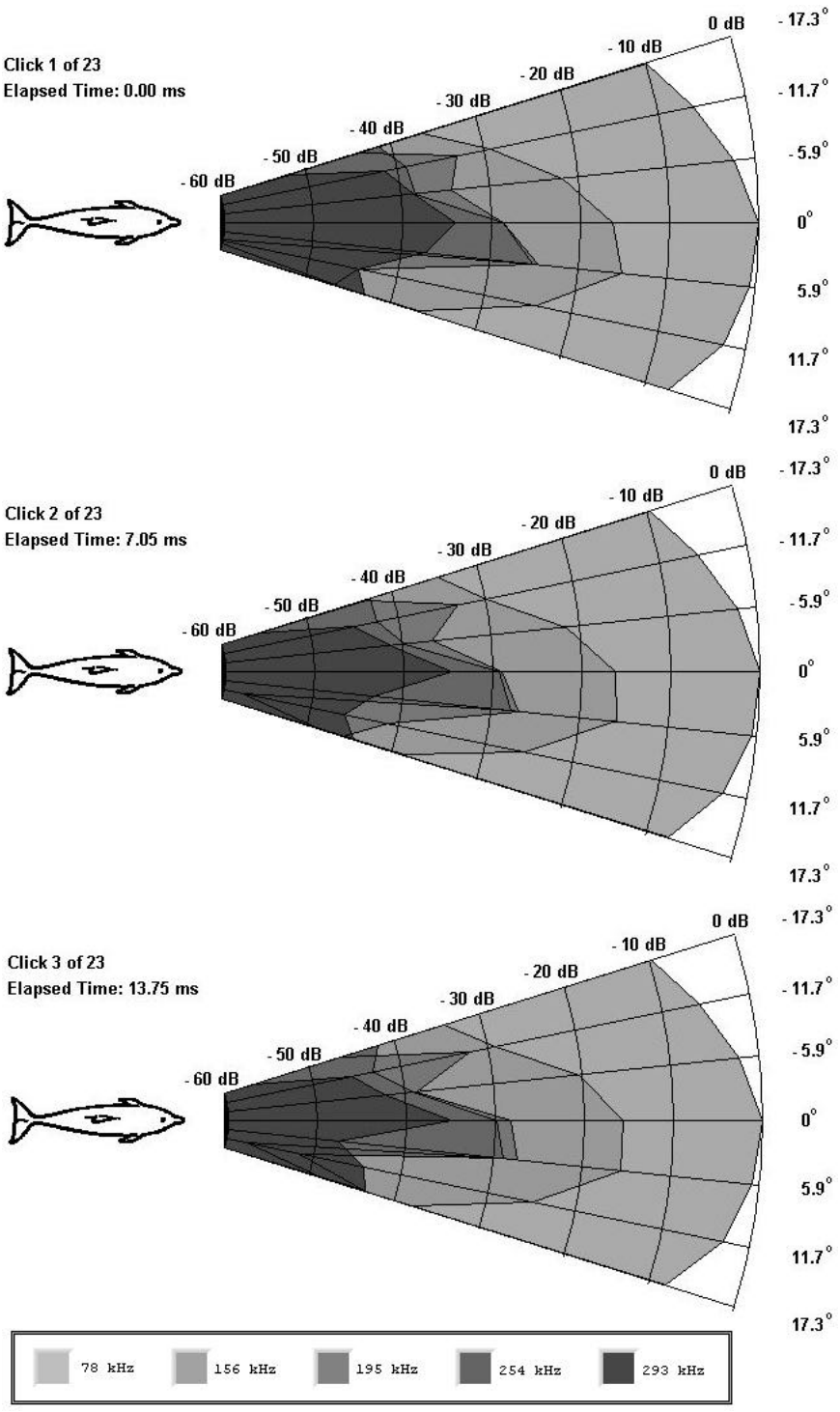

Figure 39. Trial Run 3-26 Clicks 1 through 3.

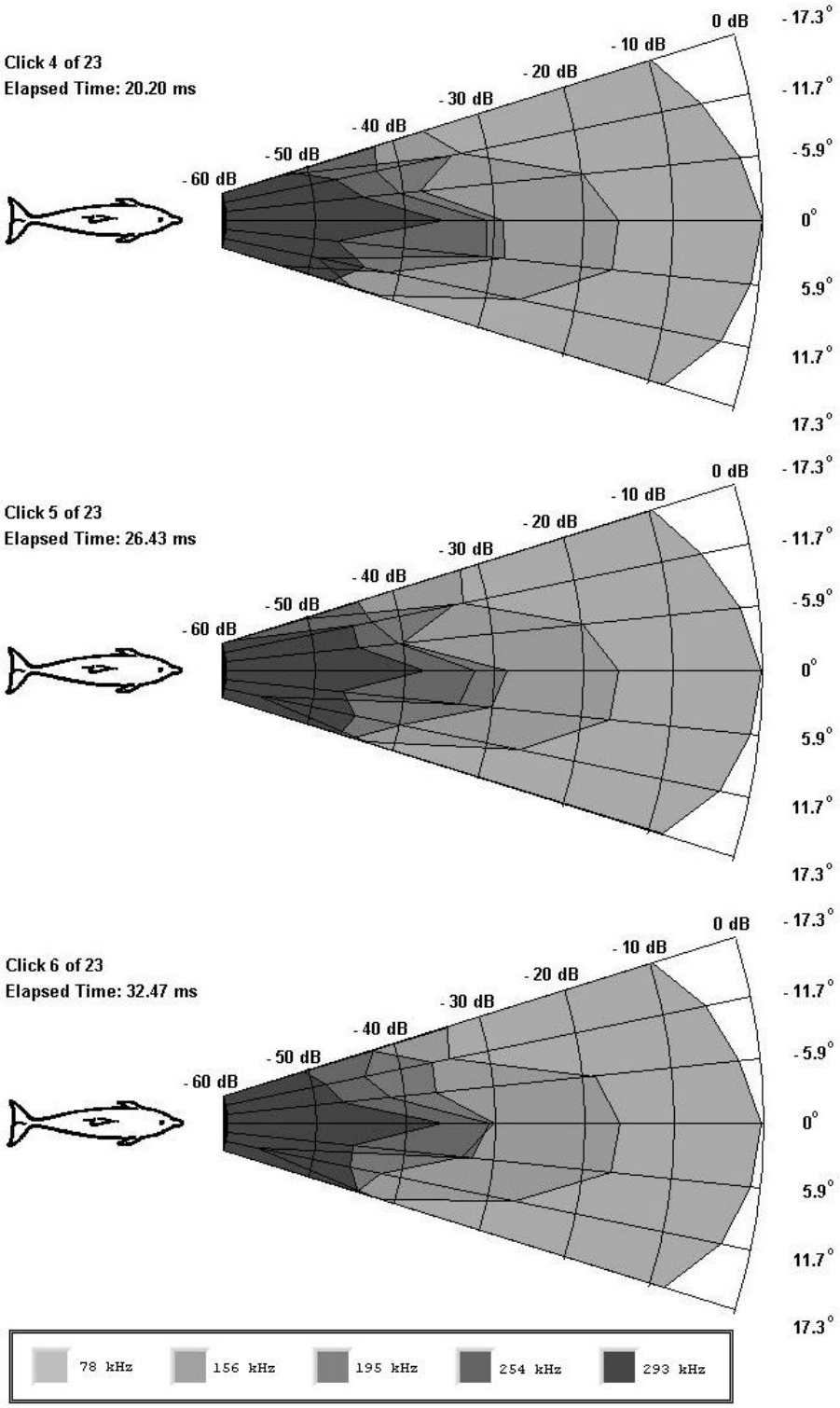

Figure 40. Trial Run 3-26 Clicks 4 through 6.

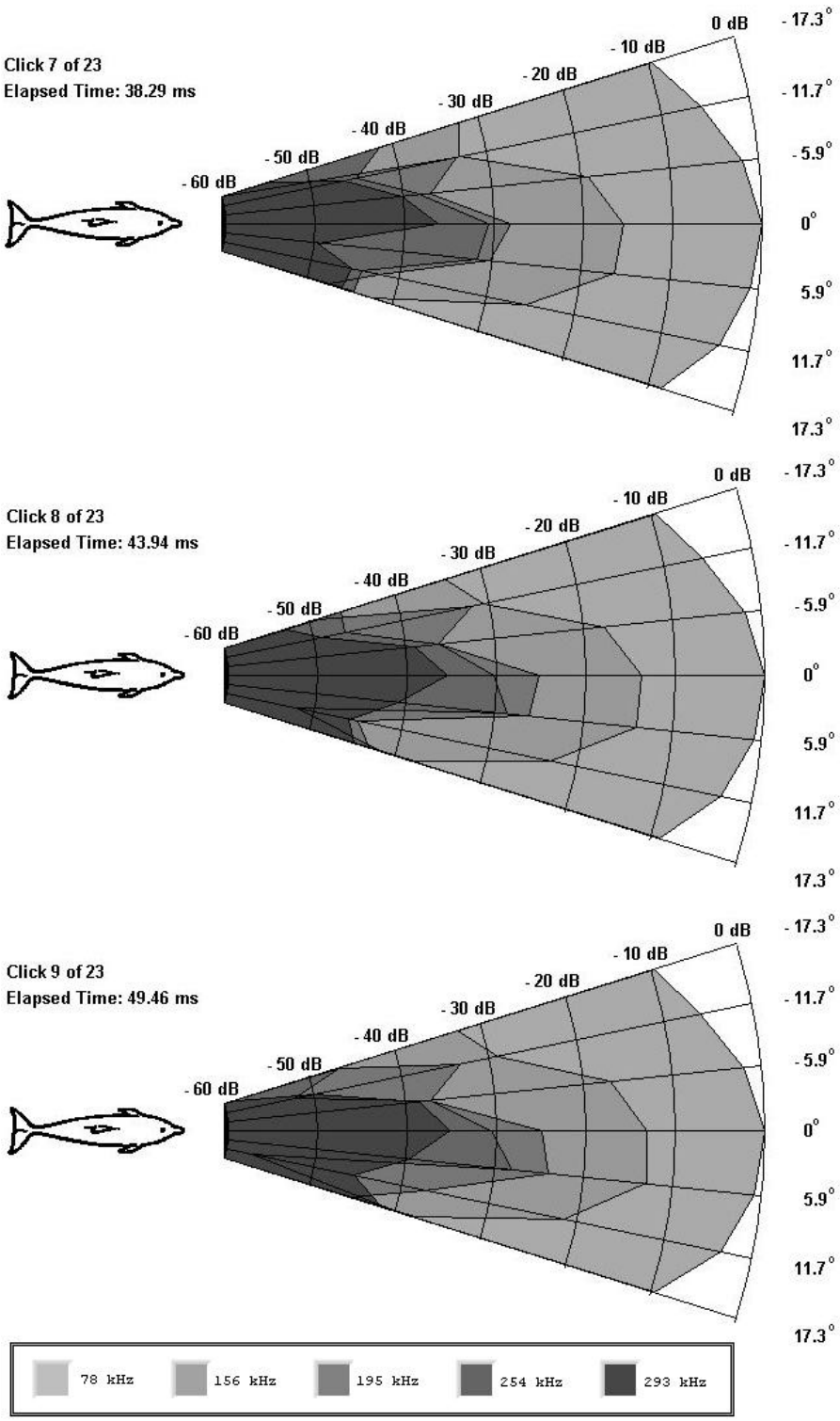

Figure 41. Trial Run 3-26 Clicks 7 through 9.

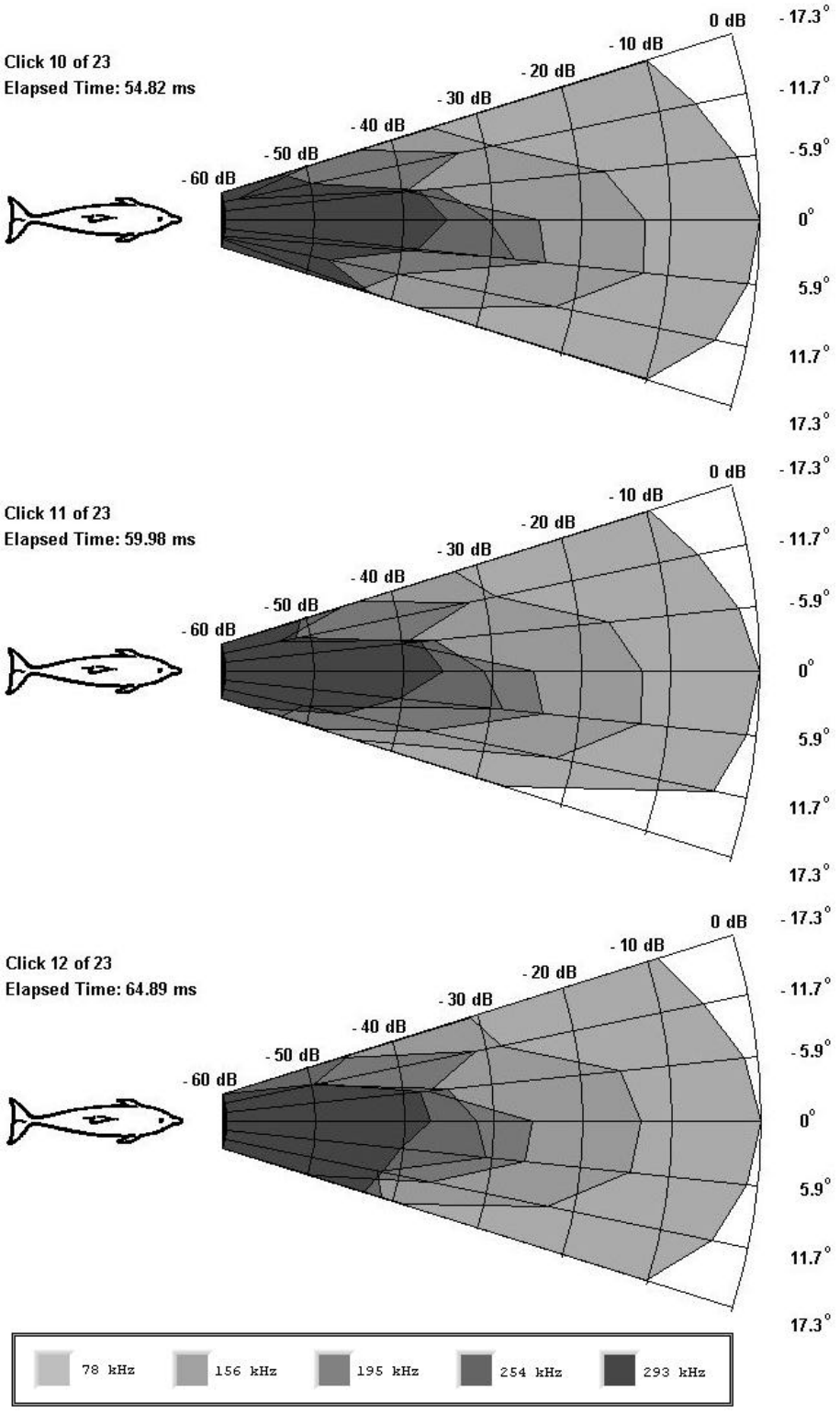

Figure 42. Trial Run 3-26 Clicks 10 through 12.

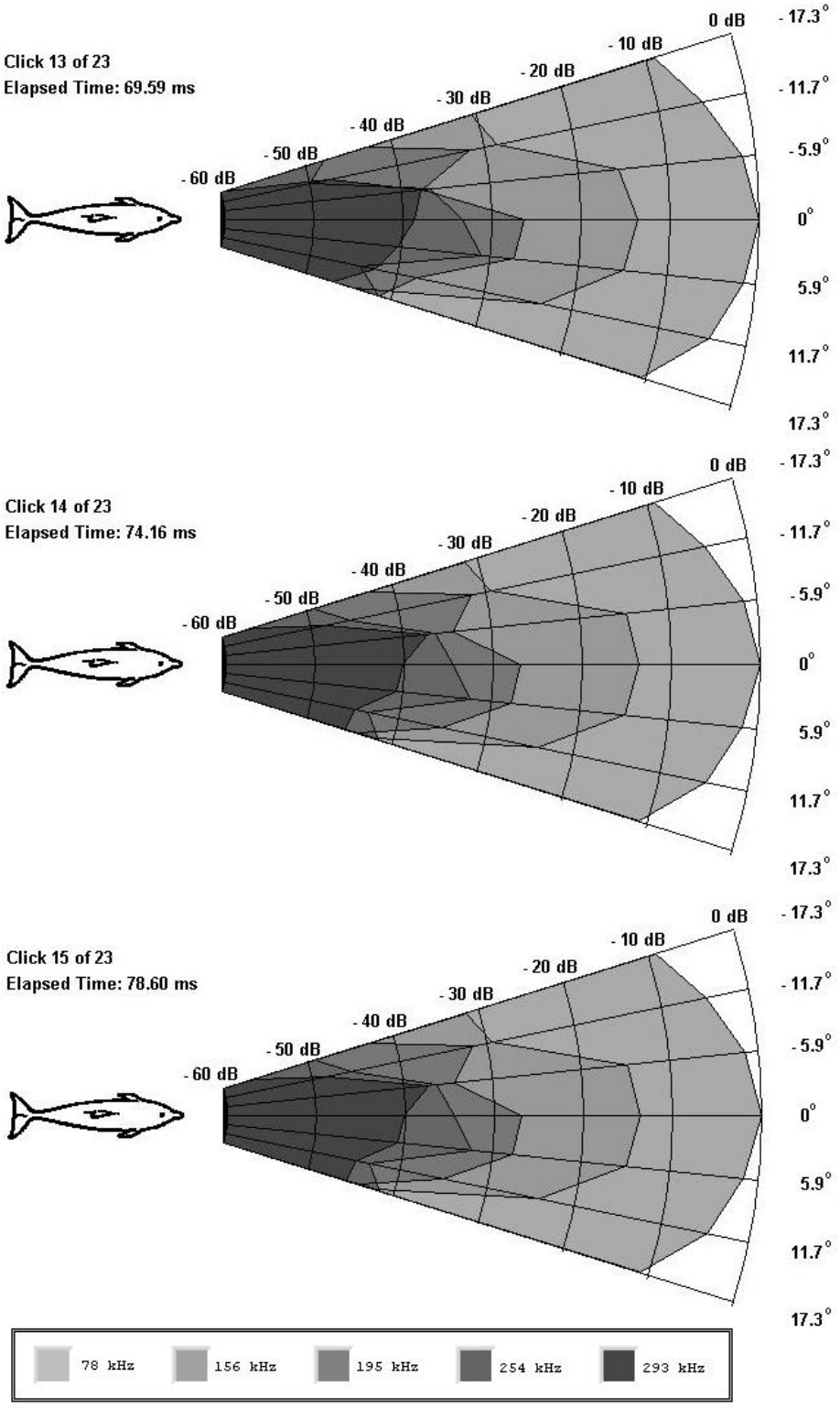

Figure 43. Trial Run 3-26 Clicks 13 through 15.

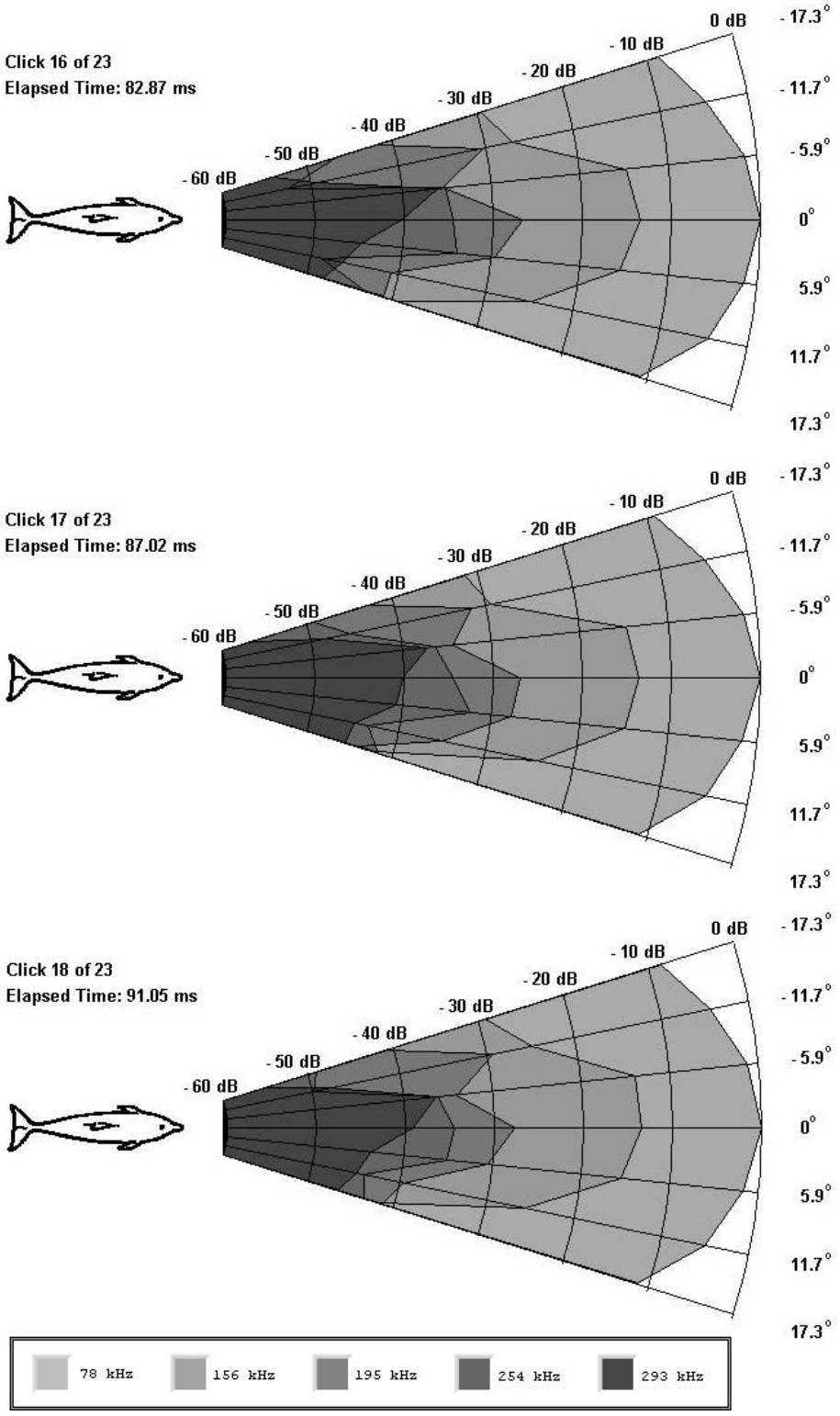

Figure 44. Trial Run 3-26 Clicks 16 through 18.

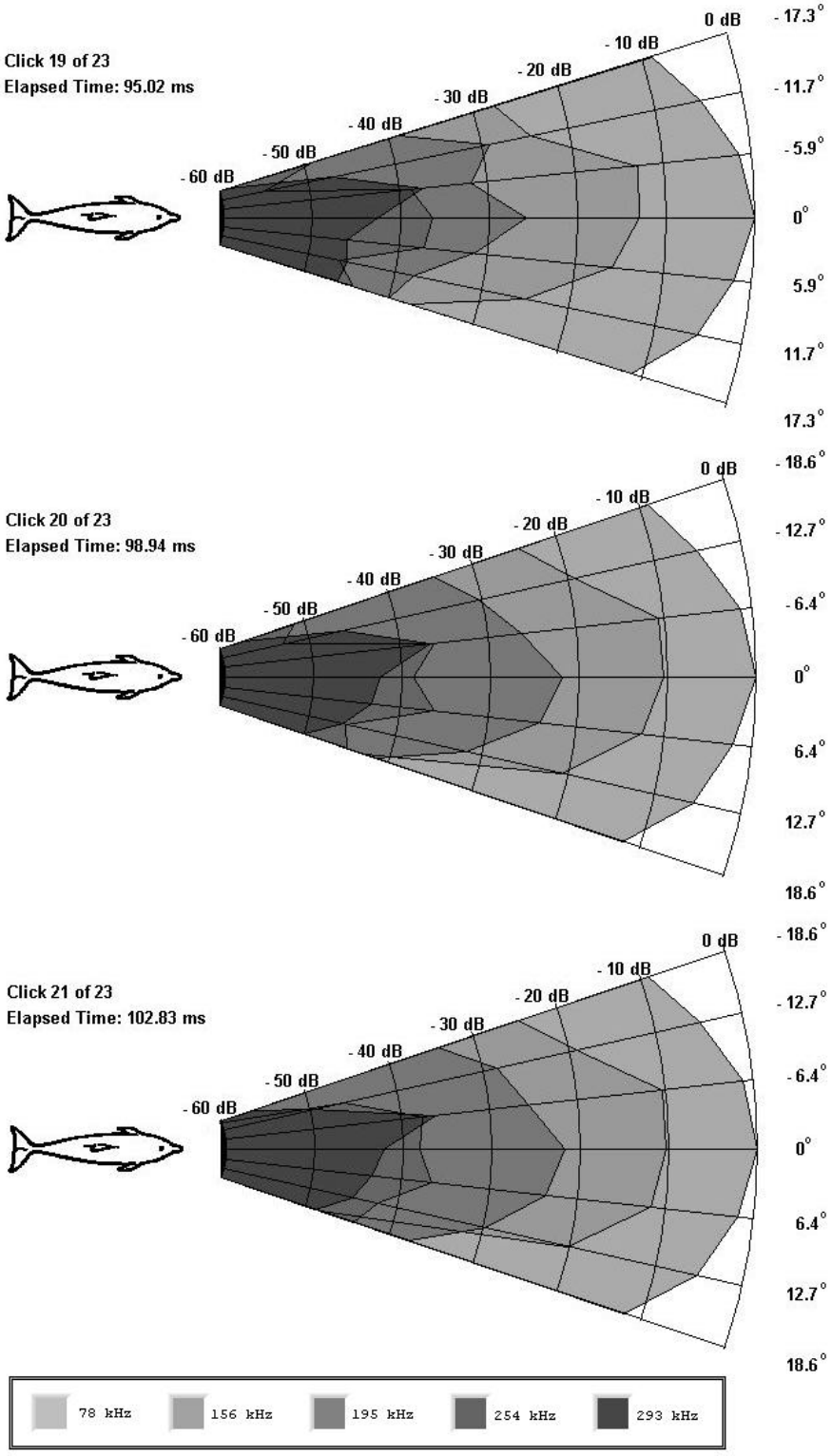

Figure 45. Trial Run 3-26 Clicks 19 through 21.

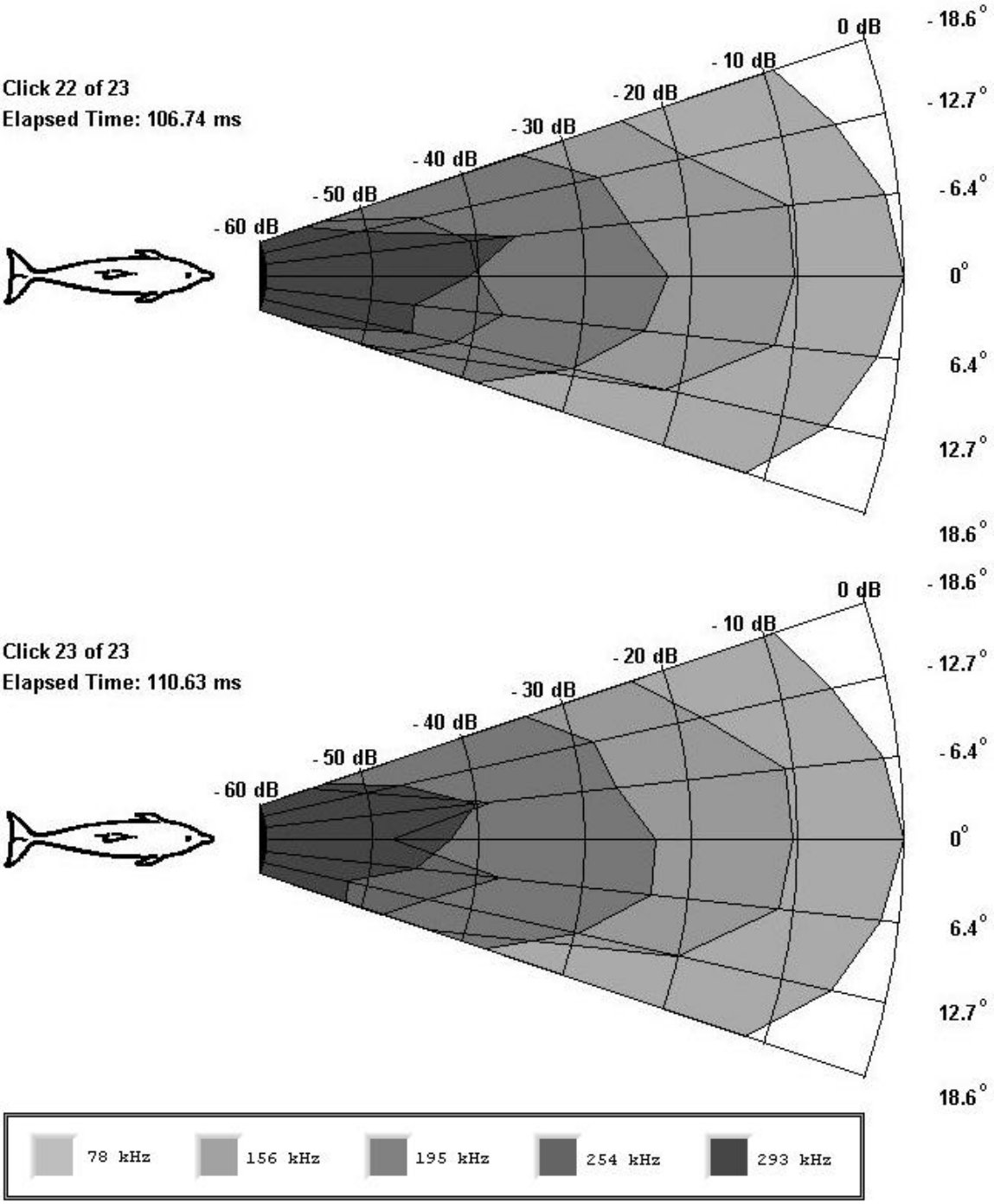

Figure 46. Trial Run 3-26 Clicks 22 and 23.

For another look at click comparison, see Click 21 in Figure 47. Striking similarities can be seen between the waveform shapes of the signals received at the -6.4° and 6.4° hydrophones.

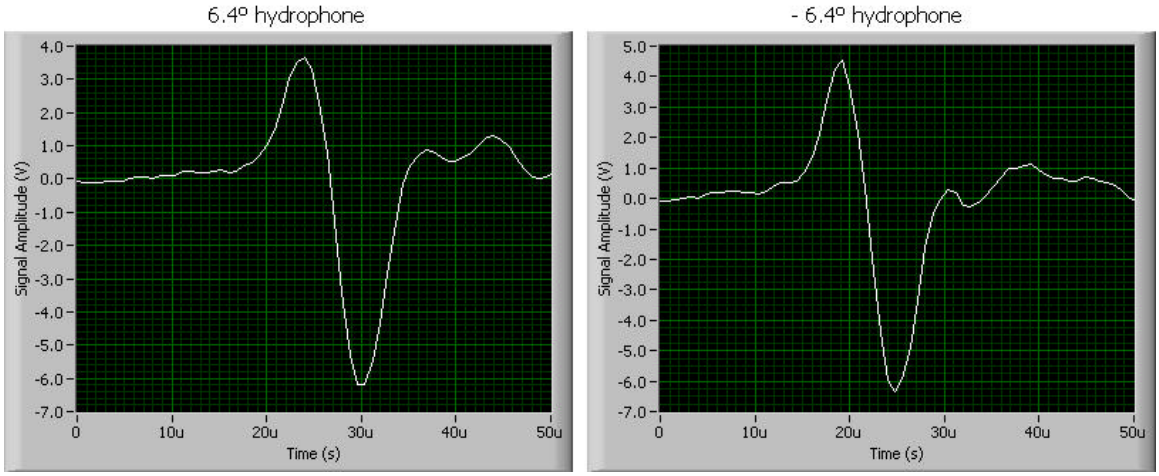

Figure 47. Click 21 received at two different hydrophones during Trial Run 3-26.

2. Vertical Plane

a. Trial Run 1-14

This trial run was the fourteenth trial run on day one, but only the fifth run with the hydrophone and camera apparatus in the vertical configuration. Figure 48 shows the 35 clicks that make up the click train, while Figures 49 and 50 display the accompanying images in which Nemo is shown to have made a “flat” and direct approach to the target. The eyecups are very prominent and contrast nicely with the dolphin and the water. Figures 51 to 59 show the plotted beam patterns of all 35 clicks in this trial run.

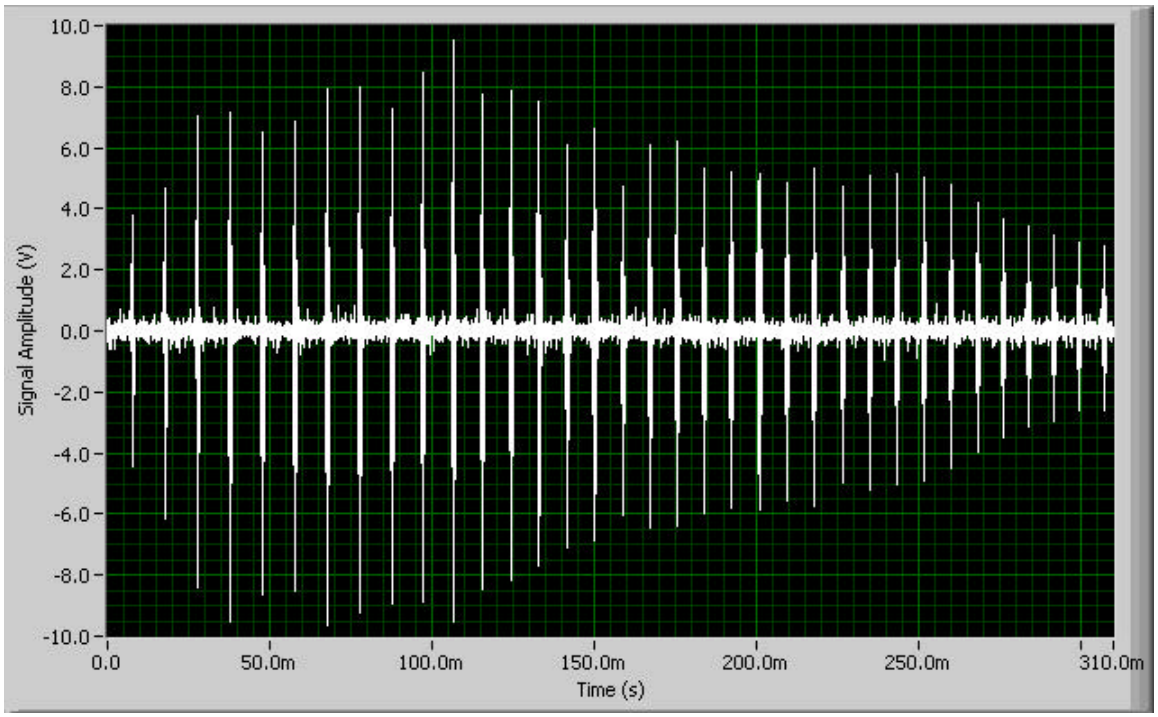

Figure 48. Trial Run 1-14 click train.

In Click 1, the EFSDL for frequencies above 250 kHz is barely noteworthy. However, by Click 4, the dolphin increased the EFSDL at the higher frequencies and concentrated the 293 kHz beam on the –5.5° hydrophone. By click 23, the 293 kHz beam was focused on the 0° hydrophone; the abrupt flatness observed in Clicks 22, 23 and 24 are most likely due to destructive interference caused by the camera lens. Click 28 was centered on the 3.0° hydrophone where the 293 kHz EFSDL increased 25 dB over that same frequency's EFSDL in Click 1. Between Clicks 4 and 35, the dolphin has increased EFSDL by 10 dB in the 293 kHz beam and steered narrow, high frequency transmitting beams more than 8° in elevation in less than 250 ms.

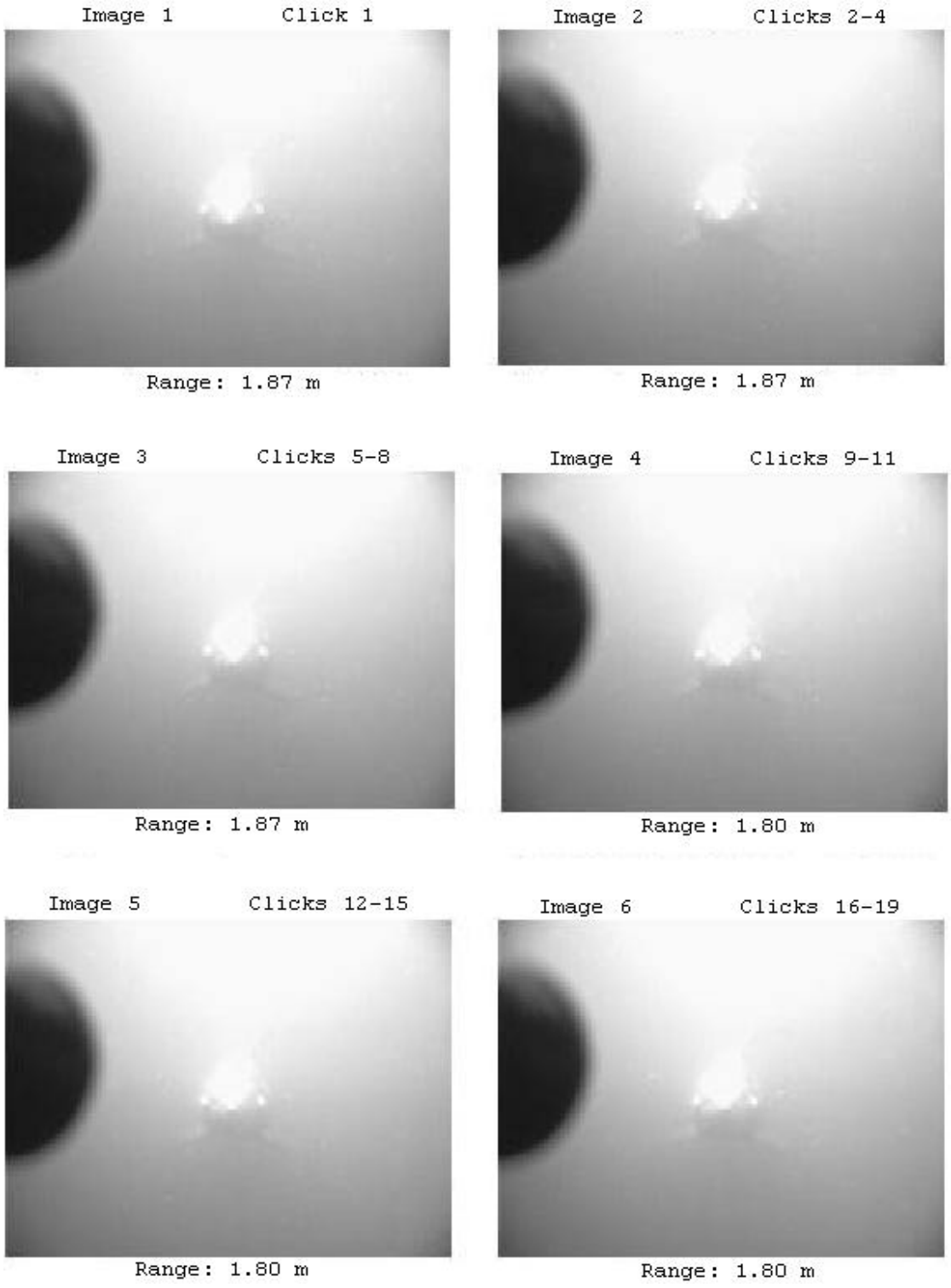

Figure 49. Trial Run 1-14 images 1 through 6

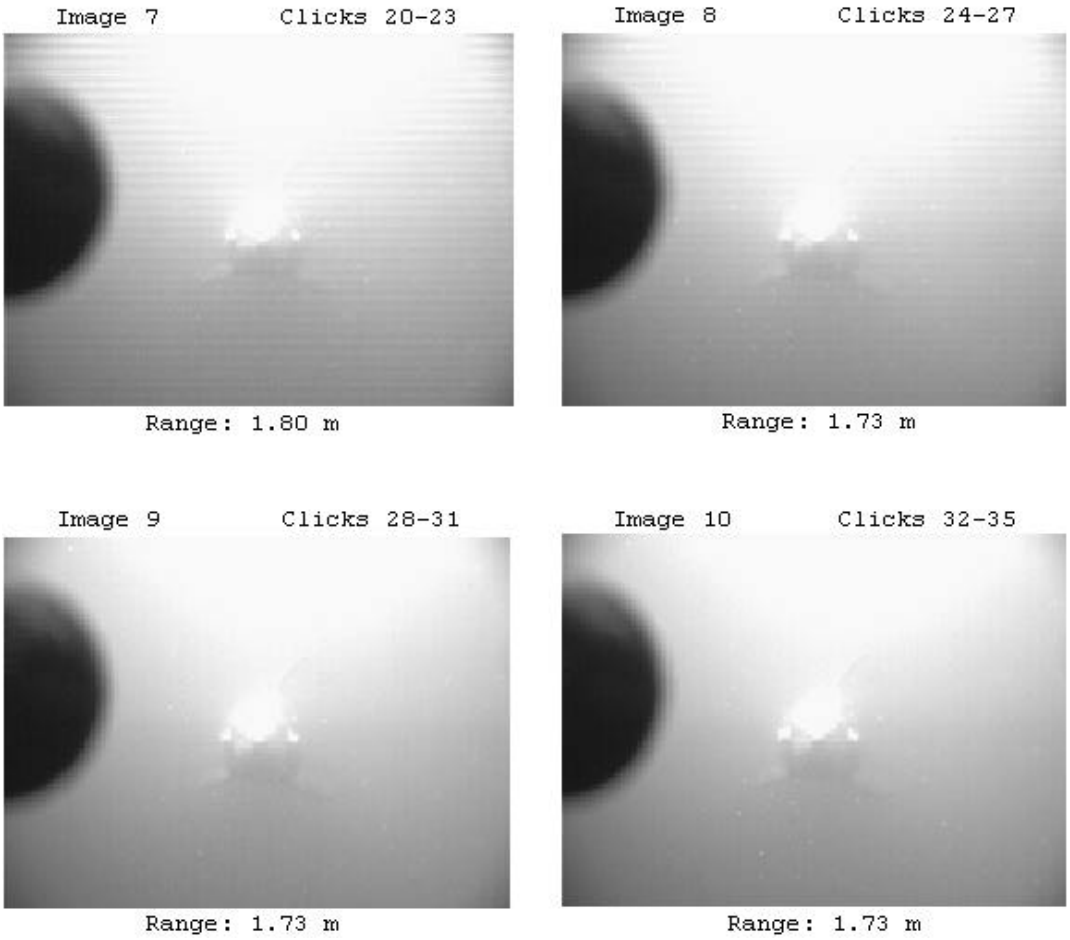

Figure 50. Trial Run 1-14 images 7 through 10.

Experiments have shown dolphins can steer their transmitting beams by moving only their melon and not their head.[Ref. 11] It is not discernable from images in the present experiment whether “Nemo” moved his head while scanning the hydrophone array or simply used his melon to steer his transmitting beams. Since no other research has plotted *Tursiops Truncatus'* high frequency transmitting beam patterns, not much is known about this field of research.

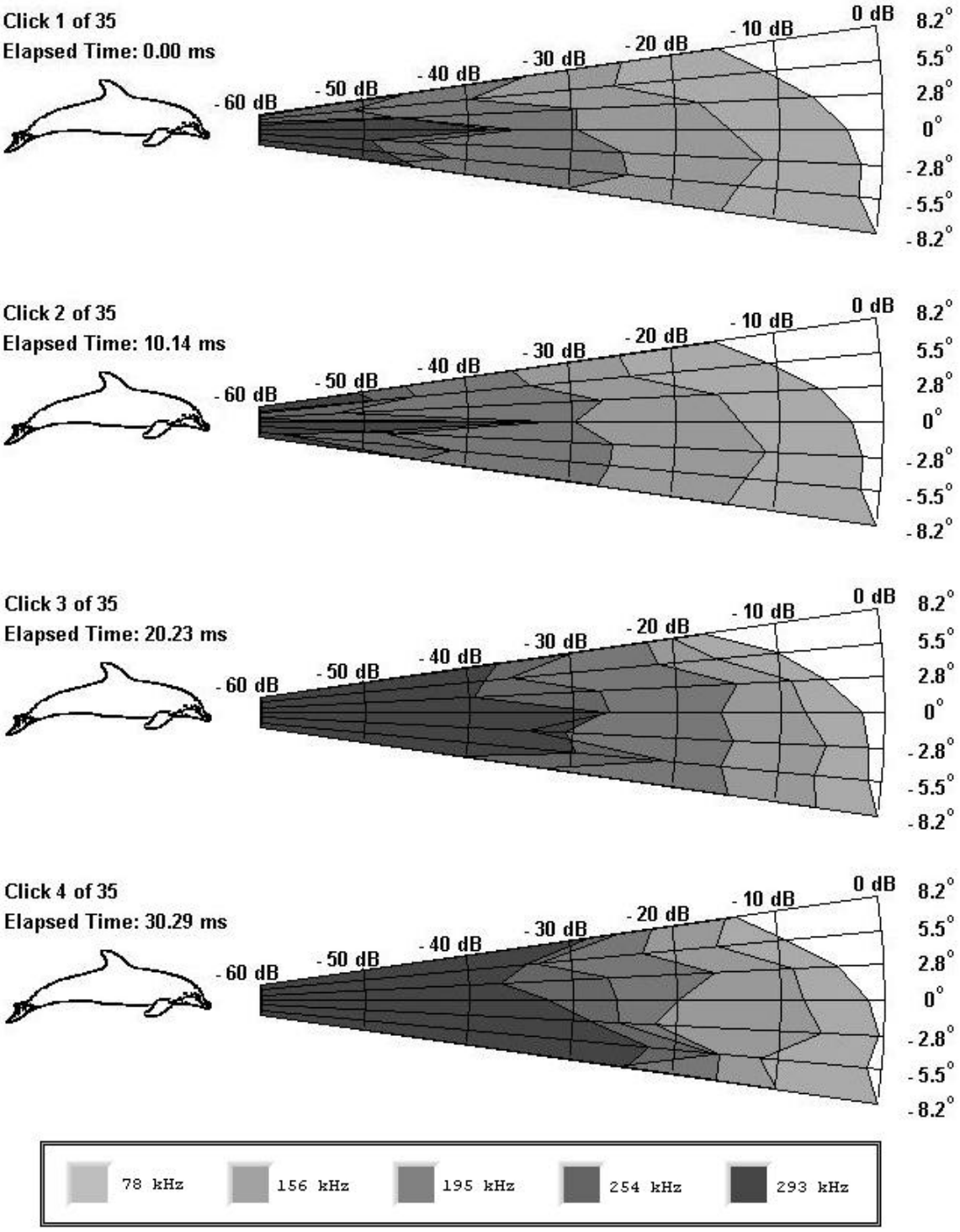

Figure 51. Trial Run 1-14 Clicks 1 through 4.

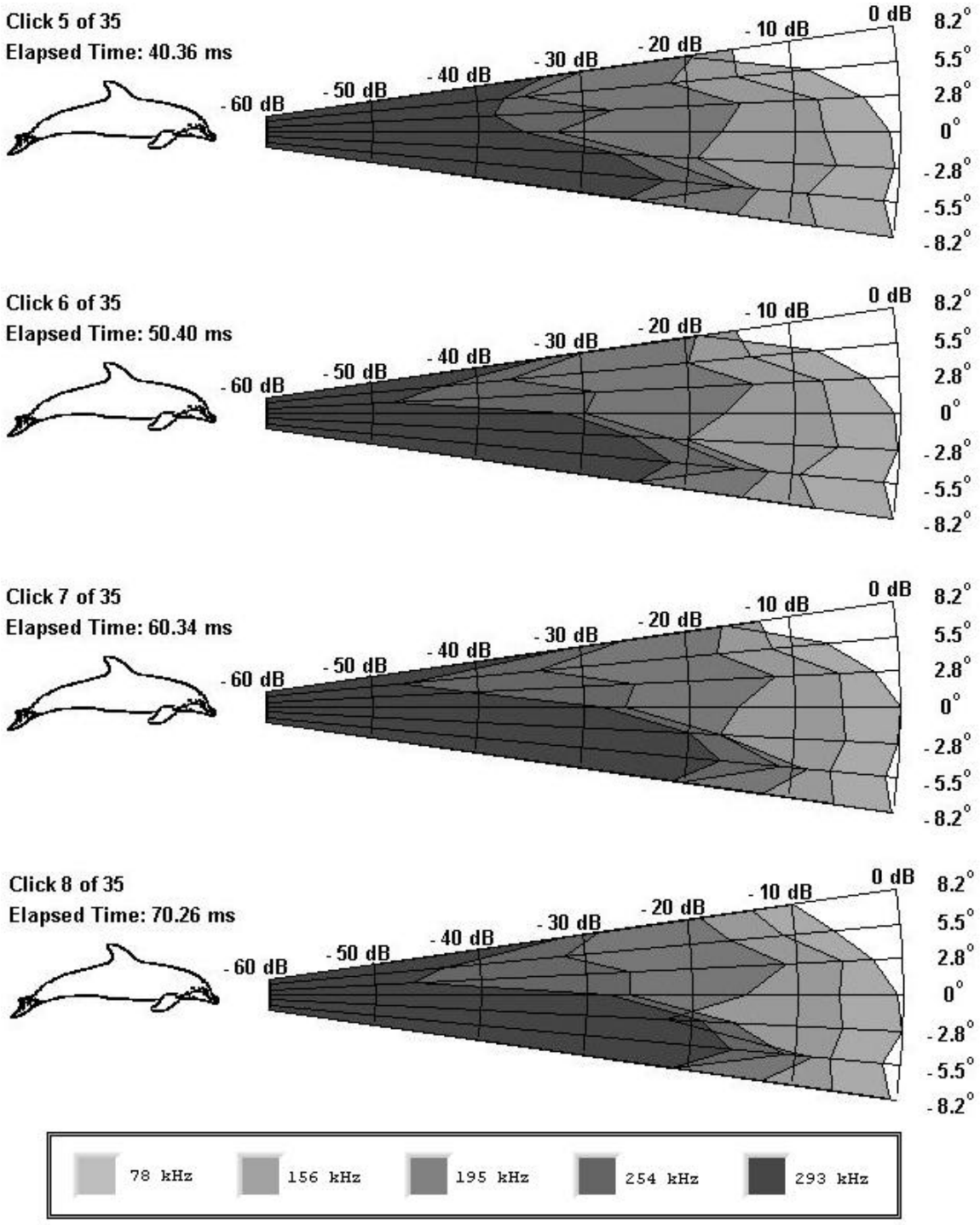

Figure 52. Trial Run 1-14 Clicks 5 through 8.

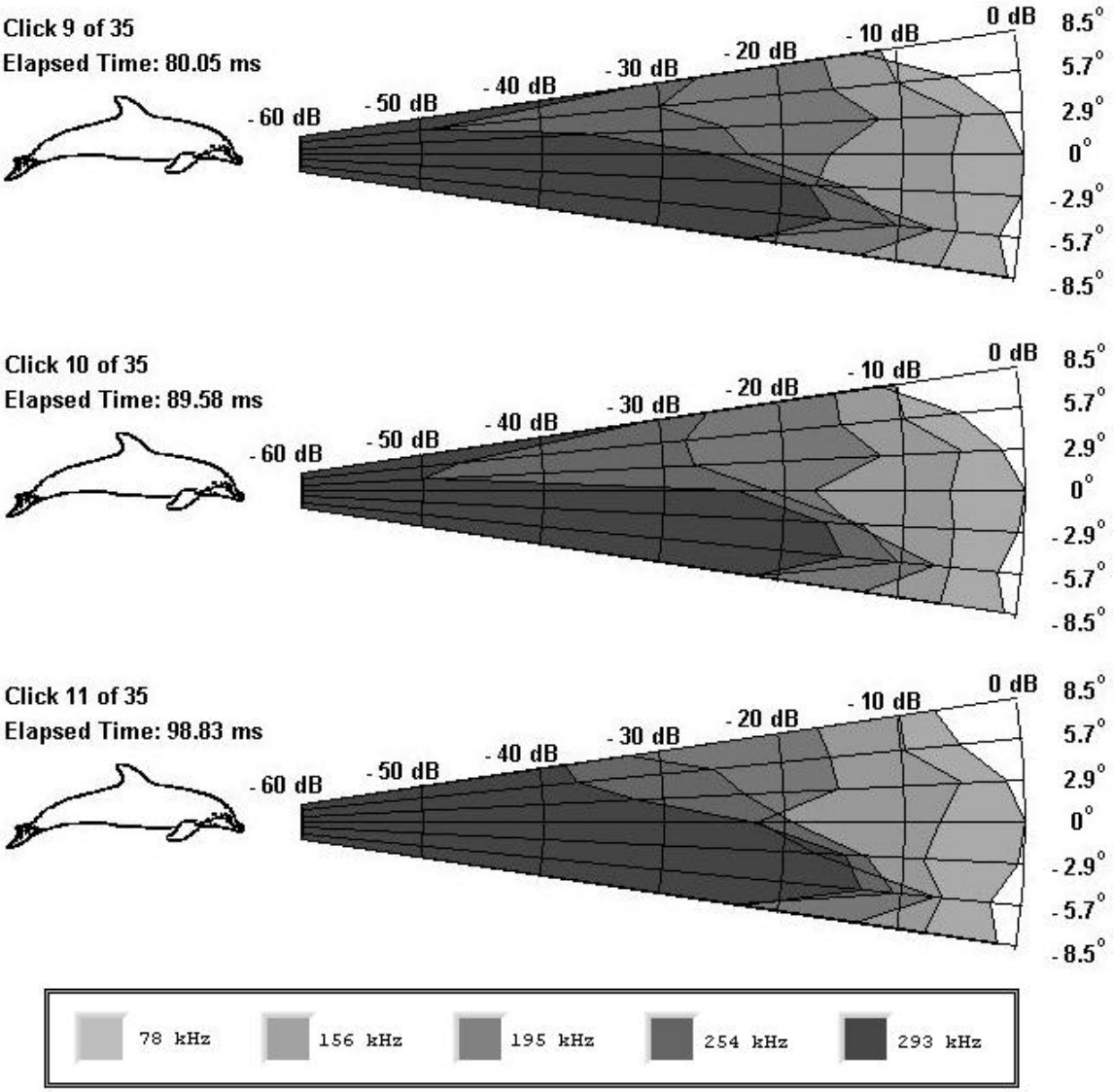

Figure 53. Trial Run 1-14 Clicks 9 through 11.

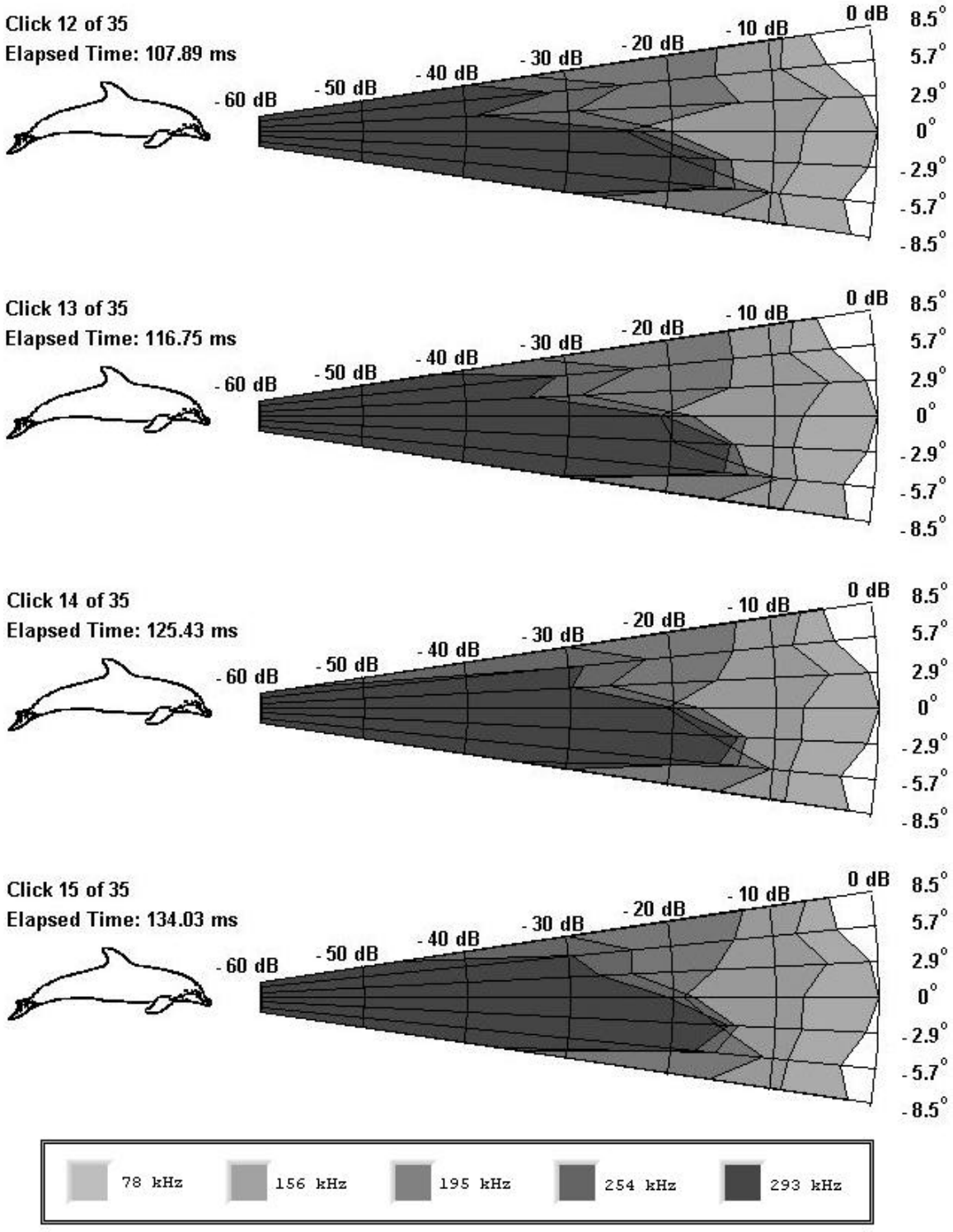

Figure 54. Trial Run 1-14 Clicks 12 through 15.

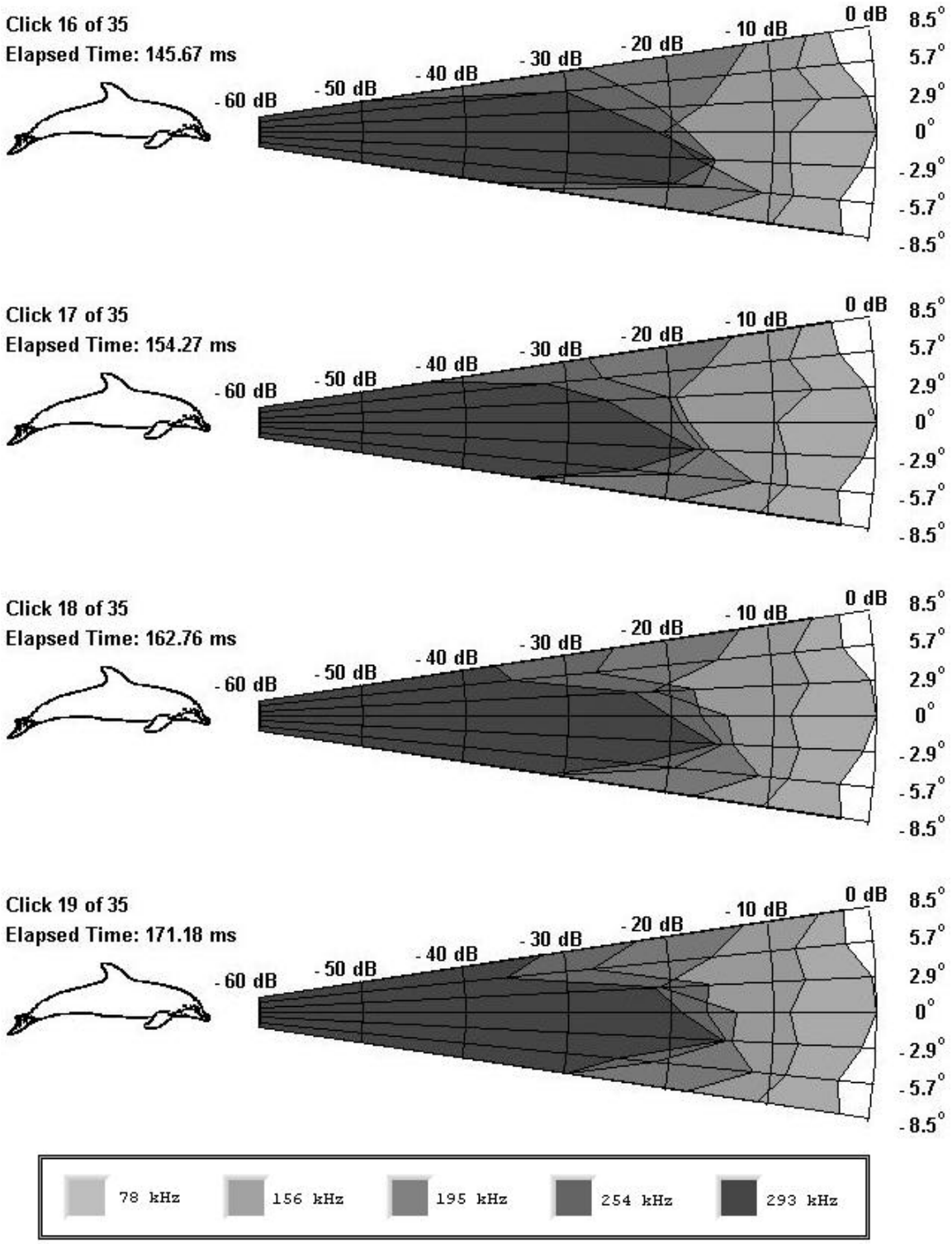

Figure 55. Trial Run 1-14 Clicks 16 through 19.

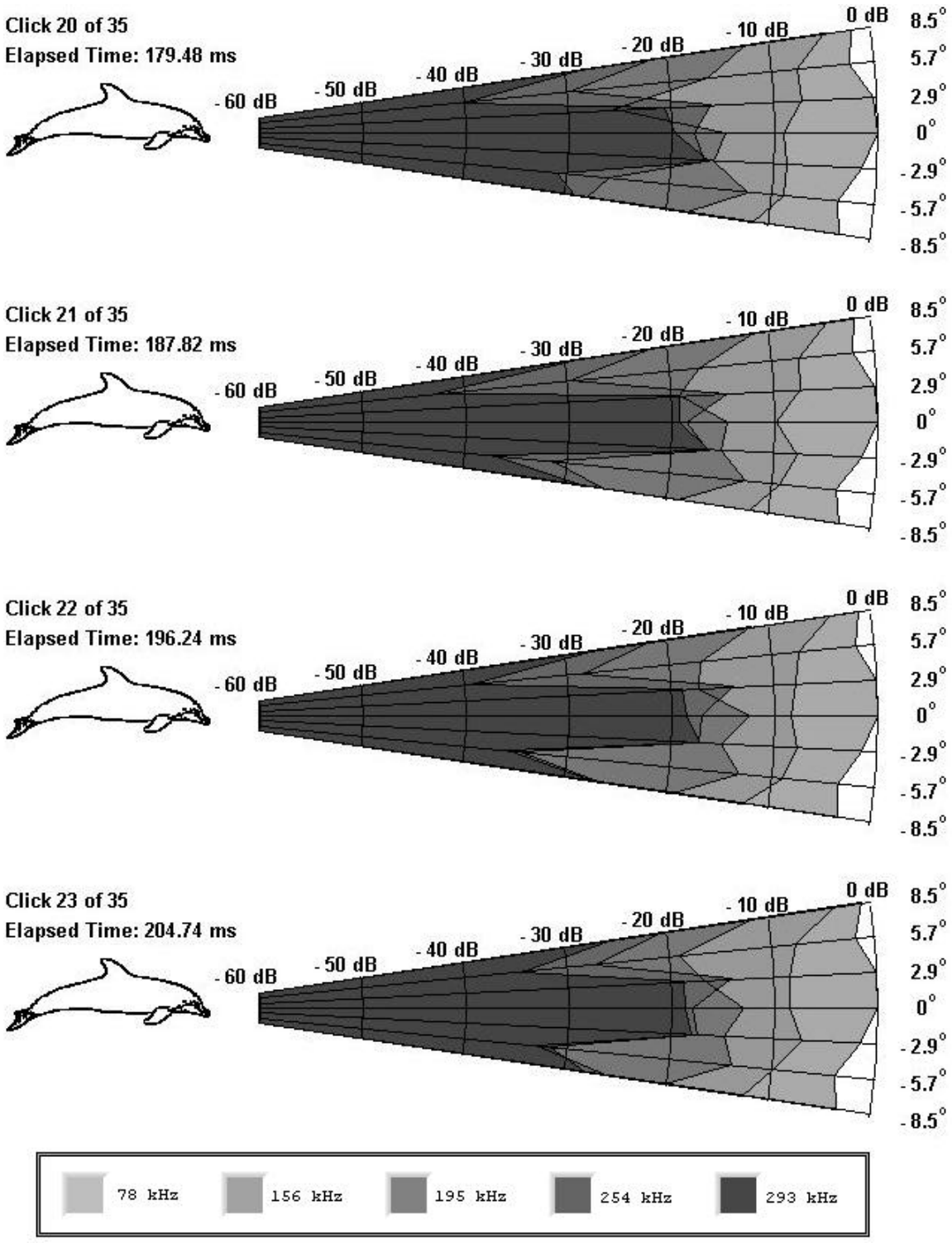

Figure 56. Trial Run 1-14 Clicks 20 through 23.

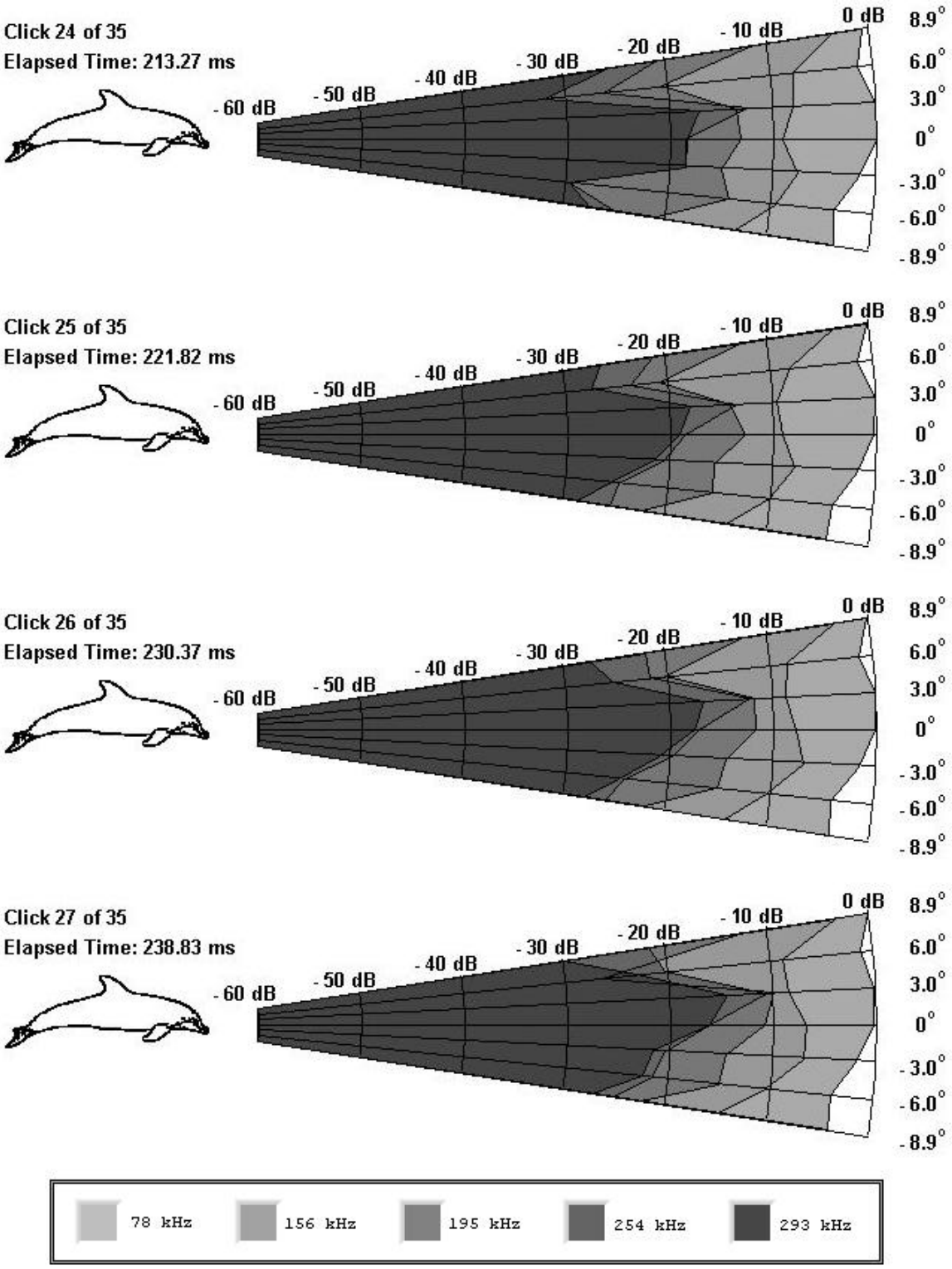

Figure 57. Trial Run 1-14 Clicks 24 through 27.

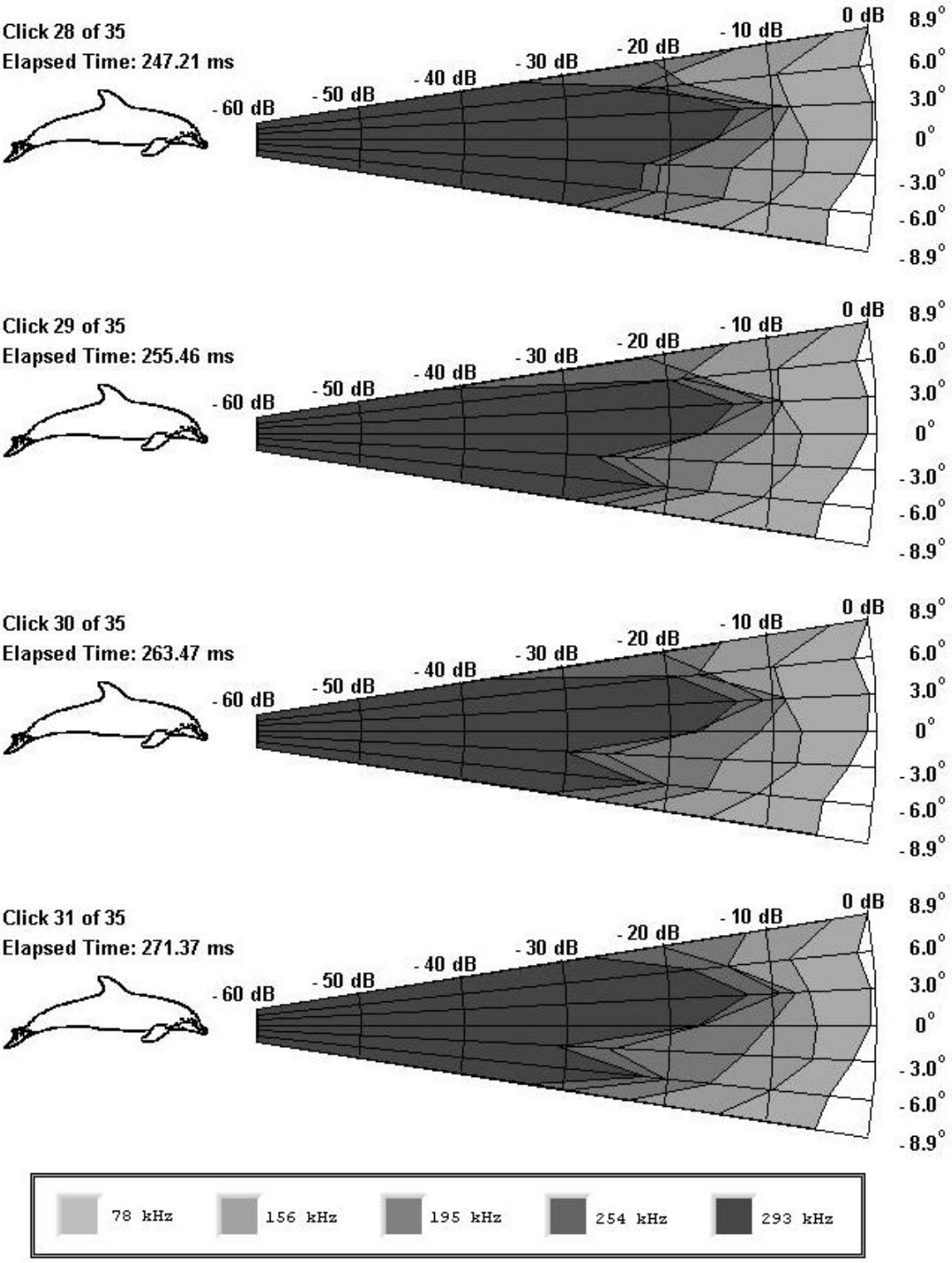

Figure 58. Trial Run 1-14 Clicks 28 through 31.

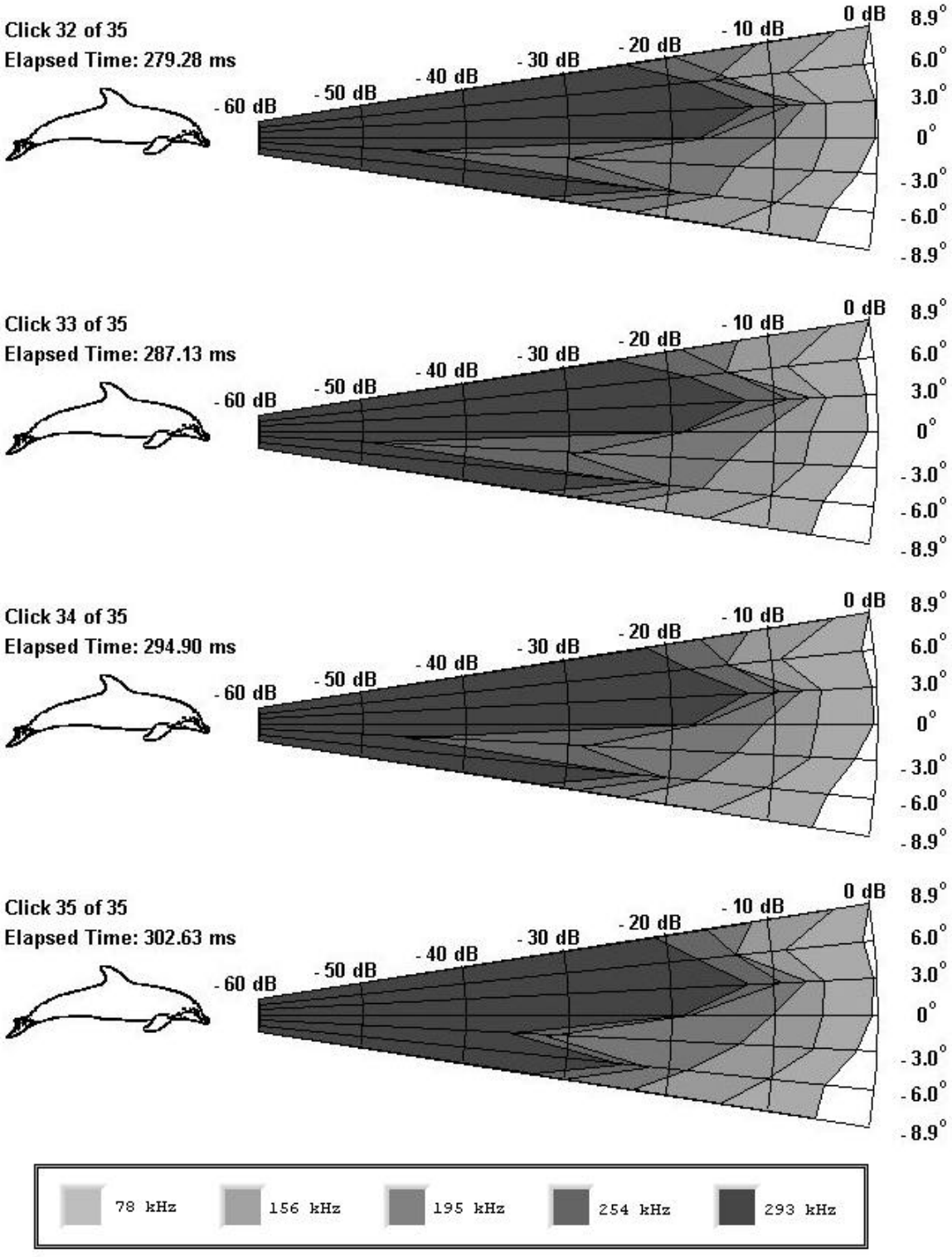

Figure 59. Trial Run 1-14 Clicks 32 through 35.

These plots clearly illustrated the inverse relationship between emitted frequencies and beam width: as frequency increased, beam width decreased.

The beam pattern plot of Click 8 shows the transmitting beam focused at –5.5° with very little energy concentration at 5.5°. The differences in both wave shape and amplitude, shown in Figure 60, are definite and clearly show how the echolocation click's wave shape contains high frequency components. Notice, the two waveforms have significantly different shapes; the waveform with two distinct negative peaks has greater EFSDLs at the higher frequencies, whereas the waveforms without this shape do not contain the high frequency components to the same degree.

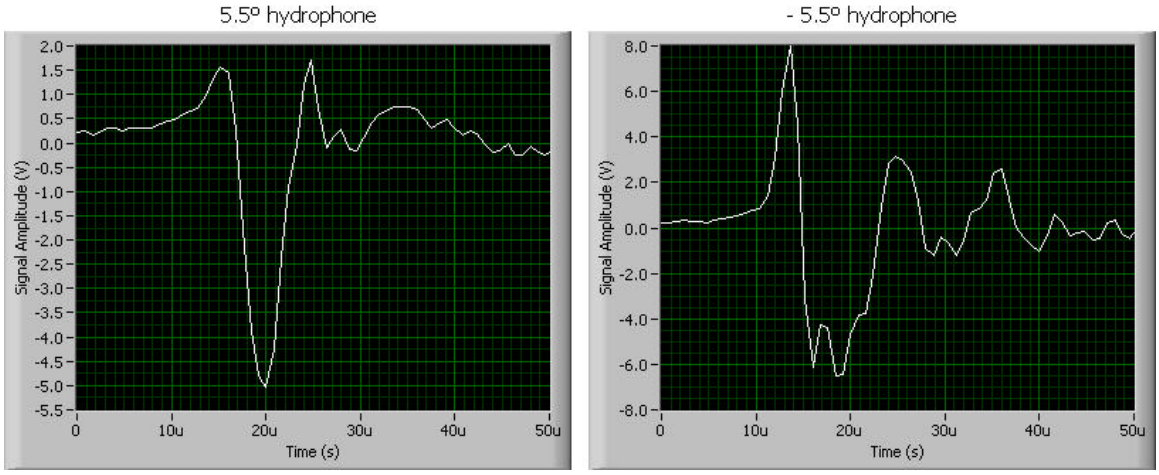

Figure 60. Click 8 received at two different hydrophones during Trial Run 1-14.

By the end of the click train, the dolphin focused his transmitting signal at 3.0°. Figure 61 again shows how the waveforms containing high frequencies (3.0°)

is radically different from that without high frequency components (-3.0°).

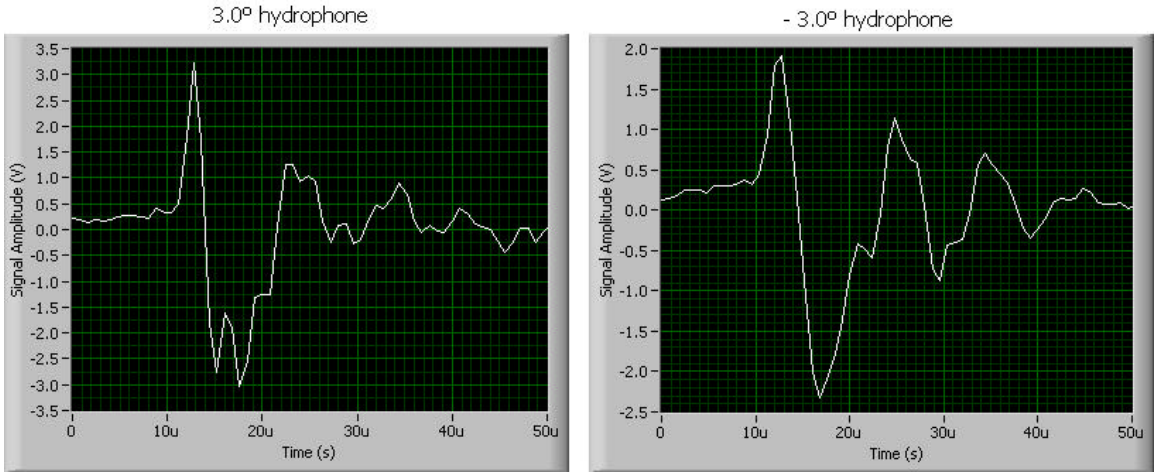

Figure 61. Click 32 received at two different hydrophones during Trial Run 1-14.

b. Trial Run 1-18

23 clicks, shown in Figure 62, and nine images, displayed in Figures 63 and 64, comprise Trial Run 1-18. This was the ninth trial run in the vertical configuration.

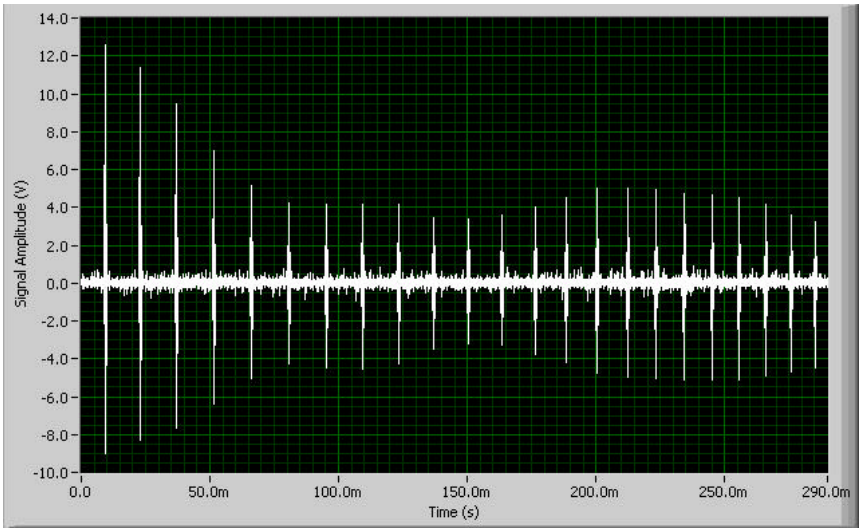

Figure 62. Trial Run 1-18 click train.

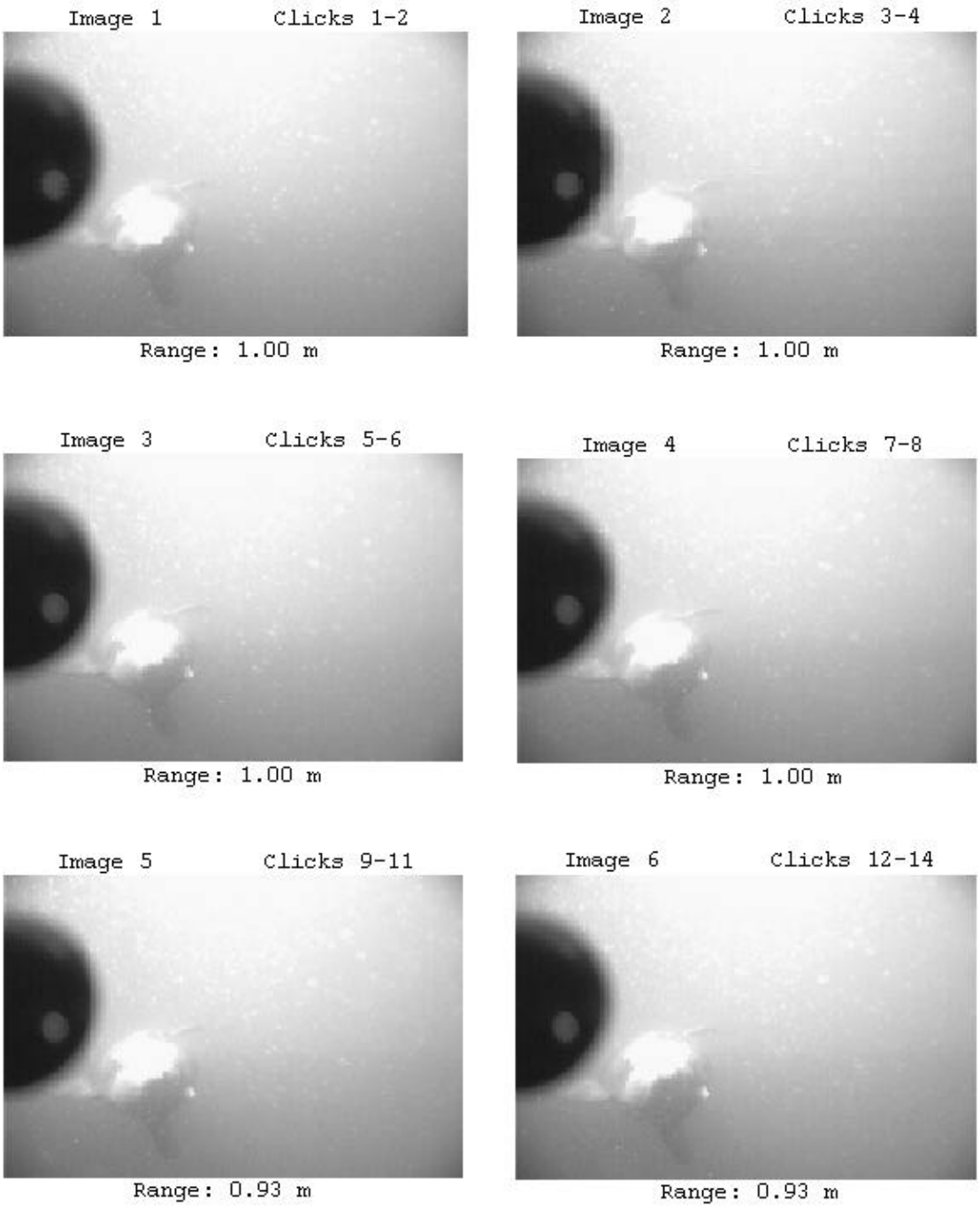

Figure 63. Trial Run 1-18 images 1 through 6.

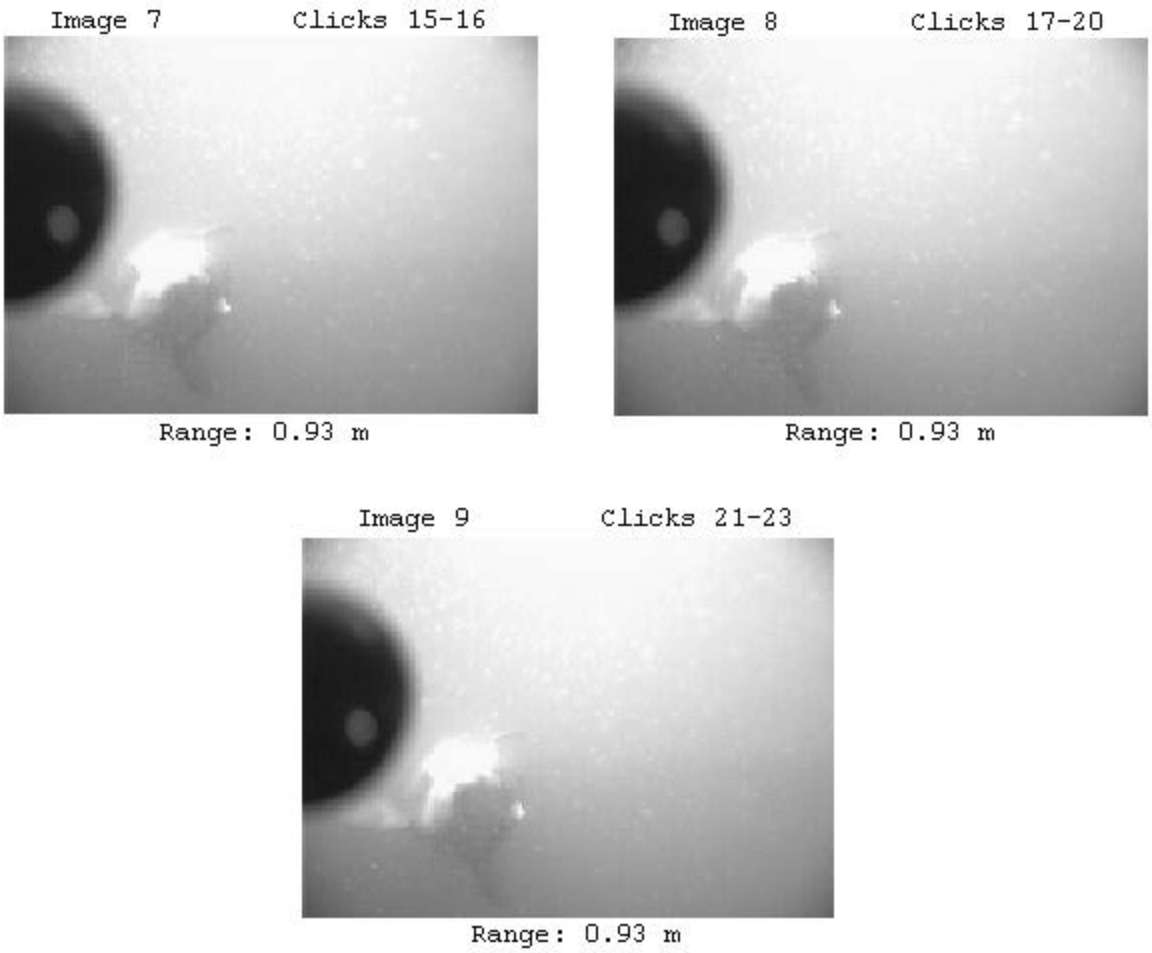

Figure 64. Trial Run 1-18 images 7 through 9.

Although the dolphin has, once again, rolled over to one side, this data set is still considered and analyzed in the vertical plane. Figures 65 to 72 show how the dolphin's sonar signals change over a period of approximately 276 ms. In Click 1, four of the five analyzed frequencies have peak EFSDLs at –10.2°. By Click 23, "Nemo" shifted the focus of his echolocation click to the 16.1° hydrophone. The 293 kHz beam focused somewhere between the 16.1° hydrophone and the 10.9° hydrophone.

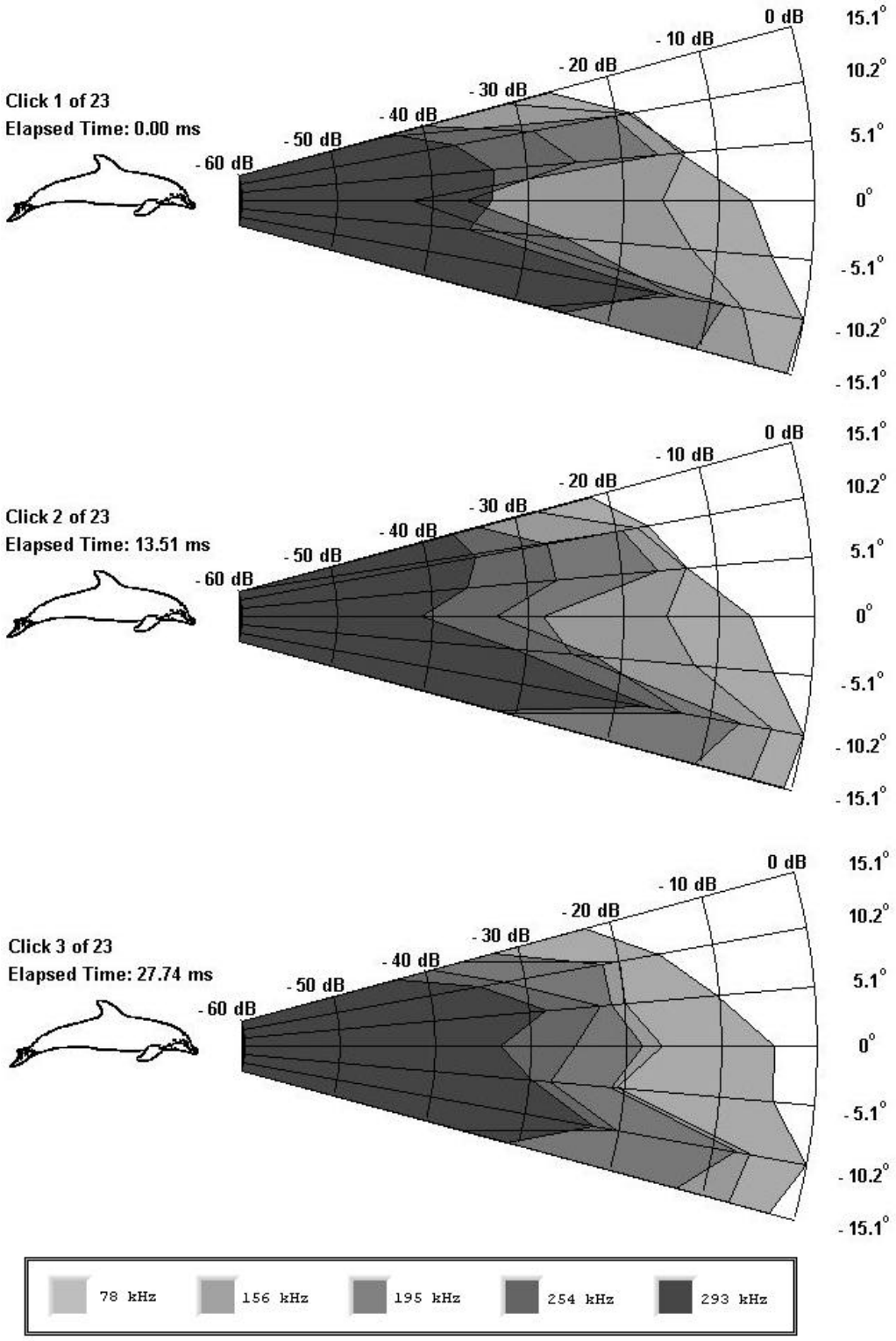

Figure 65. Trial Run 1-18 Clicks 1 through 3.

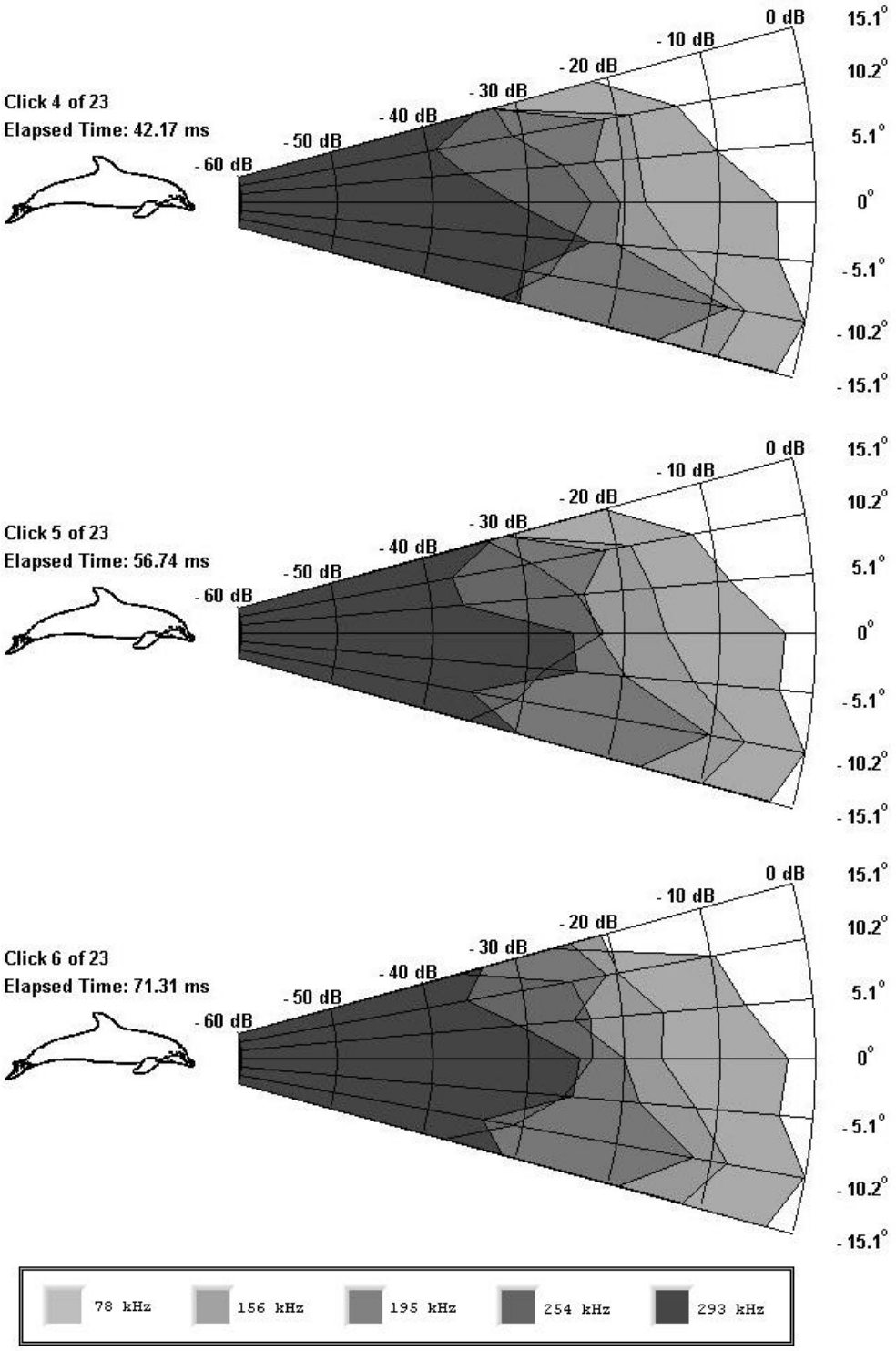

Figure 66. Trial Run 1-18 Clicks 4 through 6.

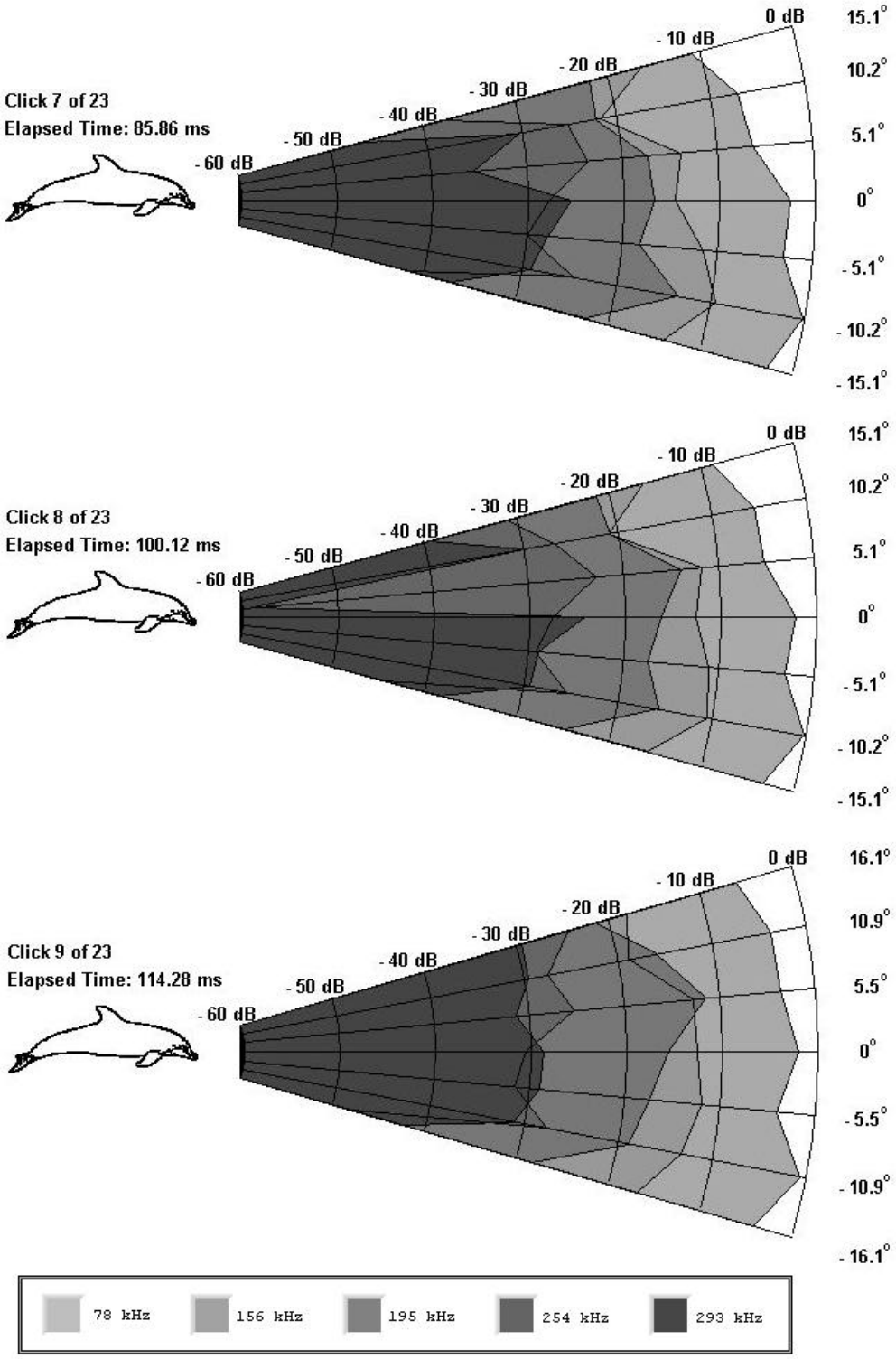

Figure 67. Trial Run 1-18 Clicks 7 through 9.

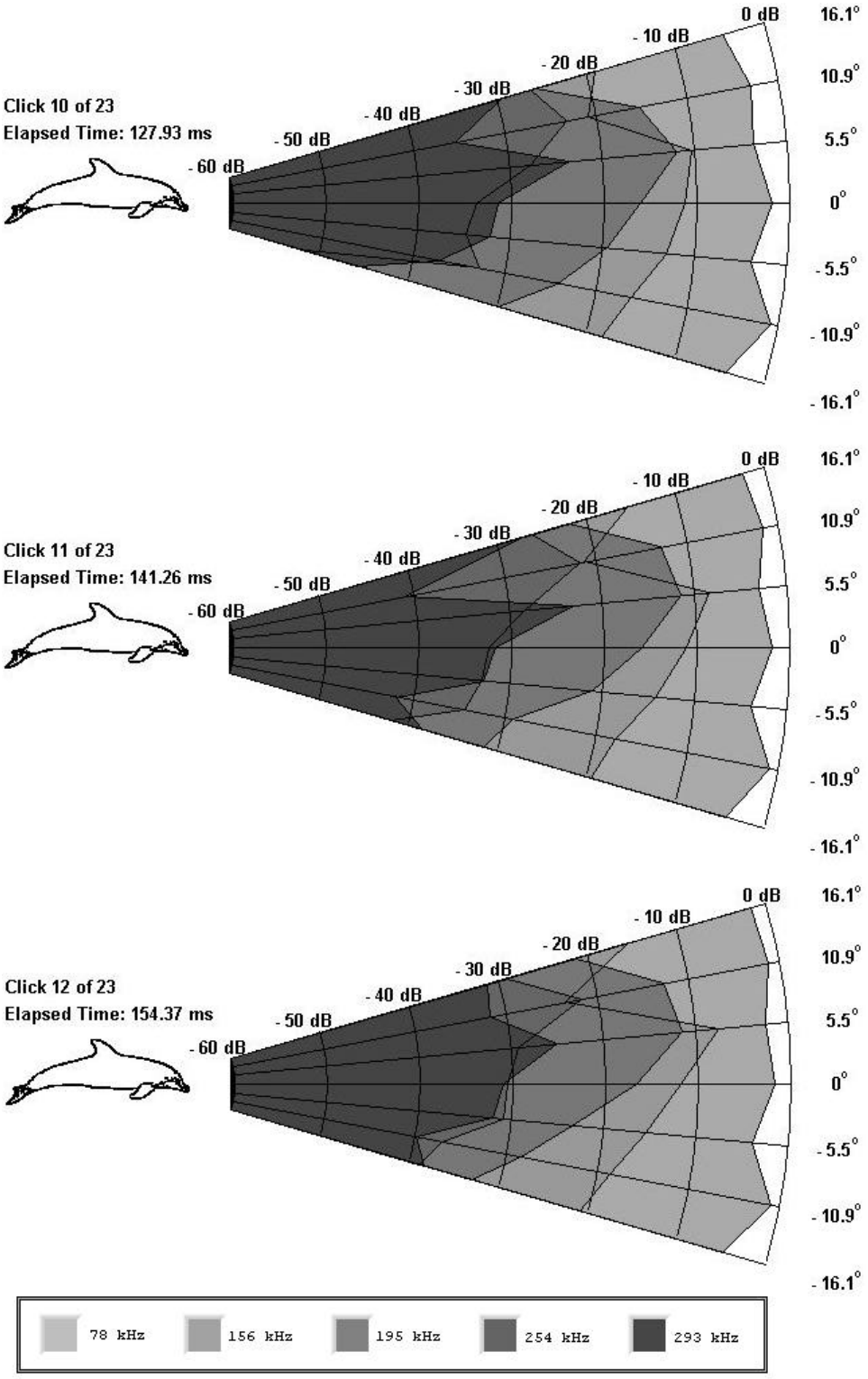

Figure 68. Trial Run 1-18 Clicks 10 through 12.

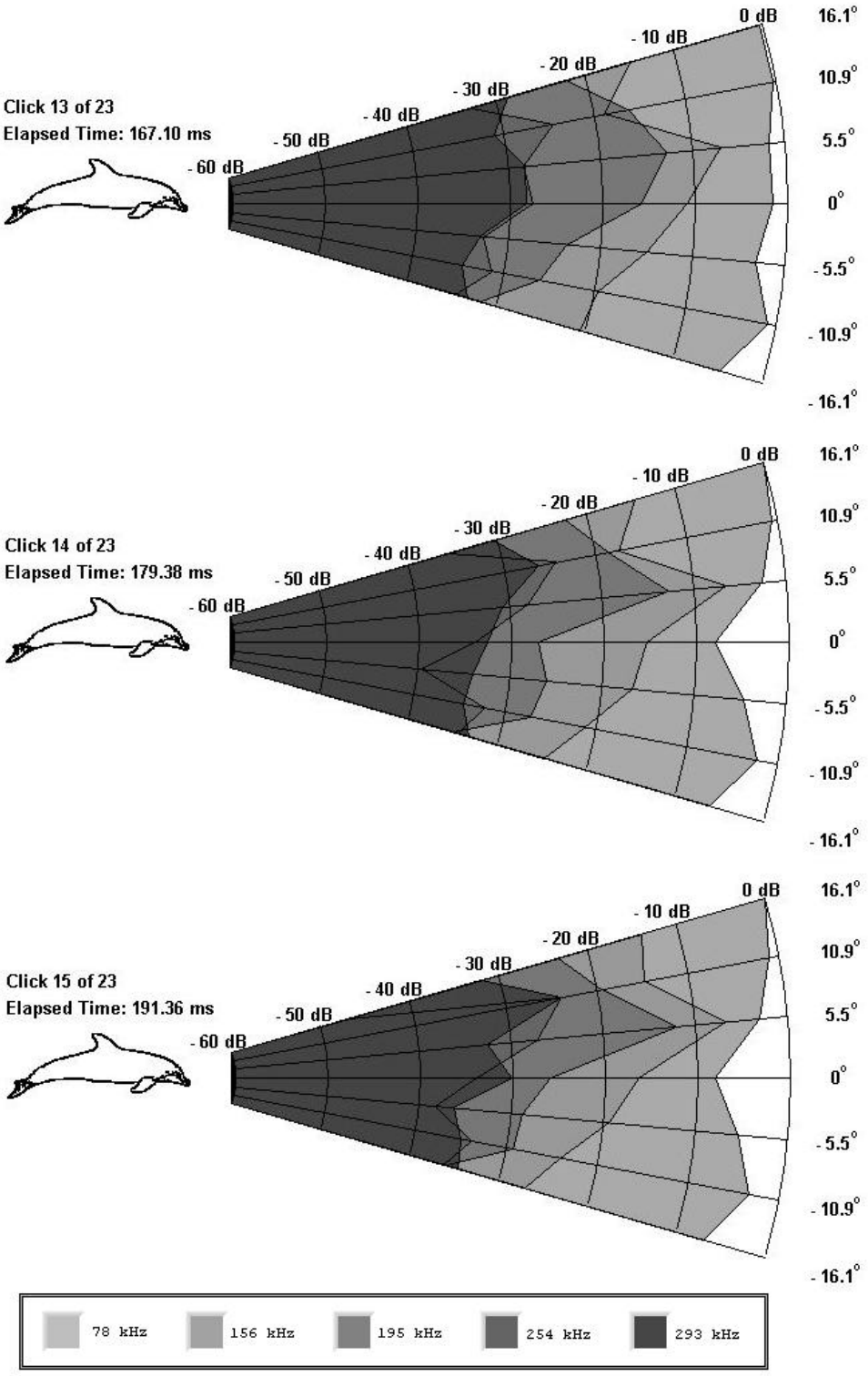

Figure 69. Trial Run 1-18 Clicks 13 through 15.

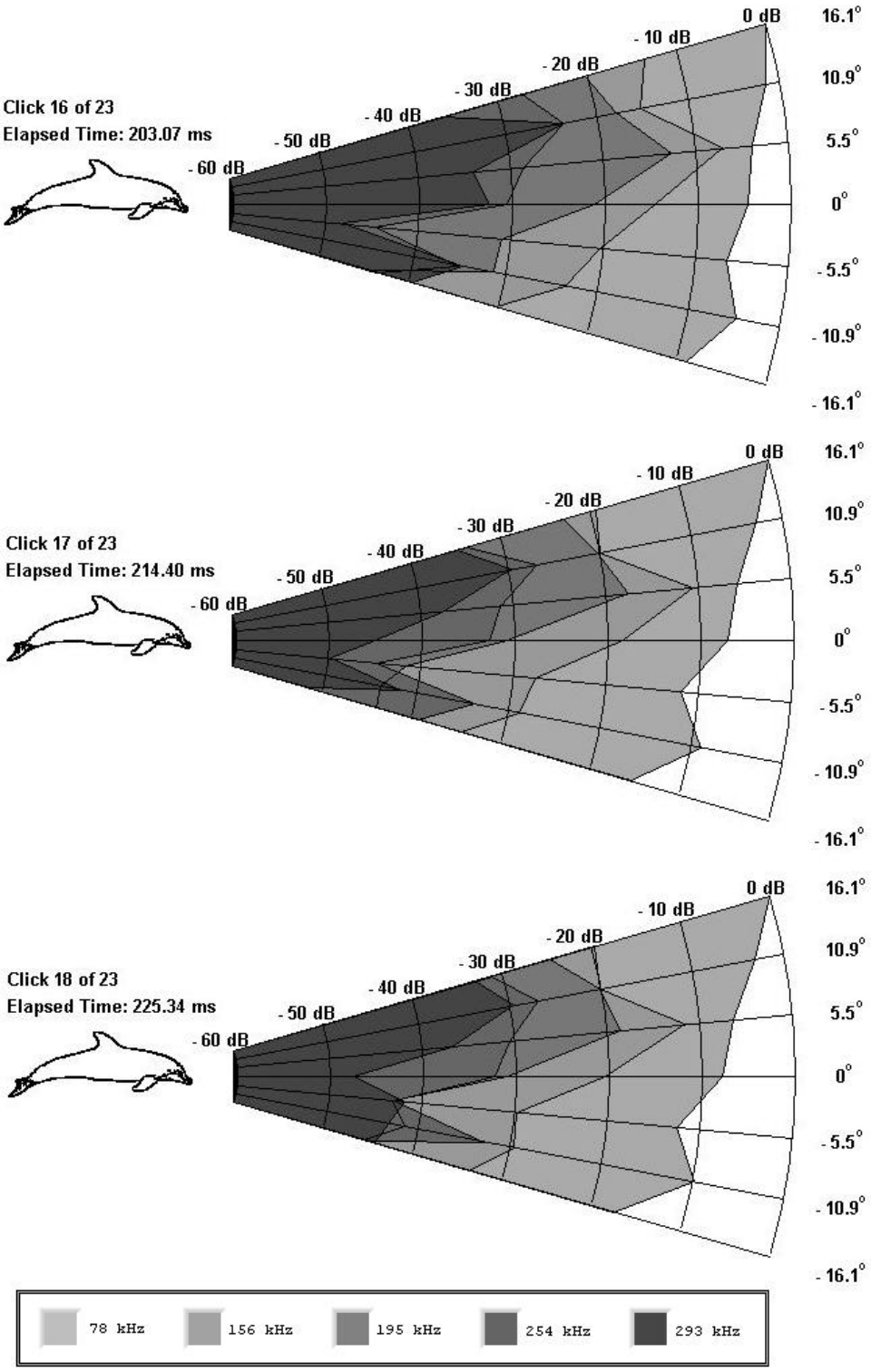

Figure 70. Trial Run 1-18 Clicks 16 through 18.

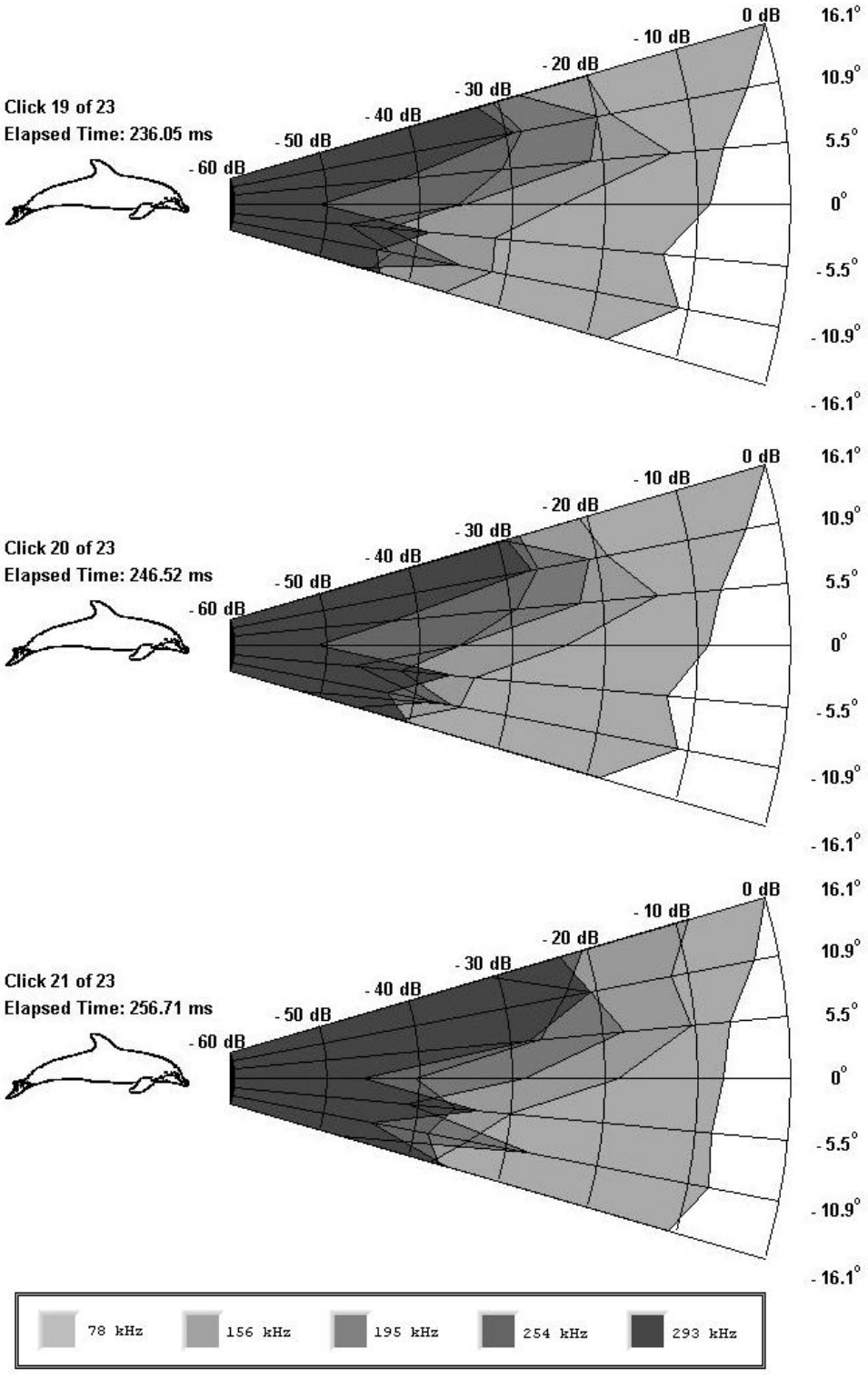

Figure 71. Trial Run 1-18 Clicks 19 through 21.

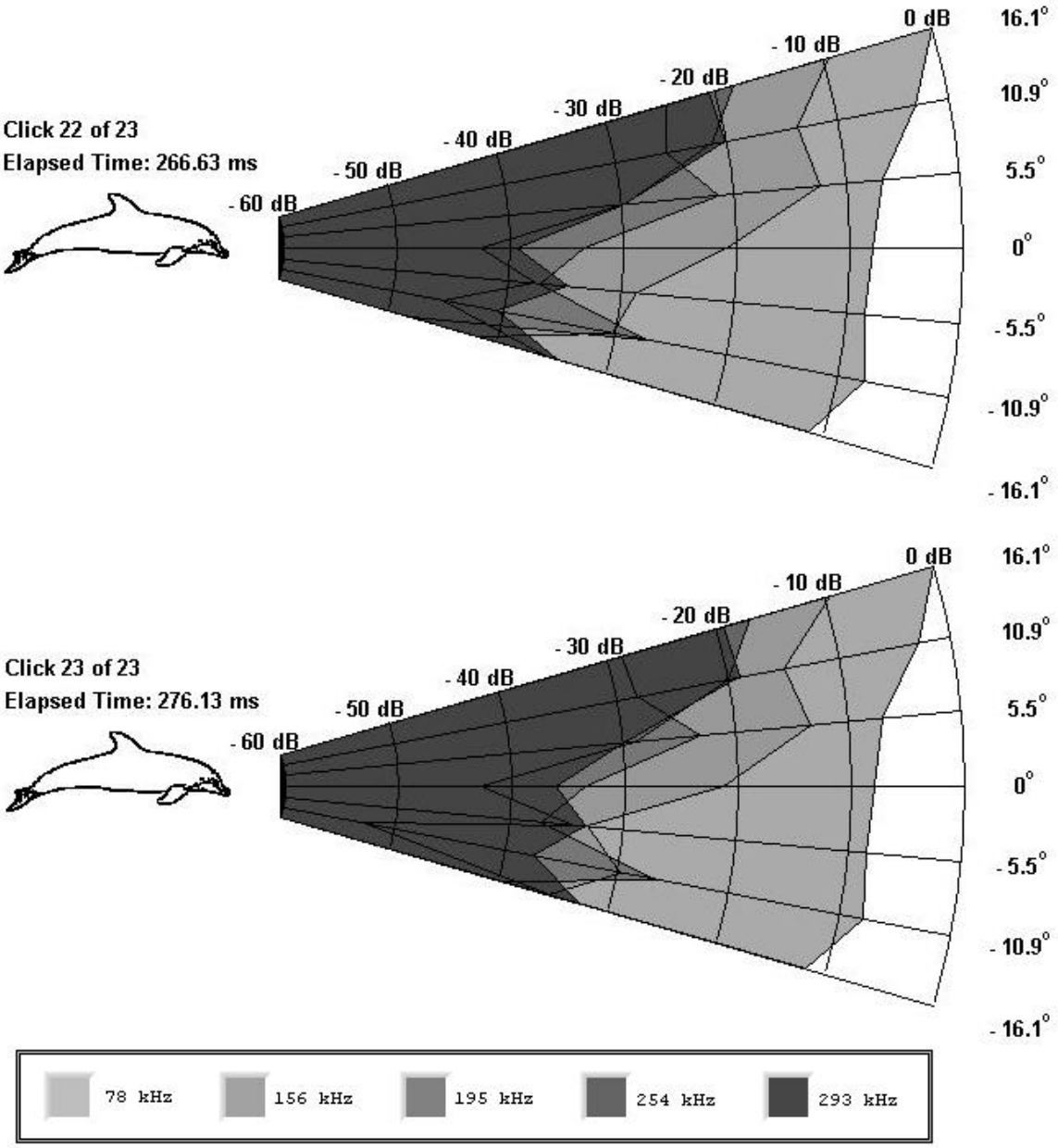

Figure 72. Trial Run 1-18 Clicks 22 and 23.

Figure 73 shows a comparison of Click 1 received at two different hydrophones. In this click, “Nemo” focused his sonar signal on the -10.2° hydrophone; the peak amplitude is more than ten times greater than the peak

amplitude seen at the 10.2° hydrophone, where the EFSDL at 293 kHz is practically 20 dB lower than the 293 kHz EFSDL at -10.2°. Again, it is observed that the waveform containing high frequencies had two negative peaks in a single cycle, whereas the signal received at 10.2° had a single peak and no significant EFSDLs at the higher frequencies.

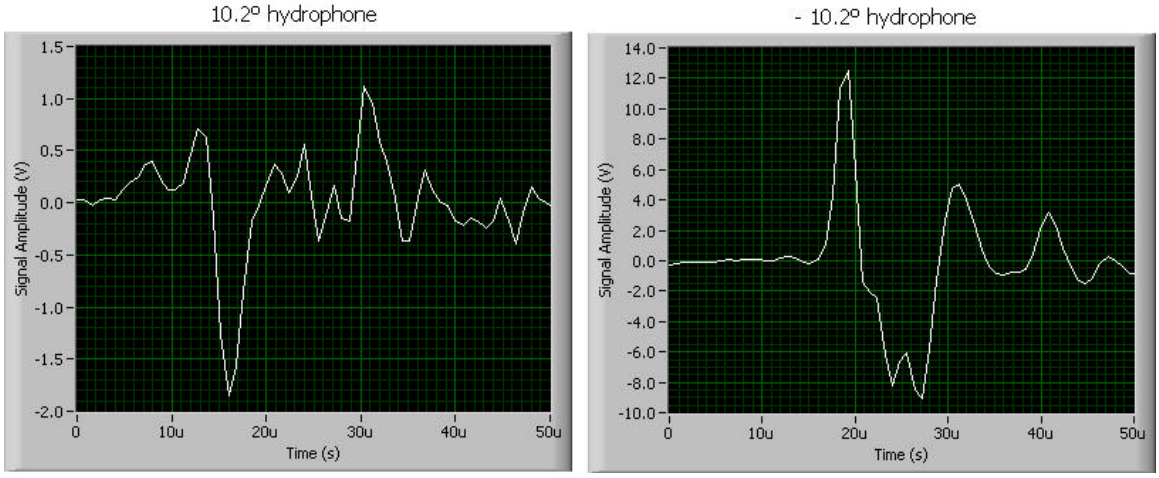

Figure 73. Click 1 received at two different hydrophones during Trial Run 1-18.

Figure 74 shows two signals from Click 18 where the 293 kHz beam is focused at 10.9°, more than 10 dB higher than that received at –10.9°. Additionally, the 293 kHz beam is 30 dB lower than the signal's peak EFSDL at 78 kHz.

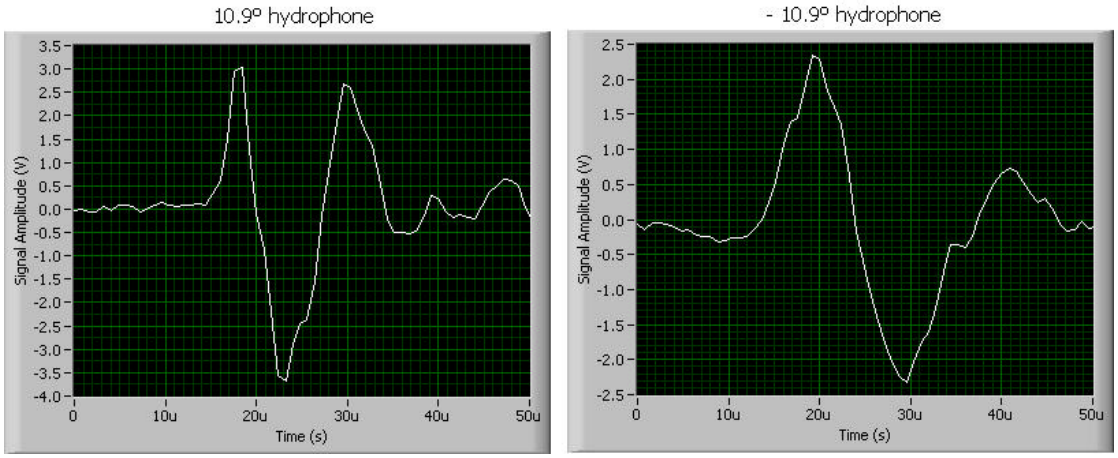

Figure 74. Click 18 received at two different hydrophones during Trial Run 1-18.

Figure 75 shows two signals from Click 23. Just as in Click 18, there is not a tremendous difference between the peak amplitudes in the two signals, however the 293 kHz component is less than 20 dB lower than the peak EFSDL (78 kHz). This difference between the 78 kHz component and the 293 kHz beam decreased by 10 dB between Clicks 18 and 23.

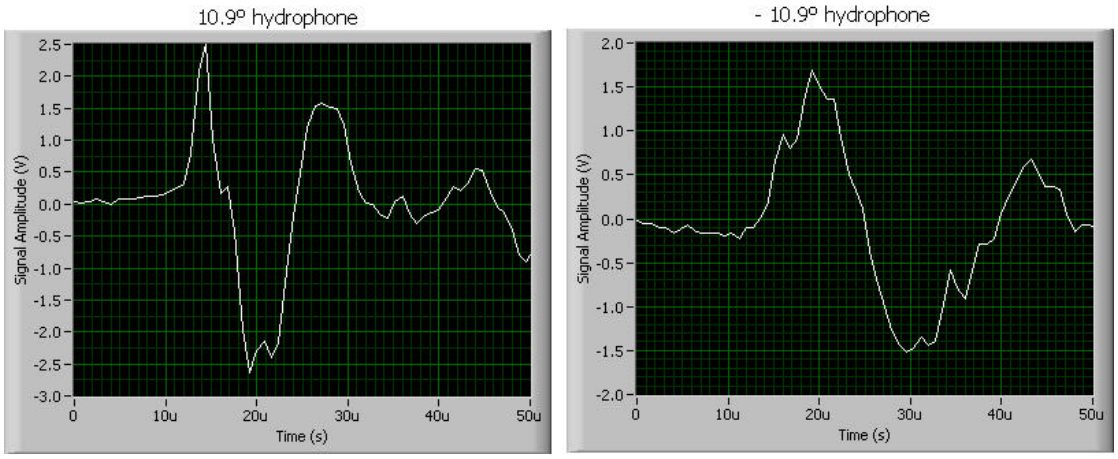

Figure 75. Click 23 received at two different hydrophones during Trial Run 1-18.

c. Trial Run 4-2

Trial Run 4-2 was the second trial run recorded on the final day of the experiment. Figure 76 shows the click train's 38 clicks with an additional click from "Old Ben", a dolphin in the adjacent pen. The first image in Figure 77 and 78 show “Nemo” almost completely rolled over to one side. In this trial run, noise was injected into the water in an effort to test the dolphin’s sonar capability. The resulting transmitting beam patterns are plotted in Figures 79 to 91.

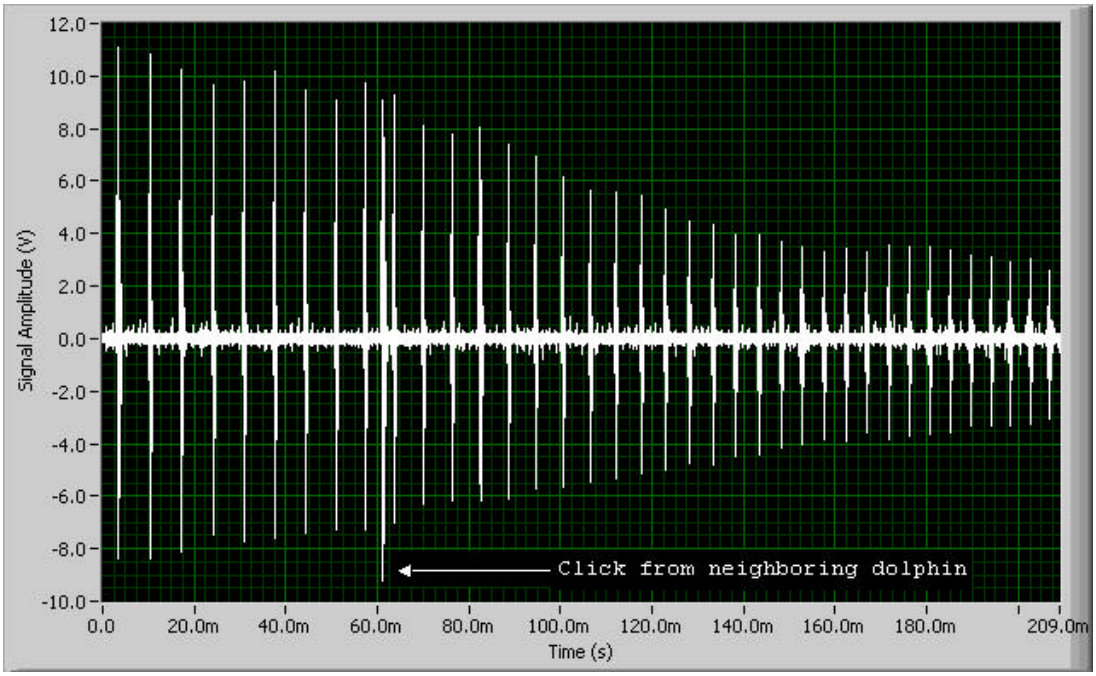

Figure 76. Trial Run 4-2 click train.

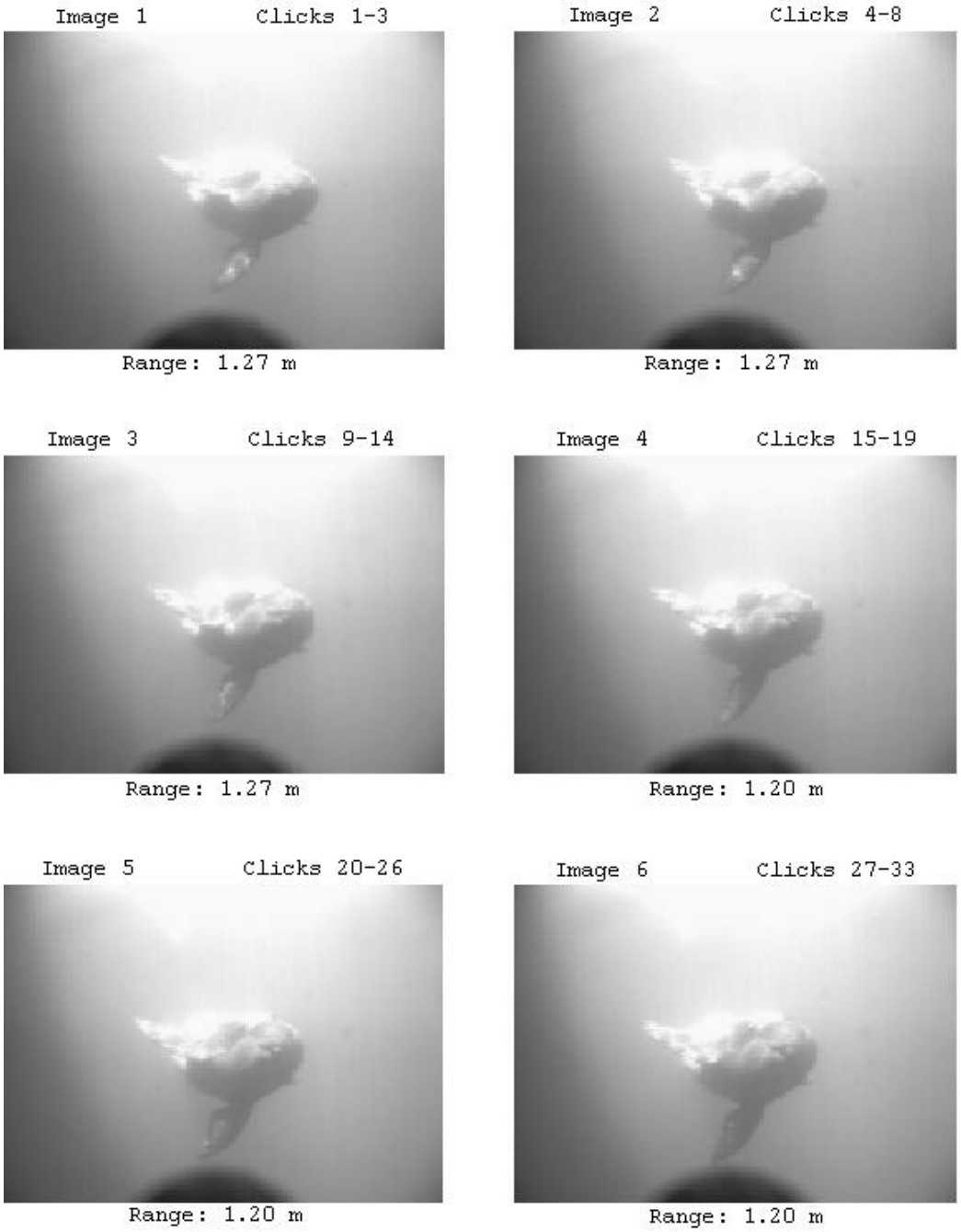

Figure 77. Trial Run 4-2 images 1 through 6.

Figure 78. Trial Run 4-2 image 7.

Throughout most of the click train, “Nemo” aimed his transmitting beam on the 4.3° hydrophone. At no time during the click train does the EFSDL at 293 kHz decrease more than 20 dB from the click's peak EFSDL. This trial run is an excellent example of how the dolphin focused narrow, high frequency beams to echolocate the target, in the presence of low frequency masking noise.

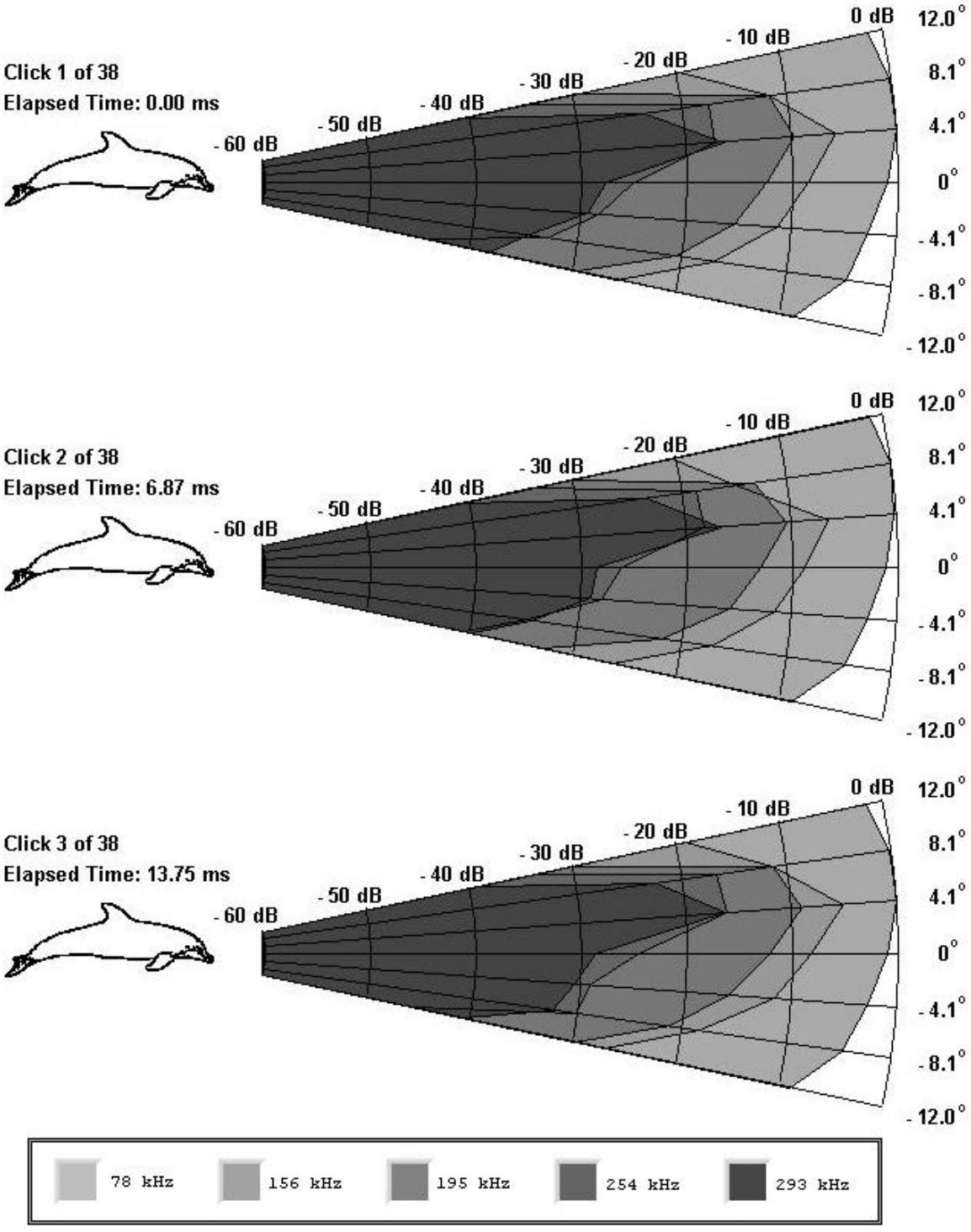

Figure 79. Trial Run 4-2 Clicks 1 through 3.

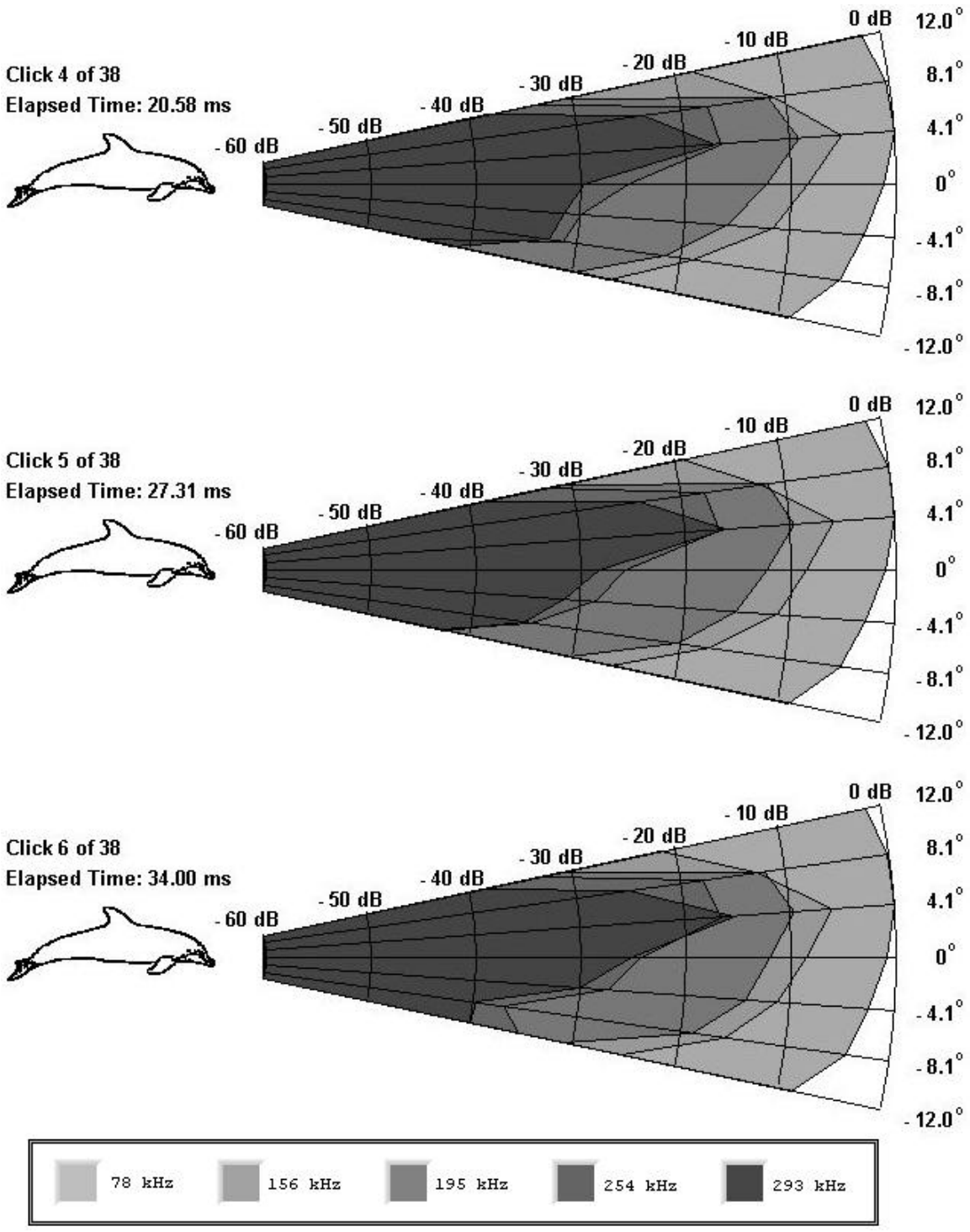

Figure 80. Trial Run 4-2 Clicks 4 through 6.

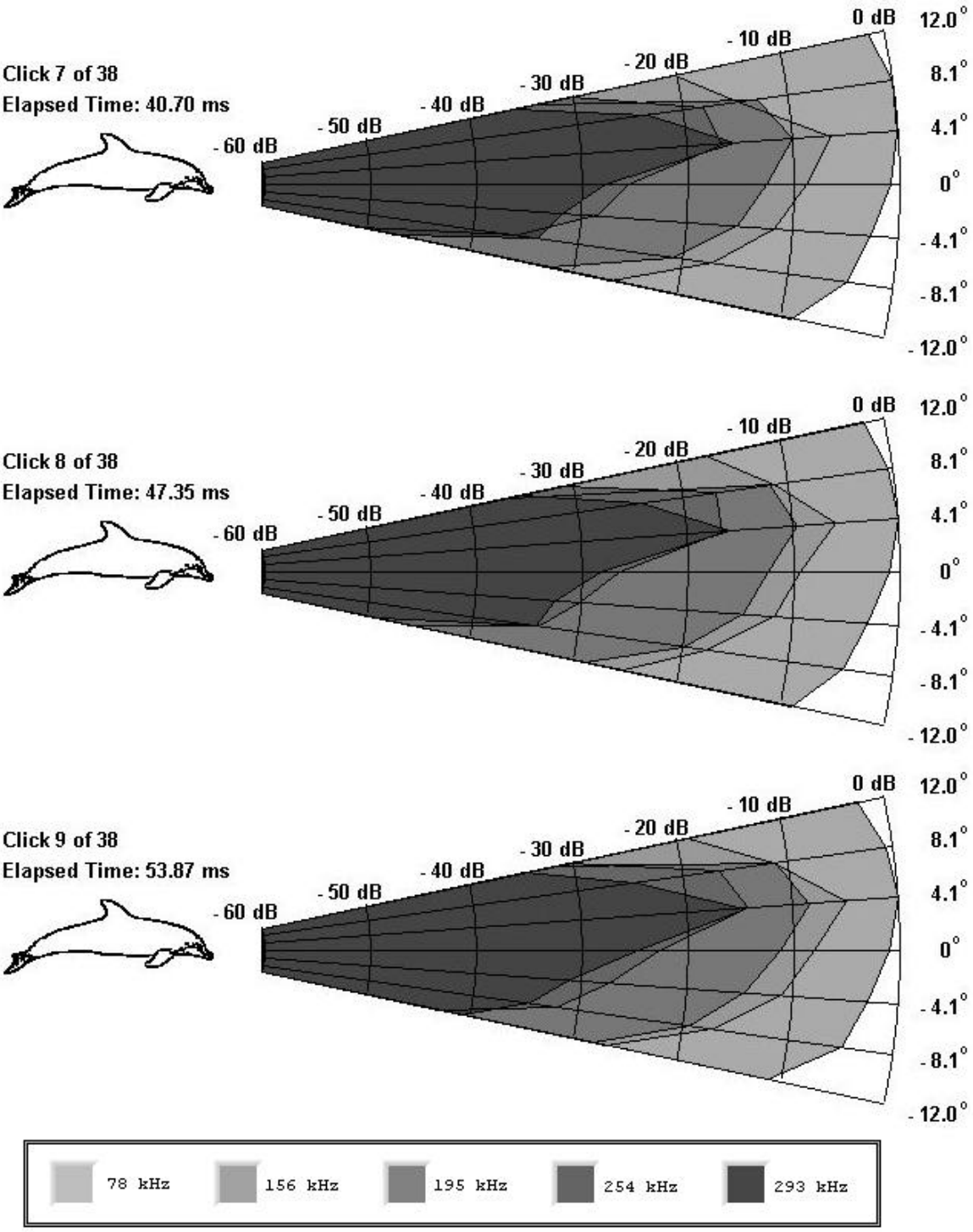

Figure 81. Trial Run 4-2 Clicks 7 through 9.

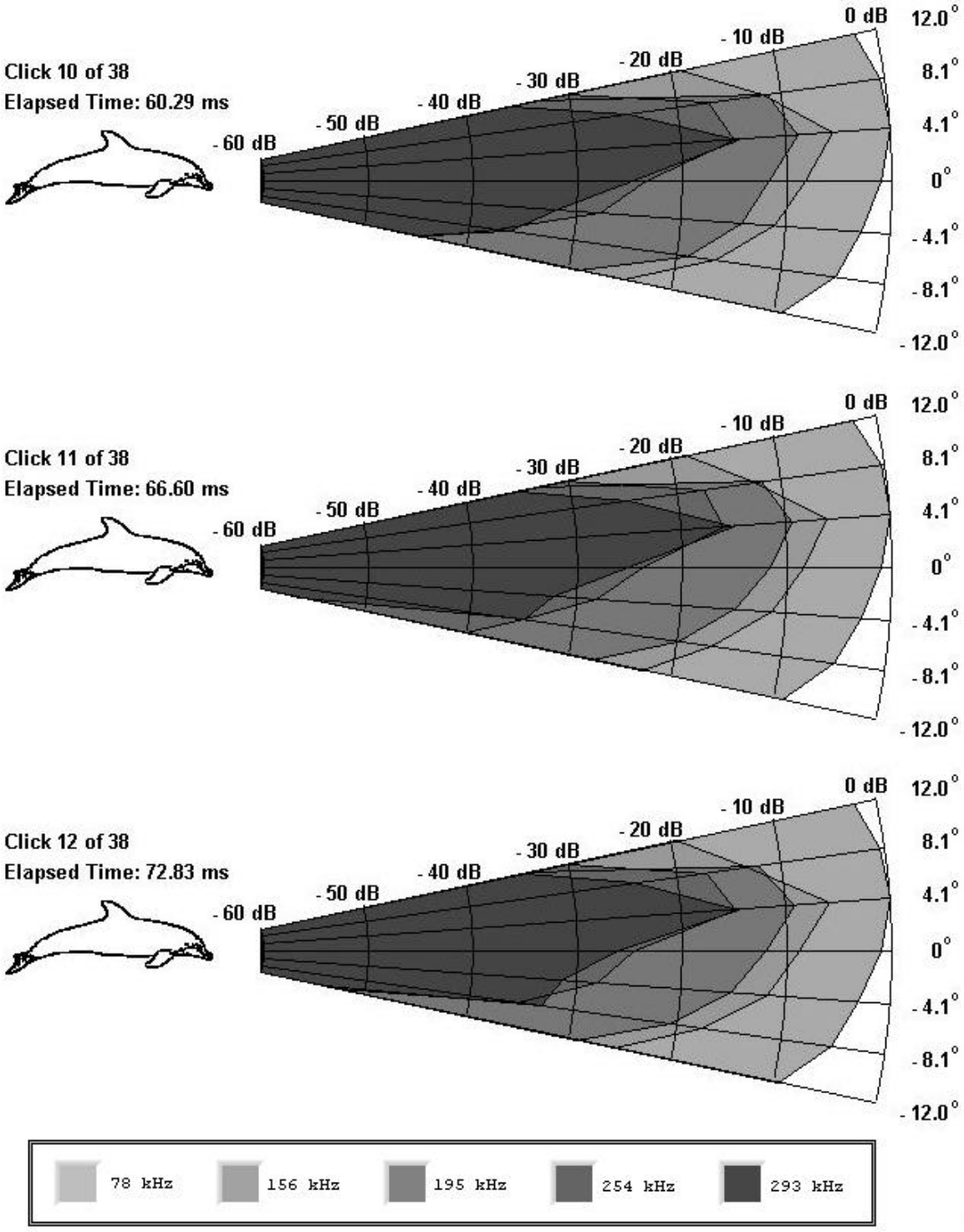

Figure 82. Trial Run 4-2 Clicks 10 through 12.

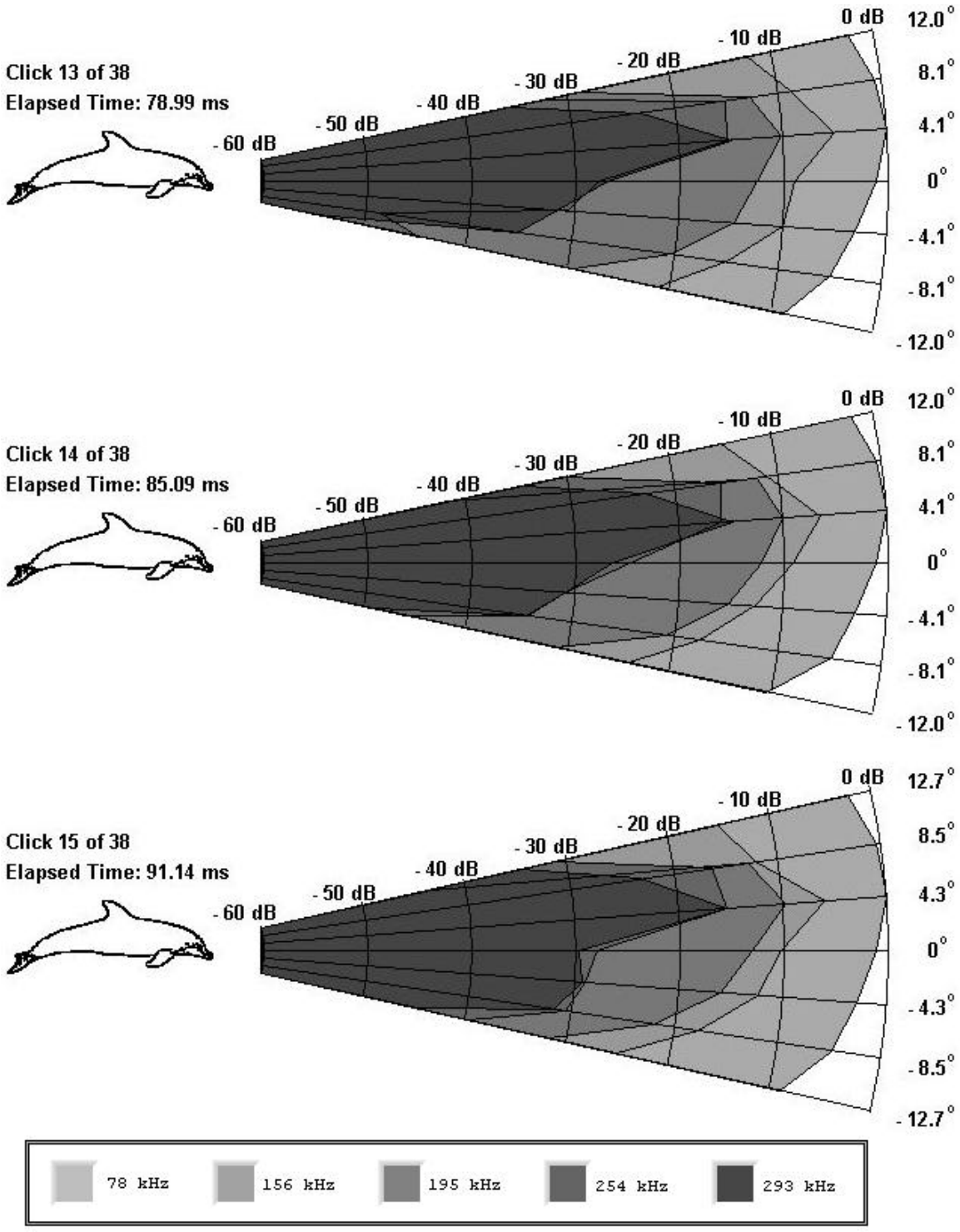

Figure 83. Trial Run 4-2 Clicks 13 through 15.

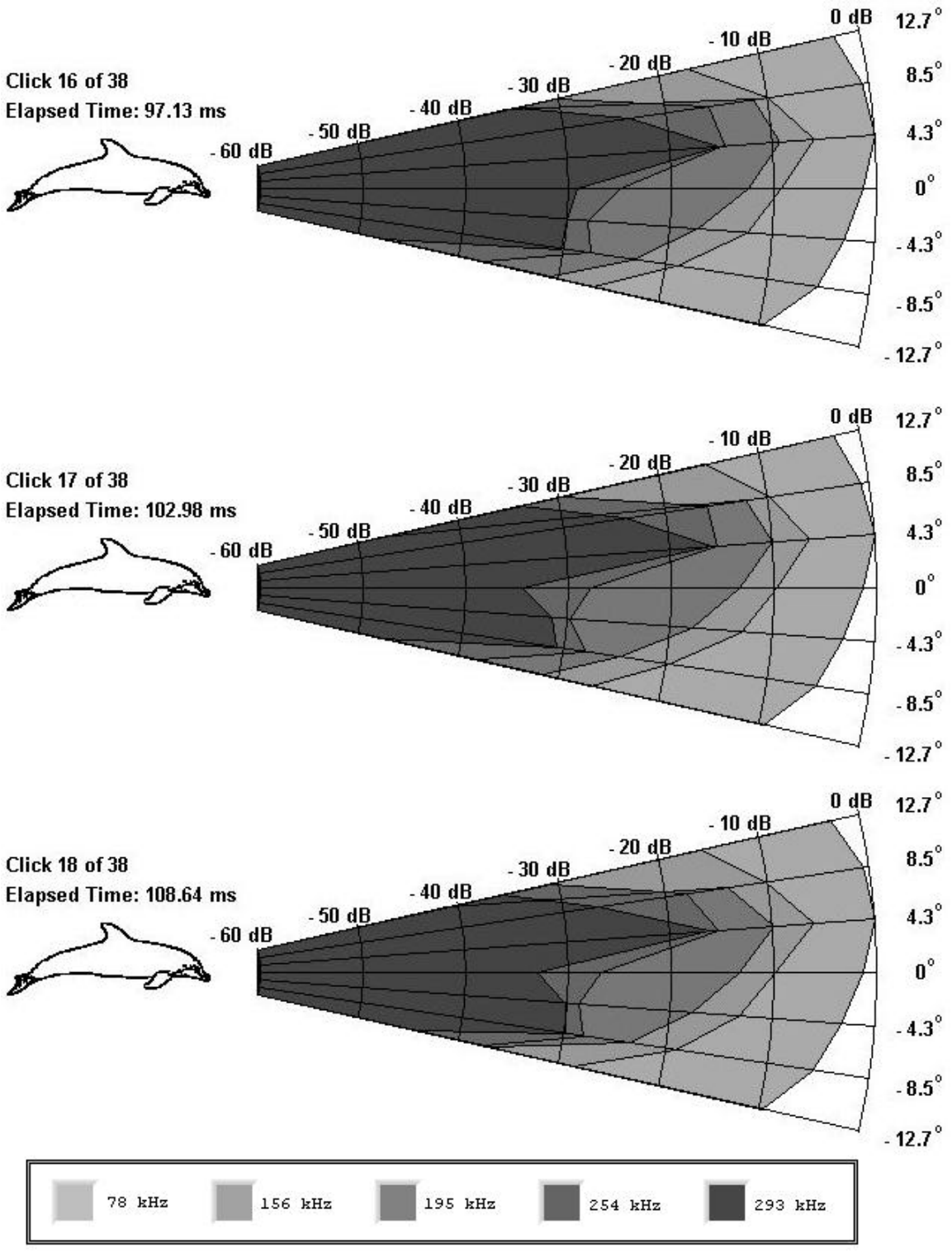

Figure 84. Trial Run 4-2 Clicks 16 through 18.

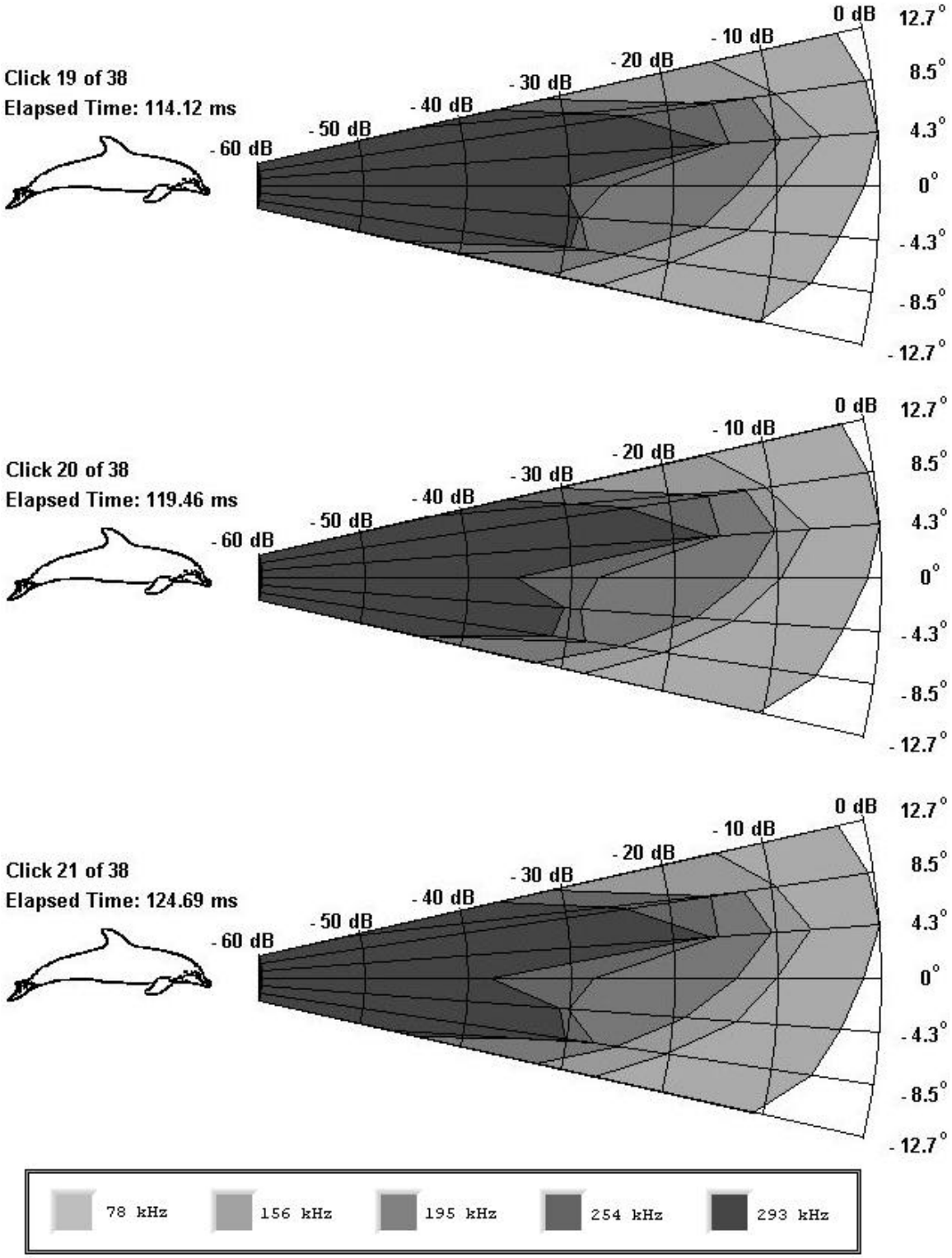

Figure 85. Trial Run 4-2 Clicks 19 through 21.

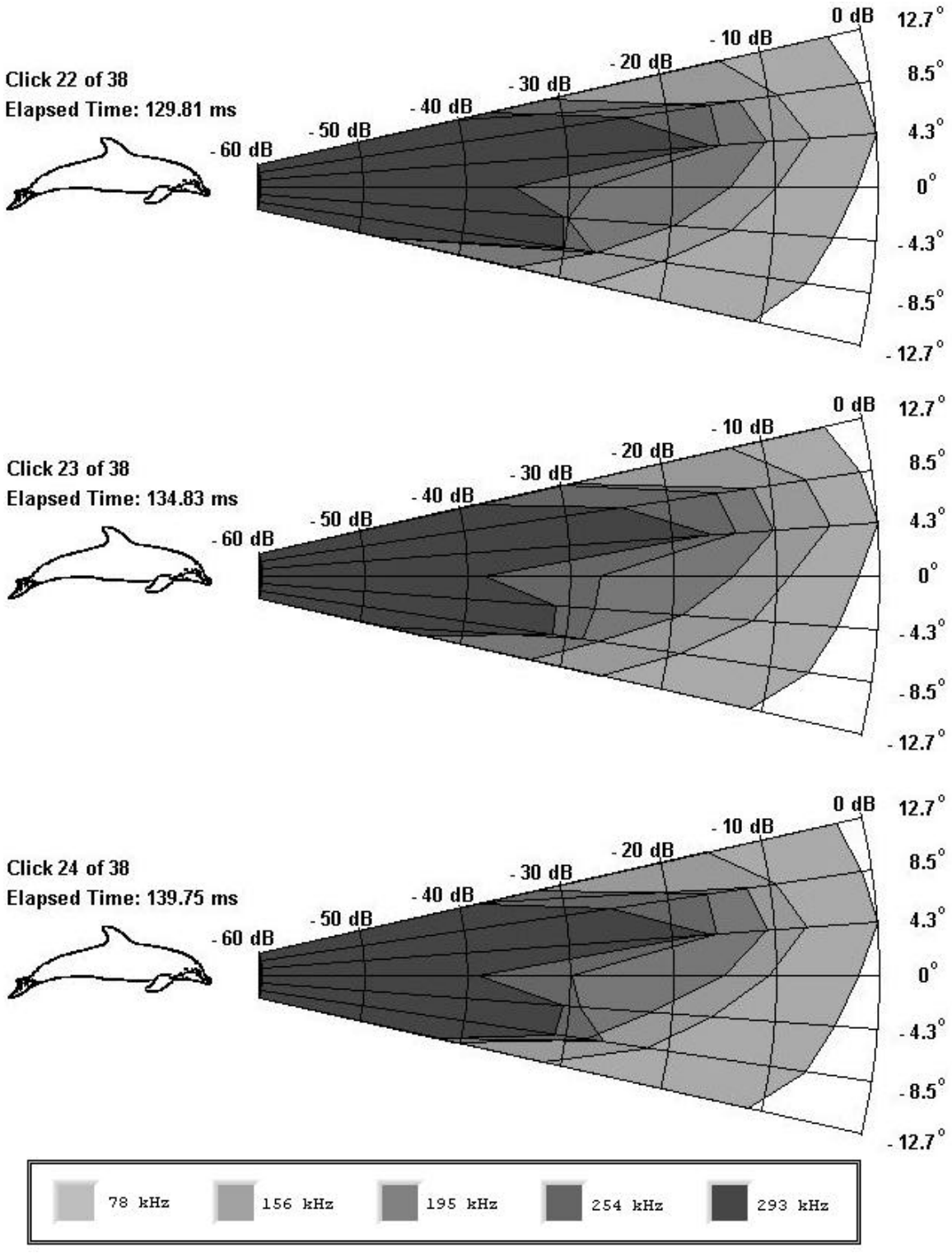

Figure 86. Trial Run 4-2 Clicks 22 through 24.

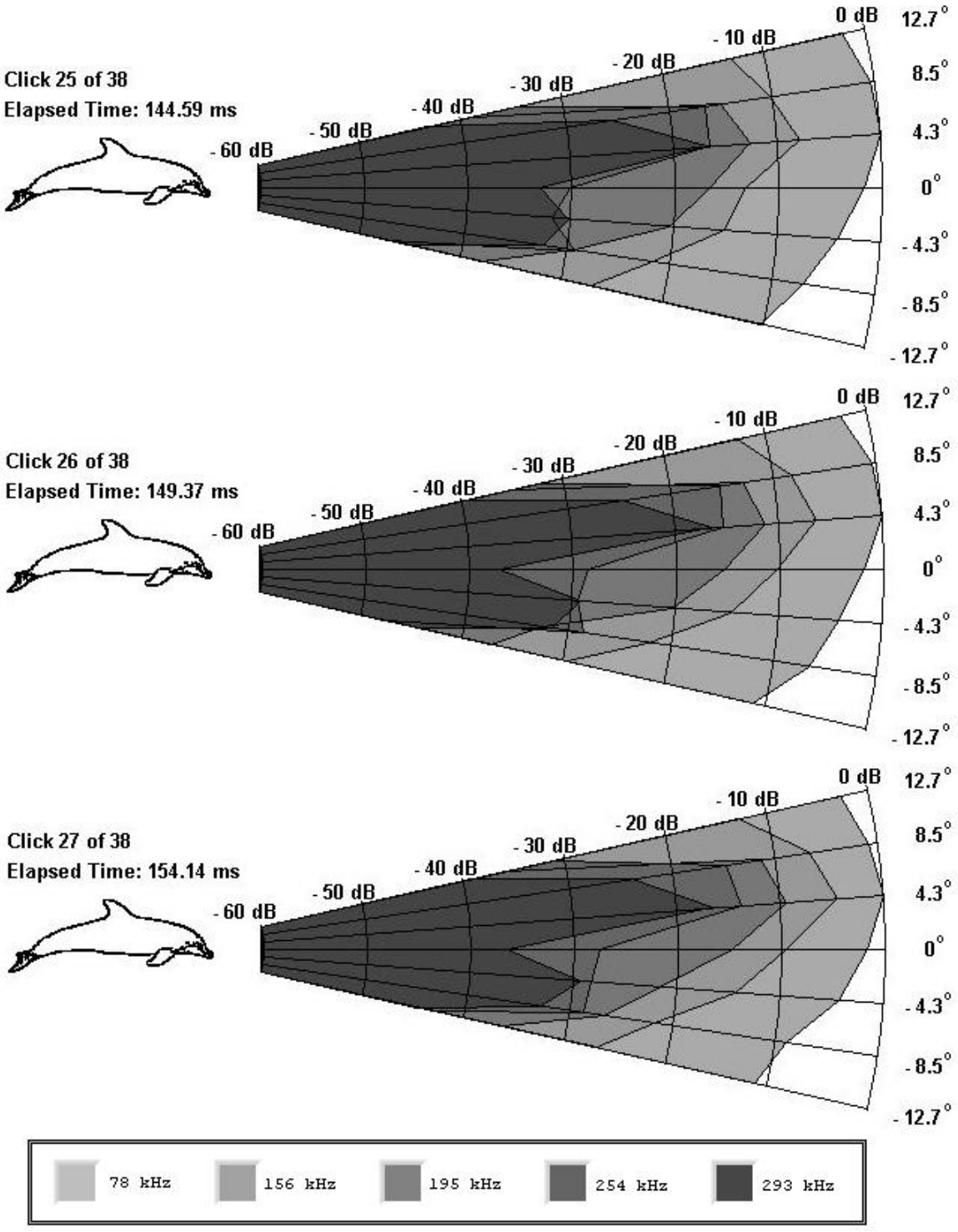

Figure 87. Trial Run 4-2 Clicks 25 through 27.

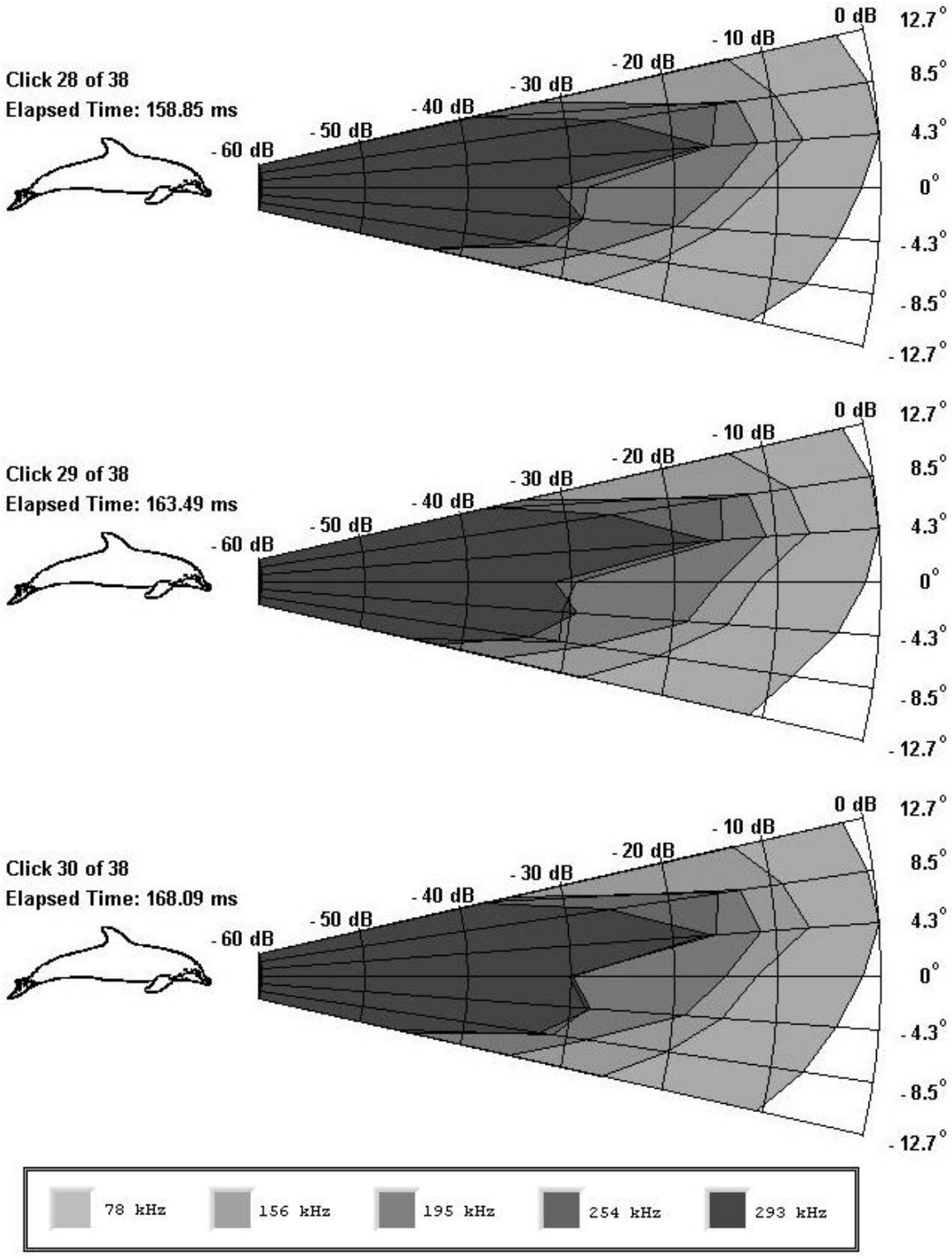

Figure 88. Trial Run 4-2 Clicks 28 through 30.

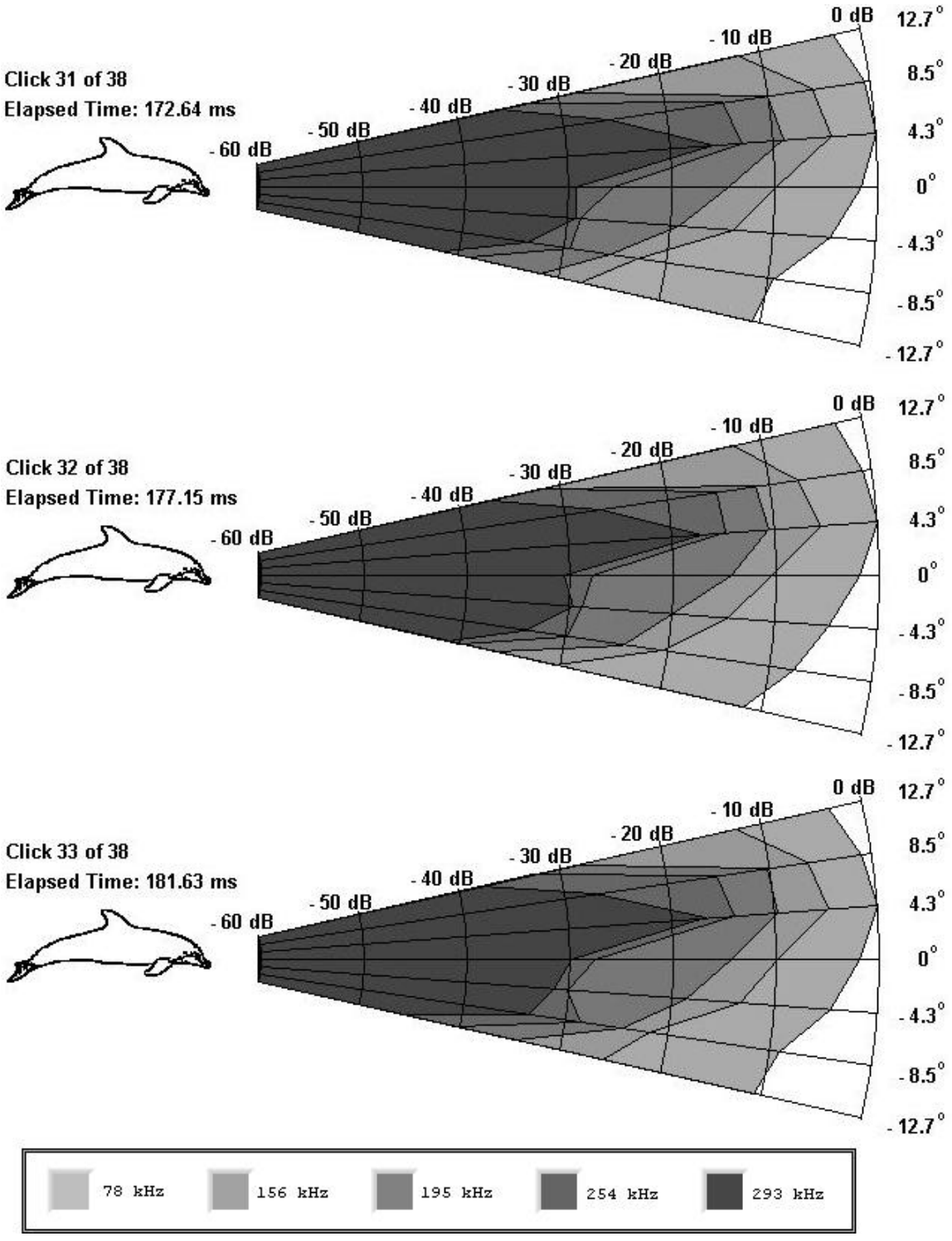

Figure 89. Trial Run 4-2 Clicks 31 through 33.

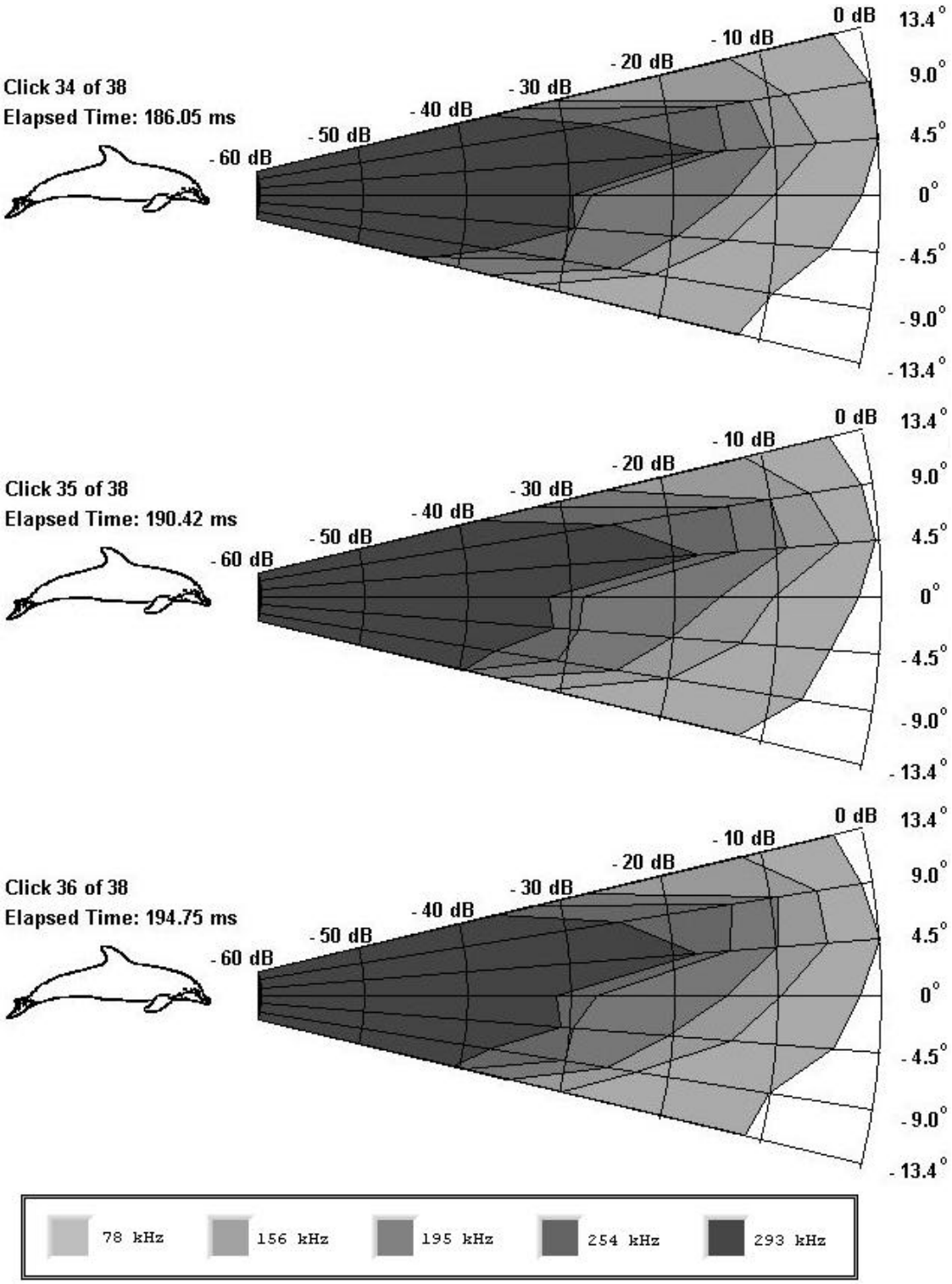

Figure 90. Trial Run 4-2 Clicks 34 through 36.

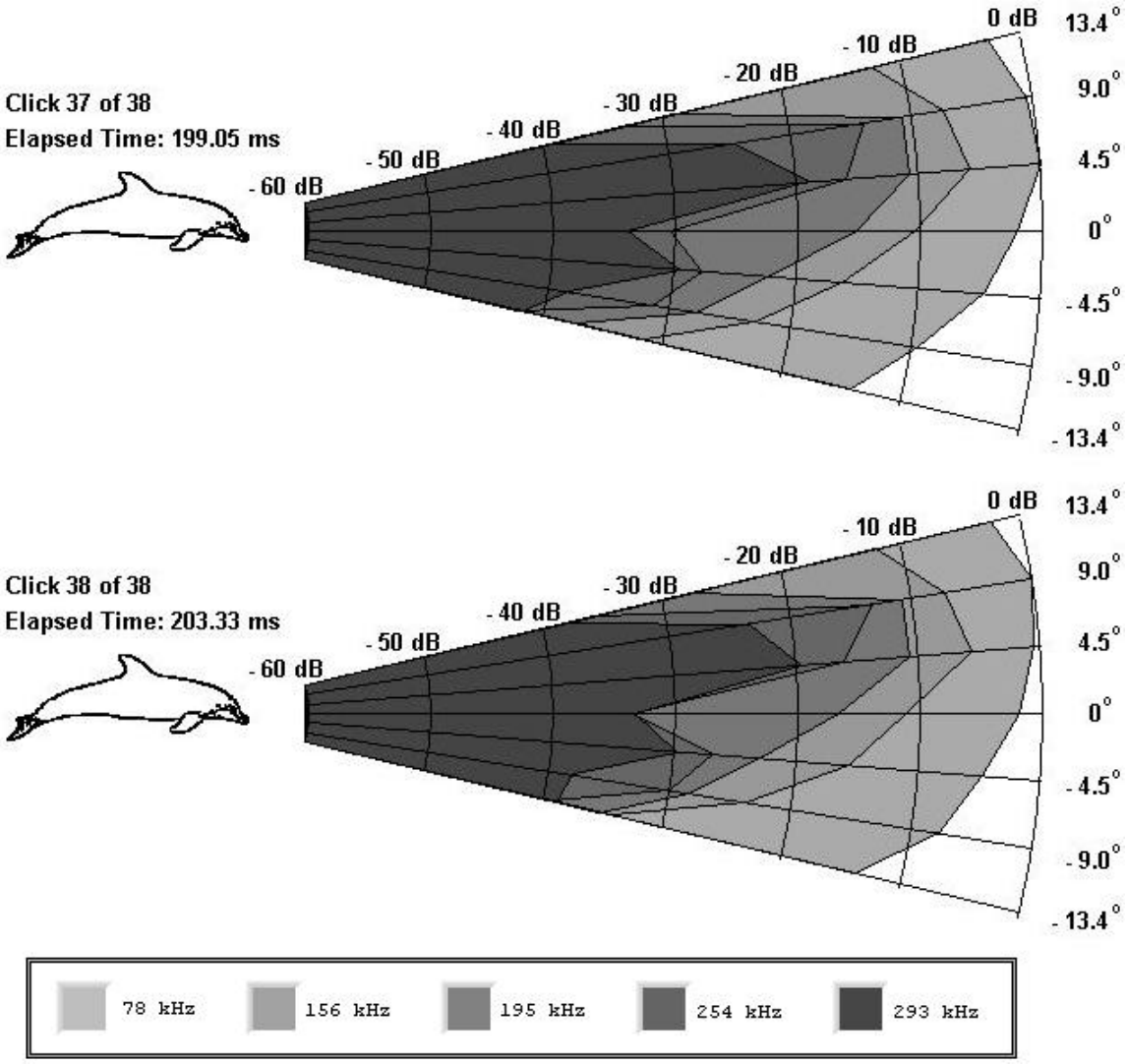

Figure 91. Trial Run 4-2 Clicks 37 and 38.

Comparison signals are shown in Figures 92 and 93. The peak amplitude and wave shape of the 4.1° time domain signal once again show the existence of the high frequency signals in Click 9. The two signals acquired in Click 21 at 4.3° and -4.3° also accentuate the differences in signals between those that do contain high frequencies

(4.3°) and the instances where high frequency components are absent.

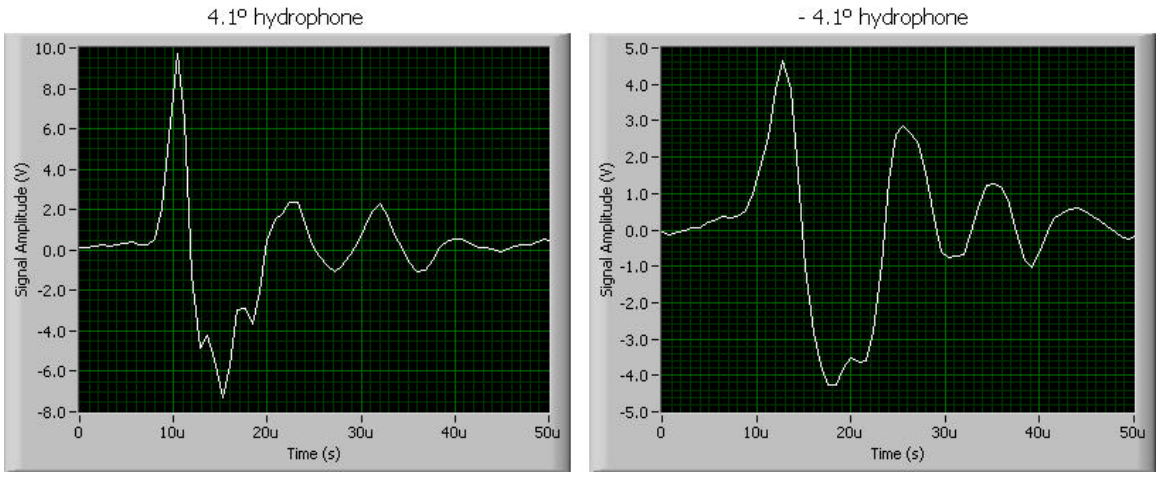

Figure 92. Click 9 received at two different hydrophones during Trial Run 4-2.

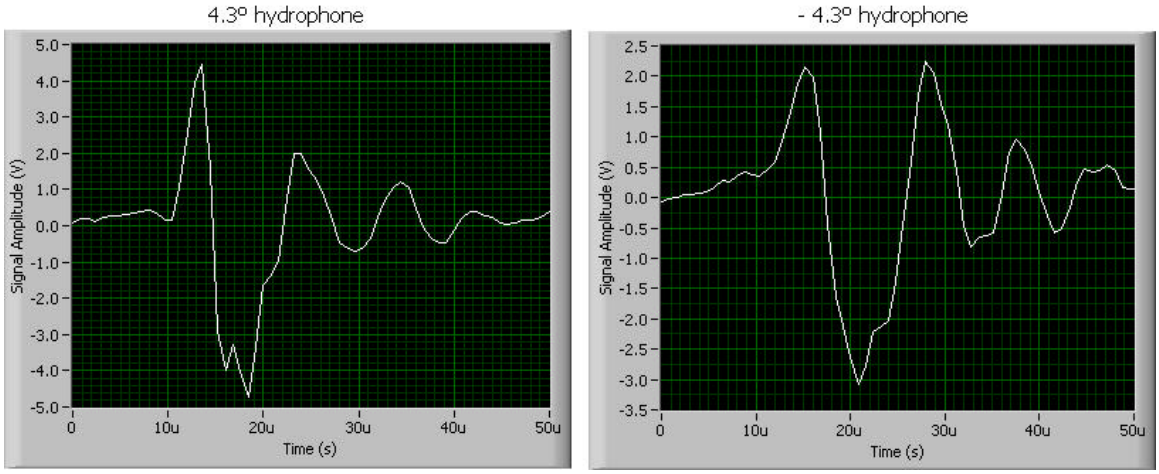

Figure 93. Click 21 received at two different hydrophones during Trial Run 4-2.

EFSDLs at 390 kHz clearly show the dolphin has the capabilities to actively use frequencies almost three times higher than previously documented *Tursiops Truncatus* sound emissions to echolocate a target. Figures 94 through

106 show plots of the signal's peak frequency (78 kHz) and the 390 kHz component.

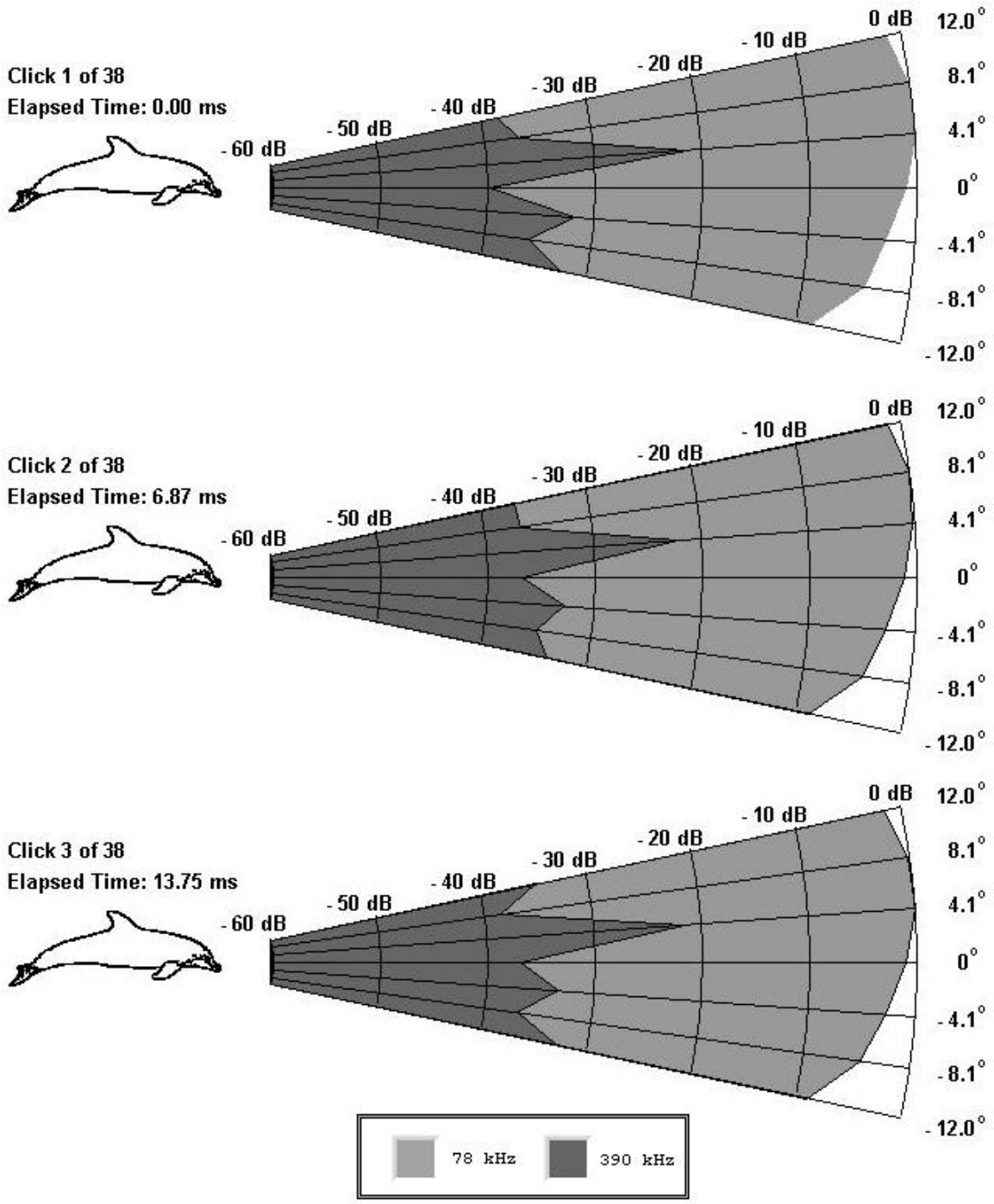

Figure 94. Trial Run 4-2 Clicks 1 through 3.

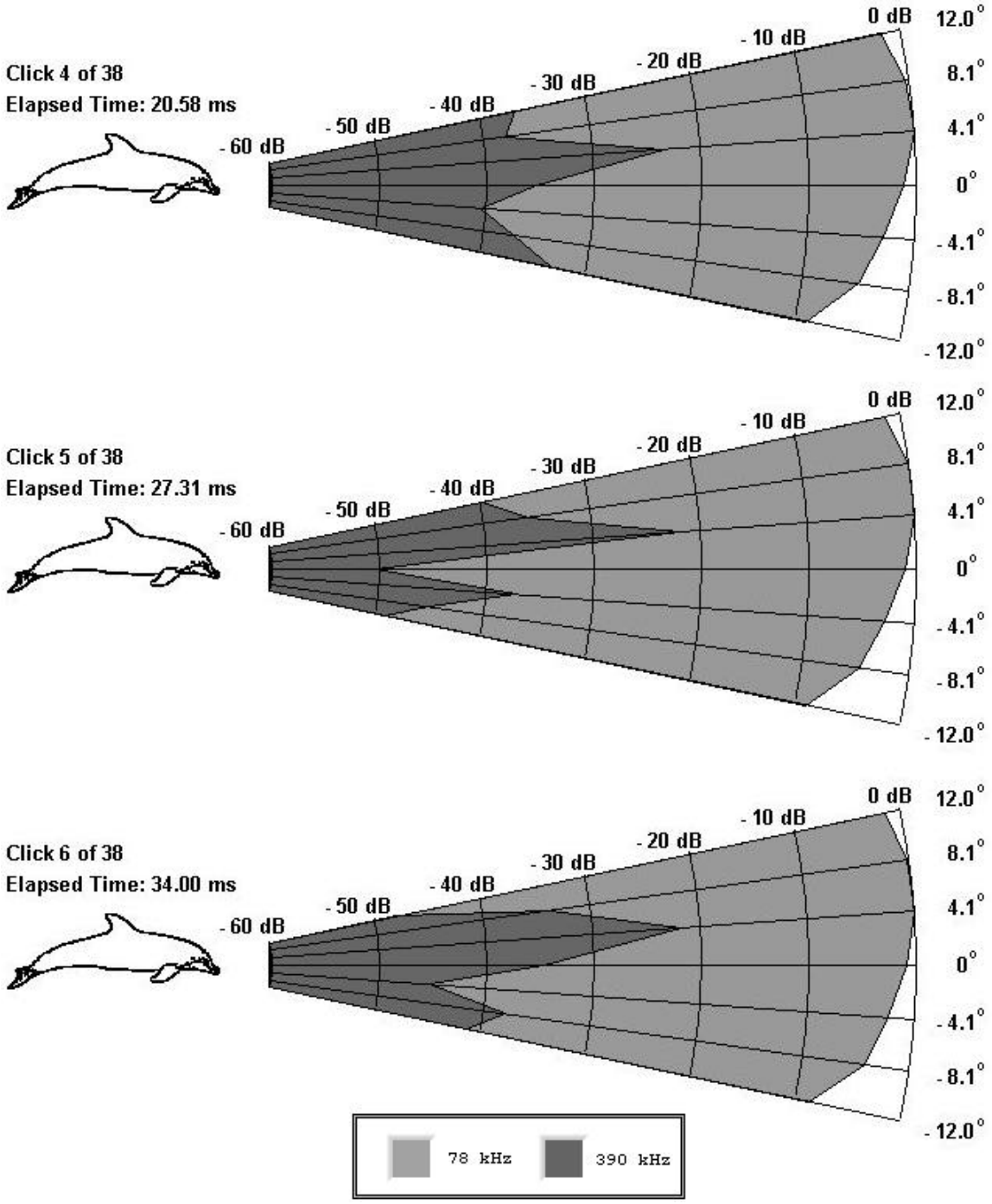

Figure 95. Trial Run 4-2 Clicks 4 through 6.

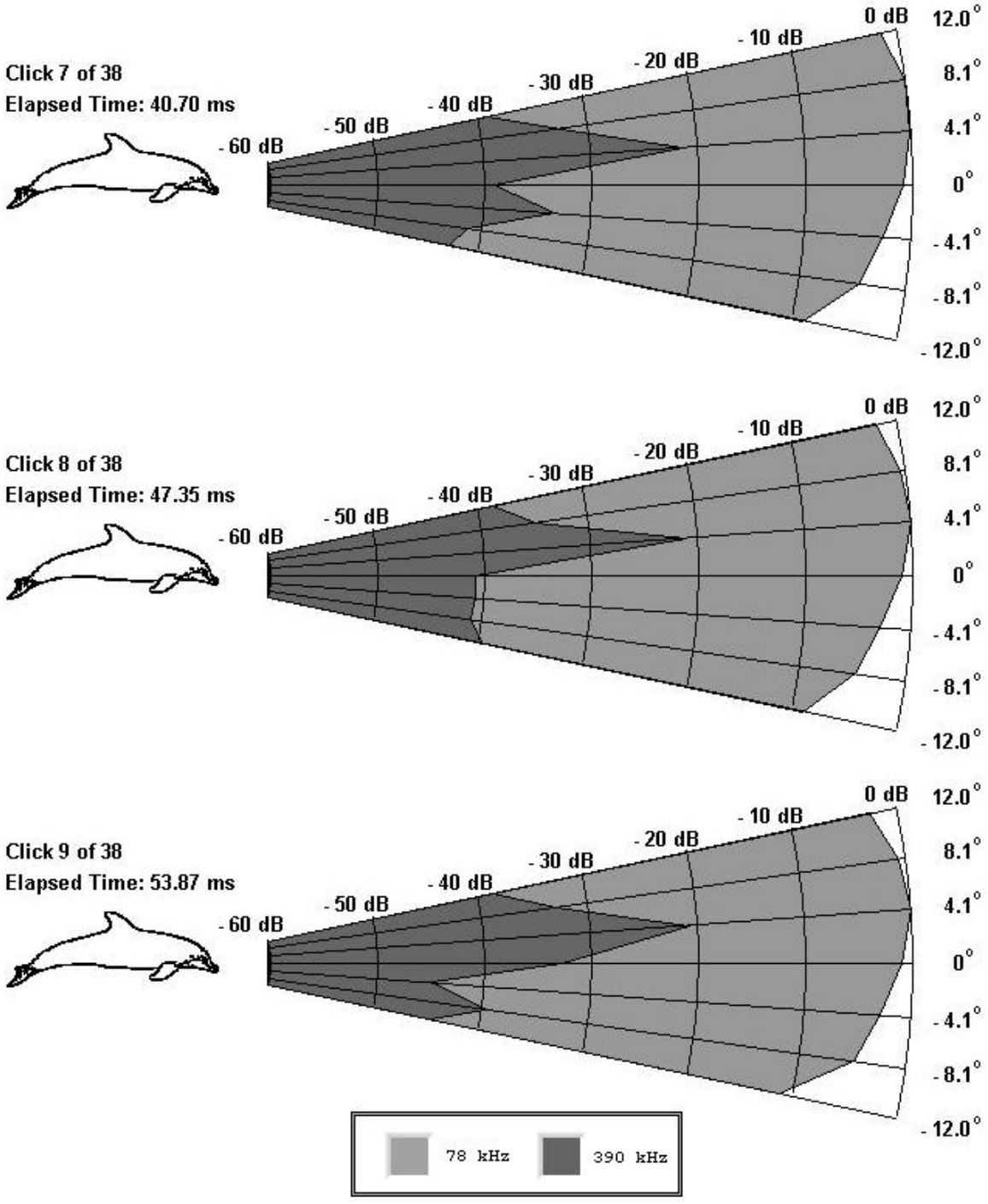

Figure 96. Trial Run 4-2 Clicks 7 through 9.

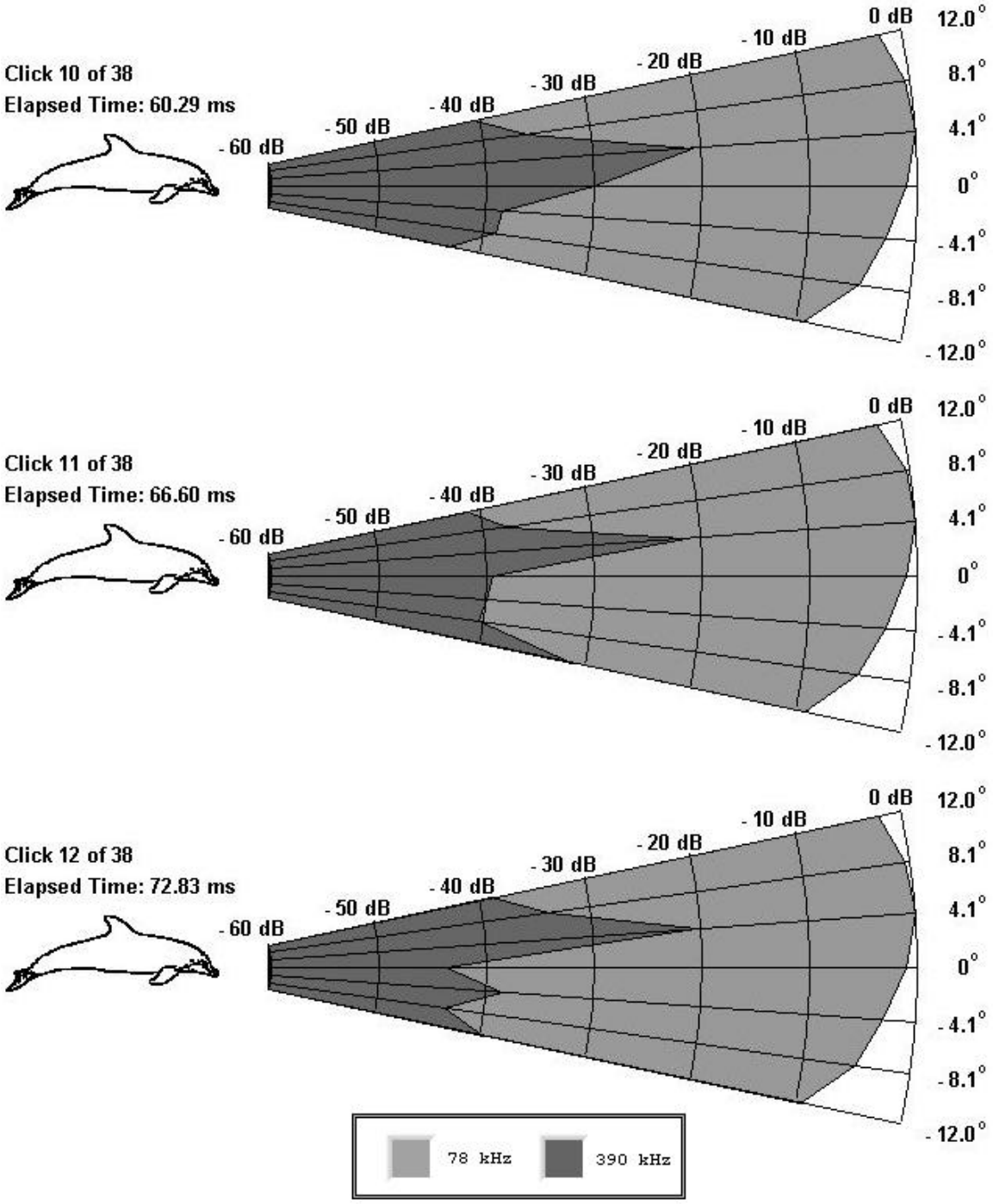

Figure 97. Trial Run 4-2 Clicks 10 through 12.

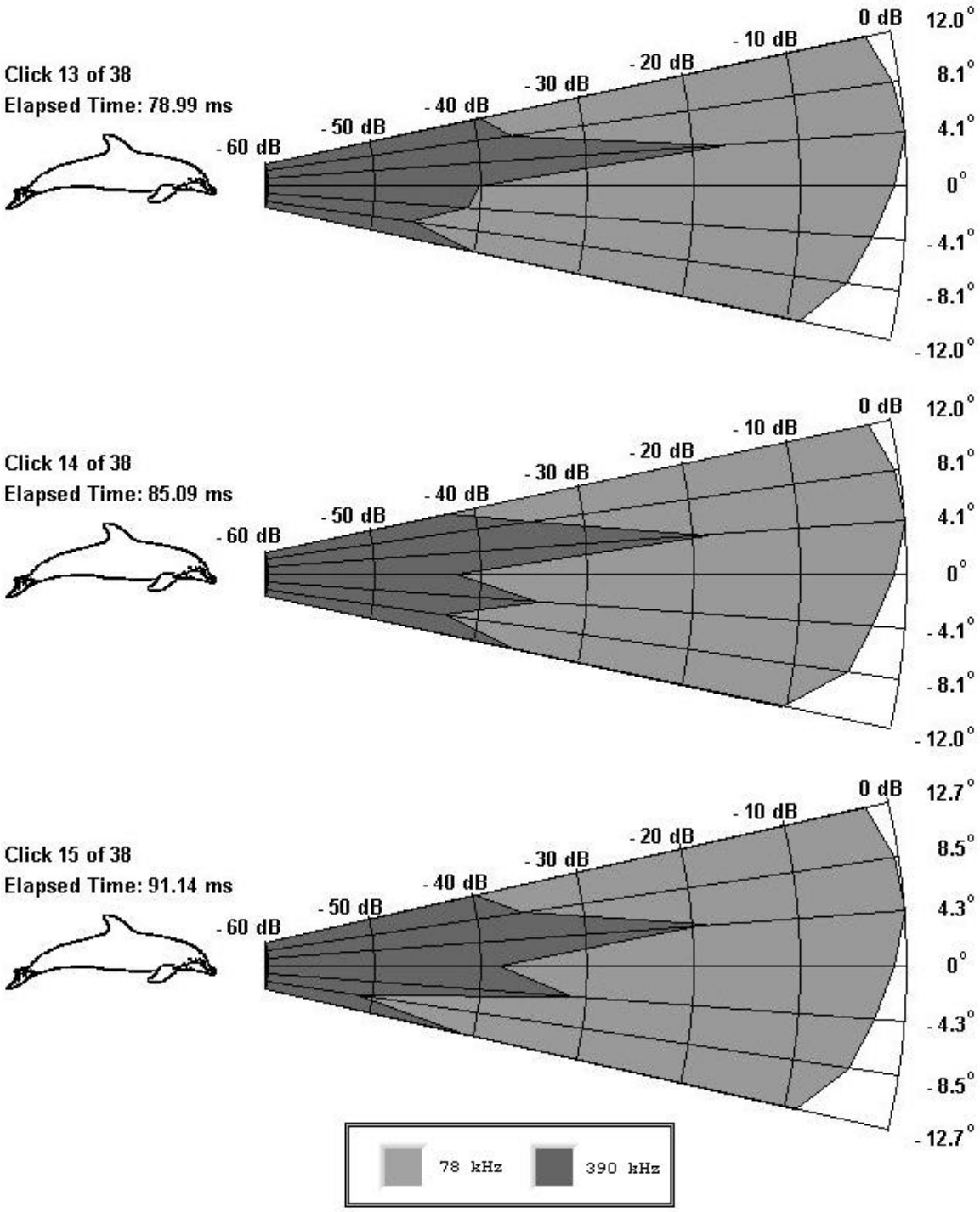

Figure 98. Trial Run 4-2 Clicks 13 through 15.

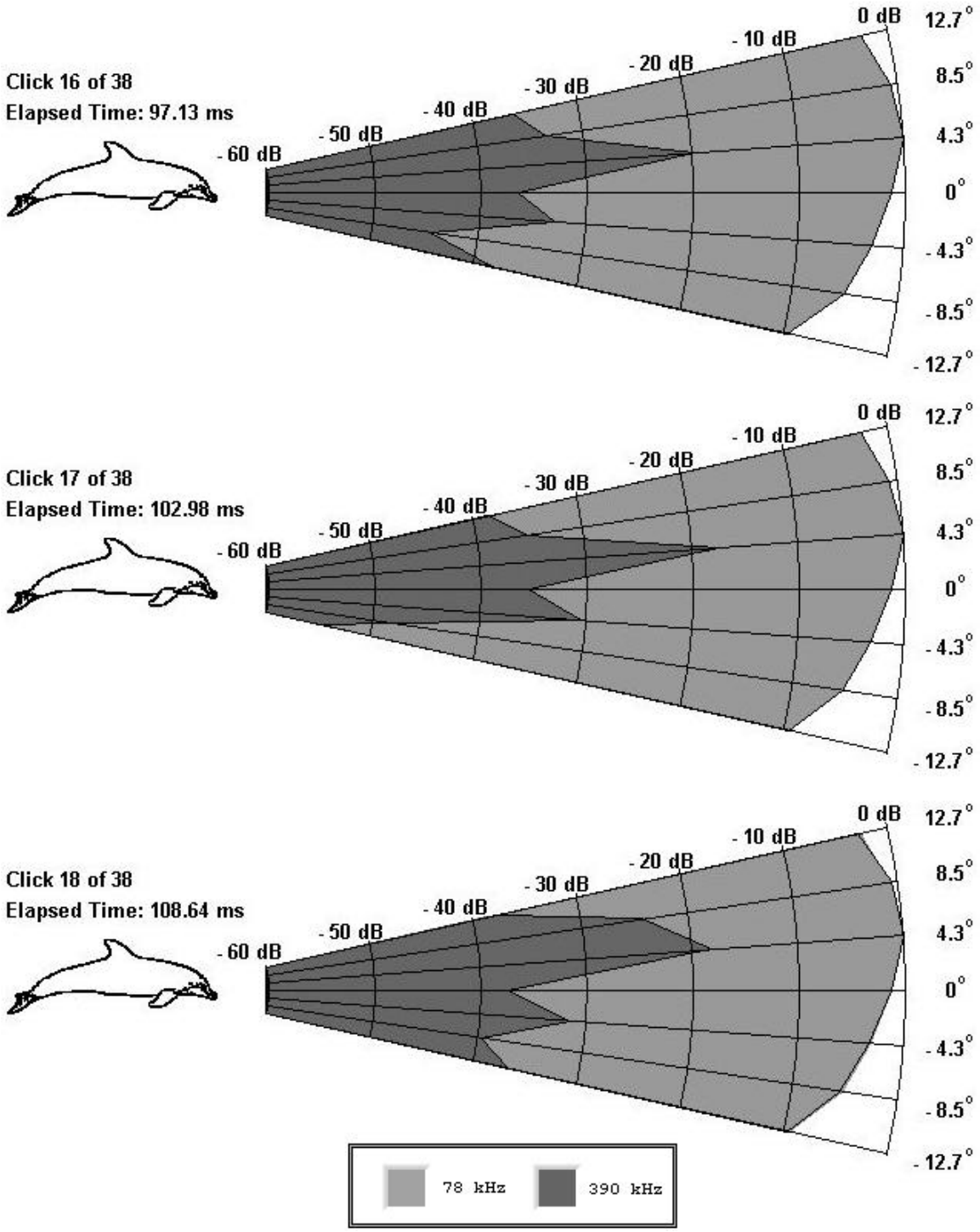

Figure 99. Trial Run 4-2 Clicks 16 through 18.

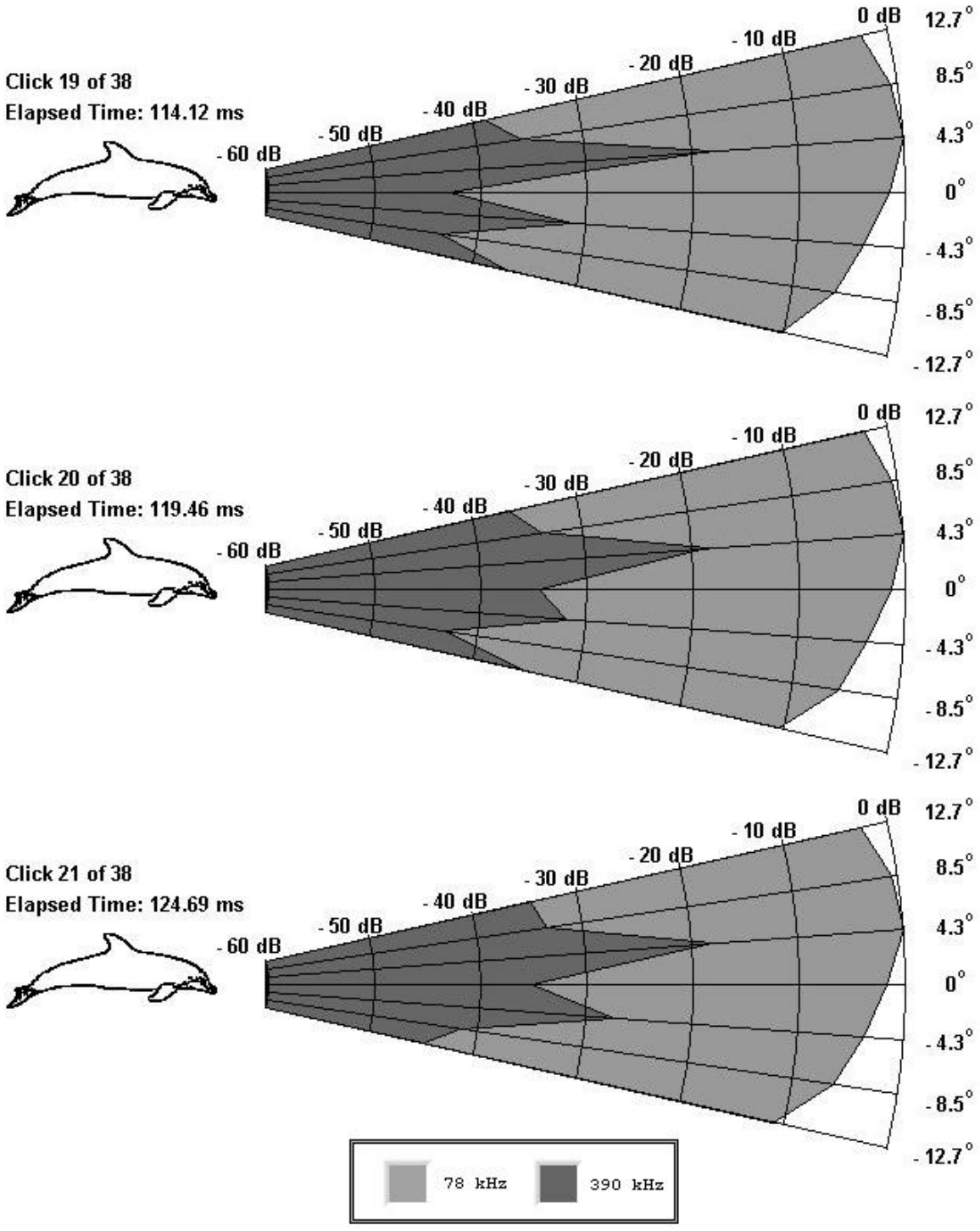

Figure 100. Trial Run 4-2 Clicks 19 through 21.

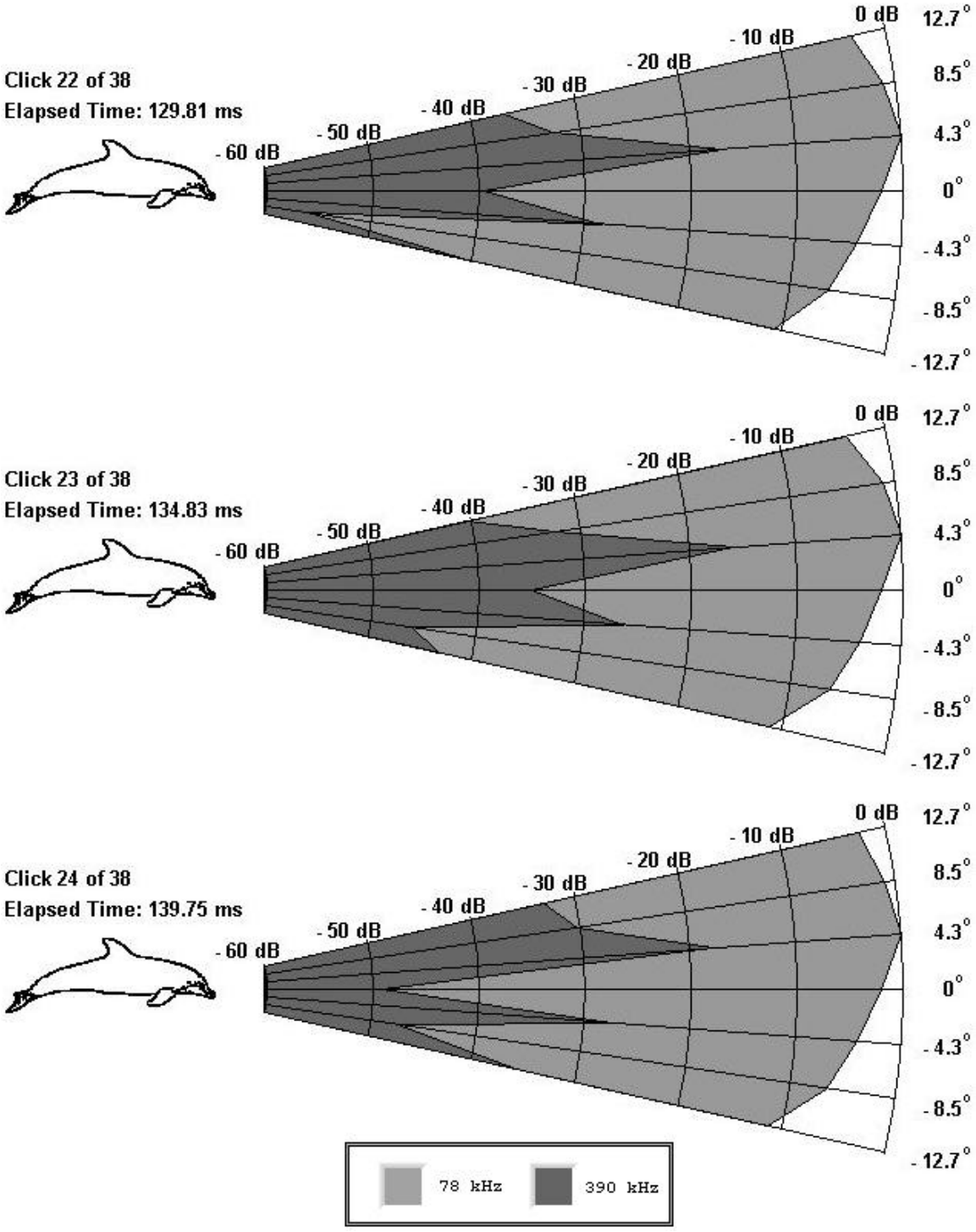

Figure 101. Trial Run 4-2 Clicks 22 through 24.

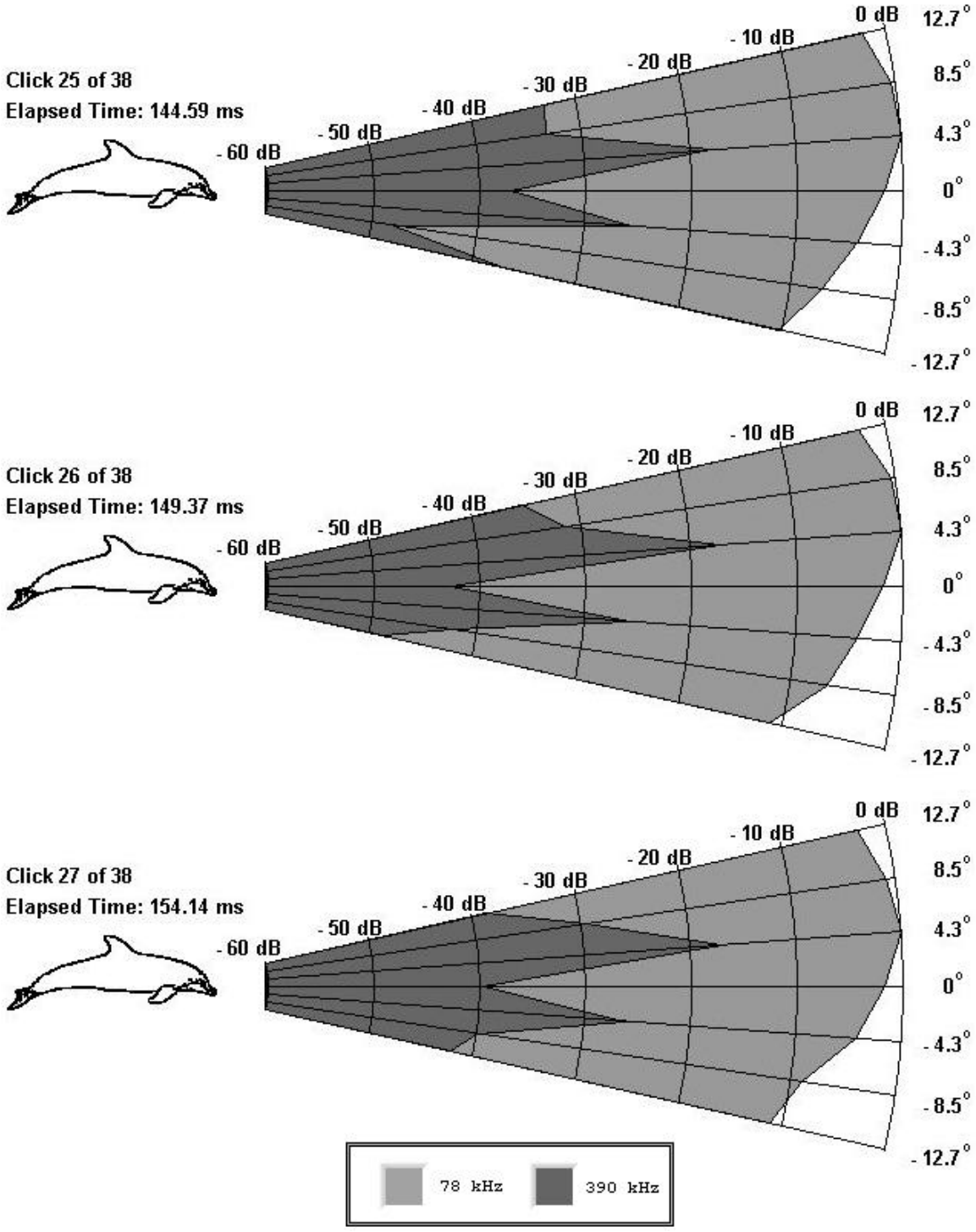

Figure 102. Trial Run 4-2 Clicks 25 through 27.

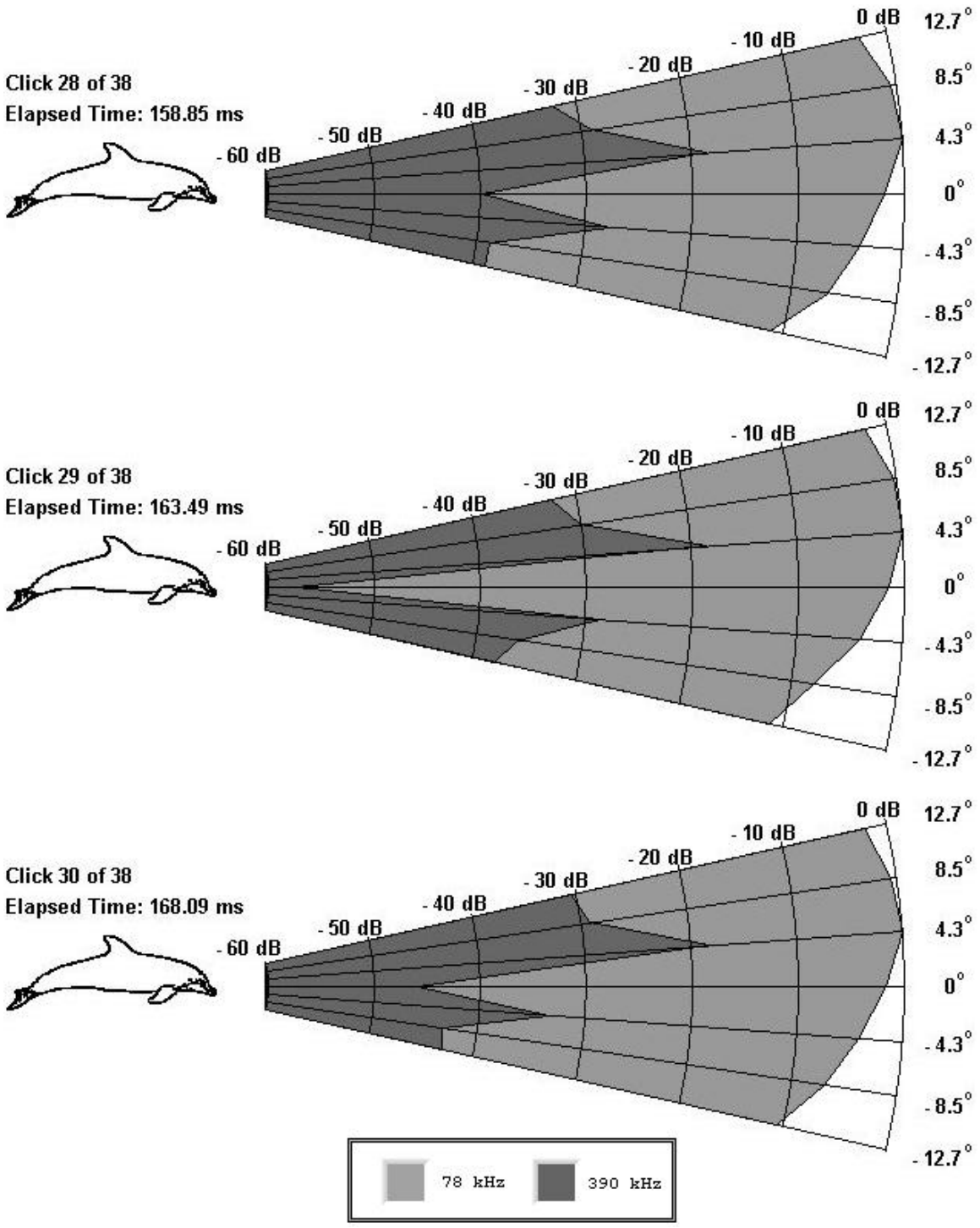

Figure 103. Trial Run 4-2 Clicks 28 through 30.

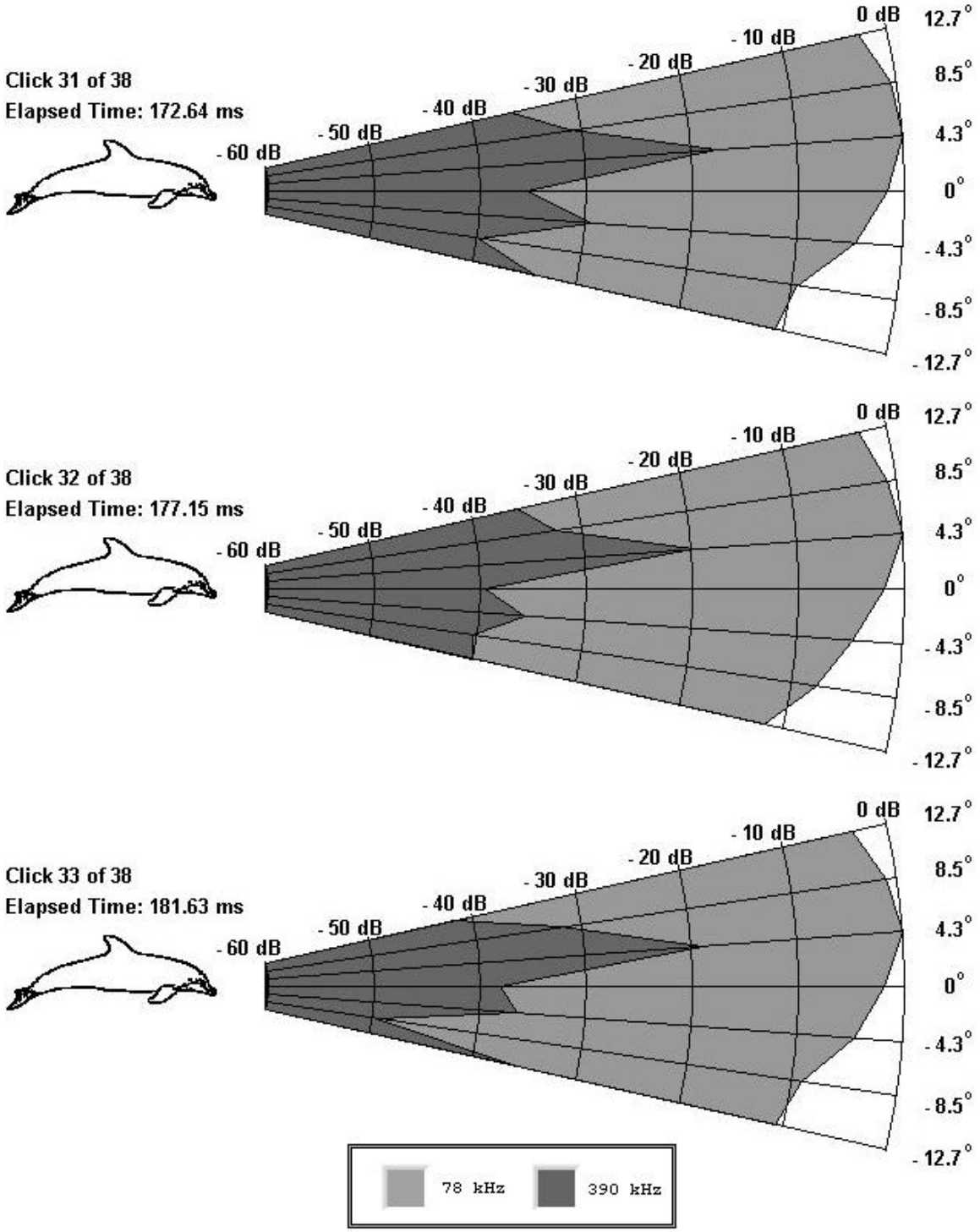

Figure 104. Trial Run 4-2 Clicks 31 through 33.

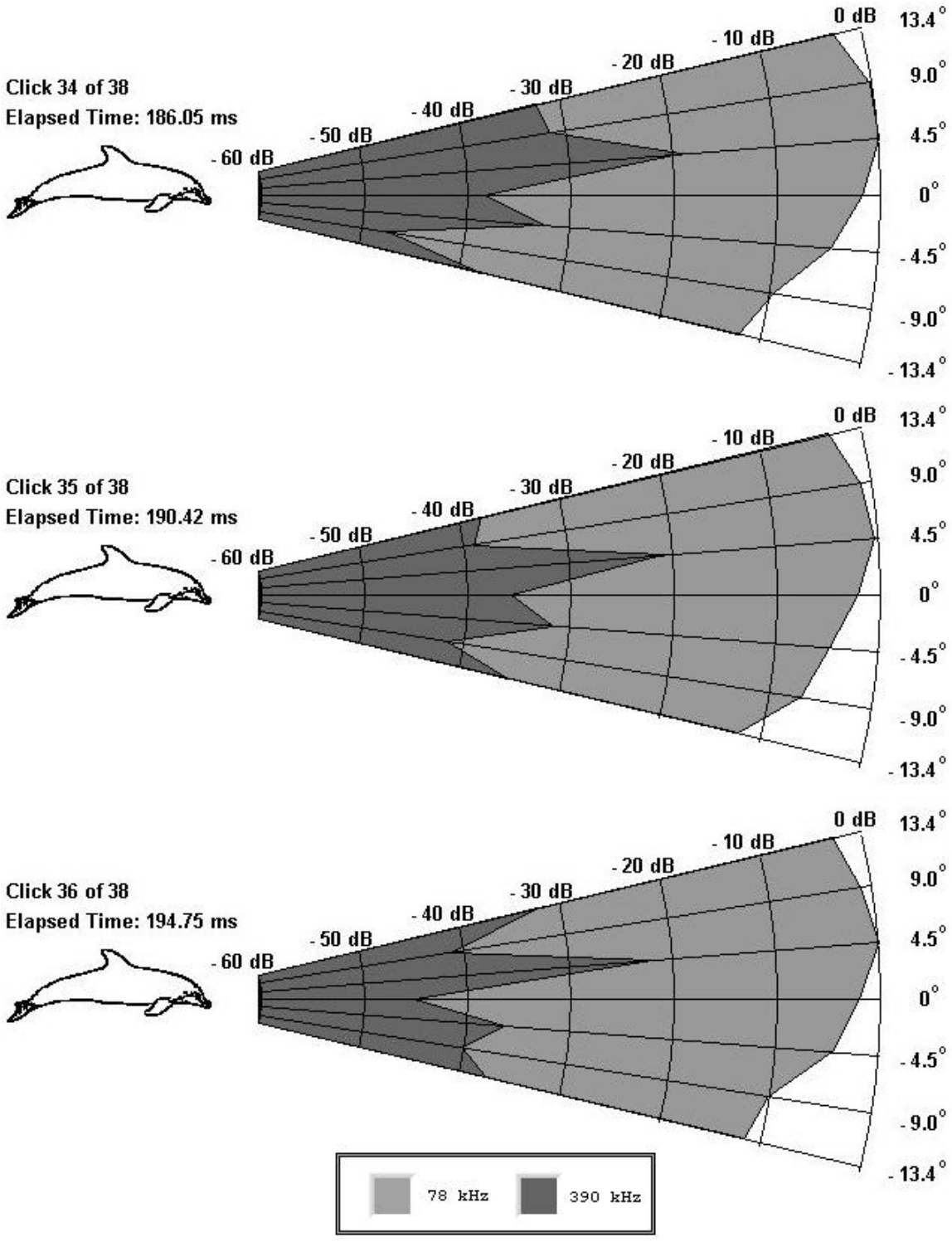

Figure 105. Trial Run 4-2 Clicks 34 through 36.

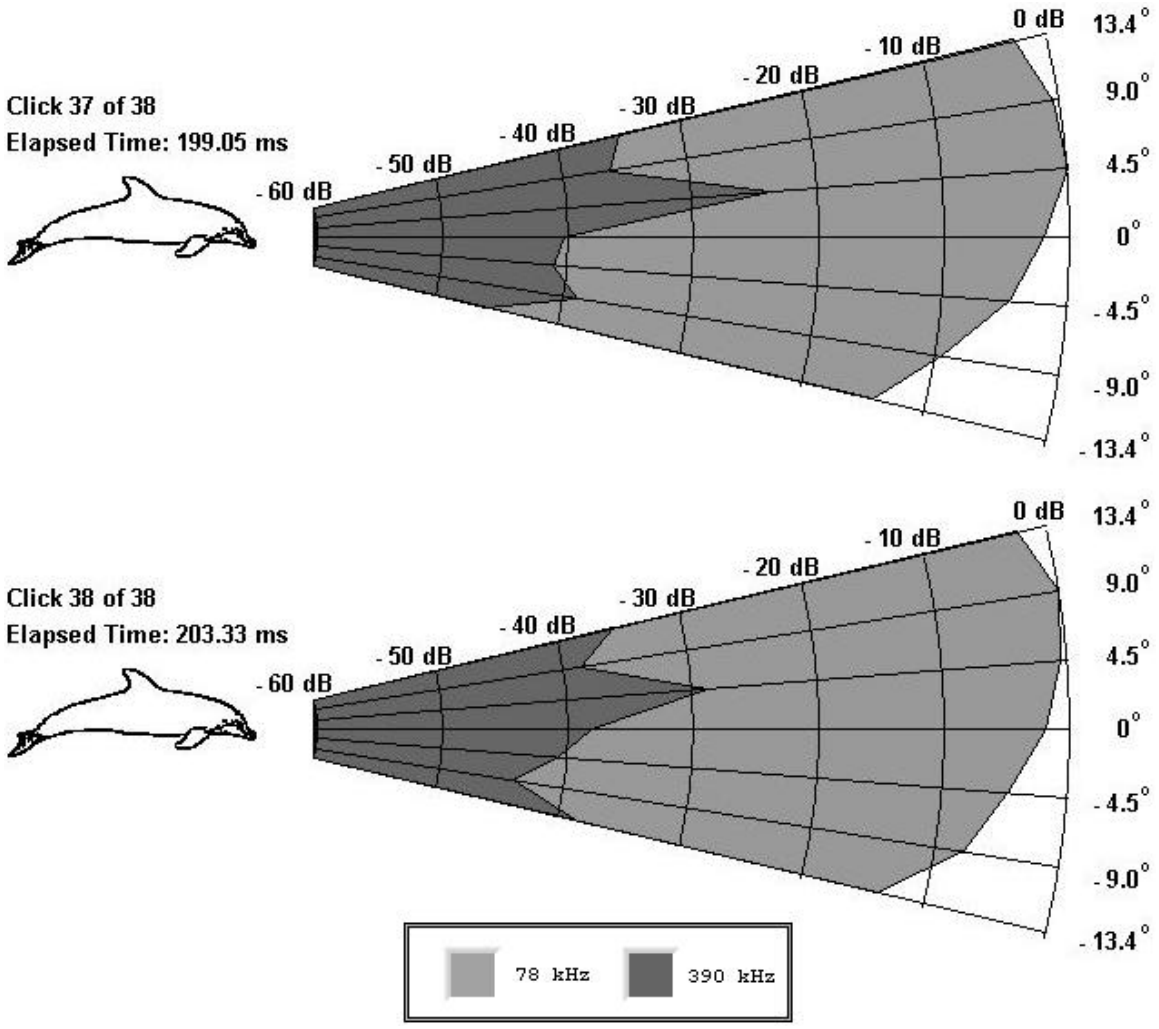

Figure 106. Trial Run 4-2 Clicks 37 and 38.

From plotted transmitting beam patterns for this trial run, it is speculated that the injected broadband noise masked the dolphin's lower frequencies and required him to rely on the higher frequencies during echolocation. Results from the TS experiment, described in Chapter III, showed that for a single cycle 100 kHz pulse at a range of 1 meter, the hydrophone and camera apparatus reflected approximately 8 percent of the incident pressure. In this

trial run, “Nemo” was approximately 1.2 meters from the target; the reflected pressure, at this range, was approximately 7 percent of the pressure incident on the hydrophone and camera apparatus. The estimated click train of reflections and the actual recorded echolocation click train are plotted in Figure 107. The time between the reflected clicks and the recorded clicks was calculated to be approximately 1.6 ms, the two way travel time for an echolocation click to leave the dolphin’s melon, strike a target at a range of 1.2 meters and return to the dolphin.

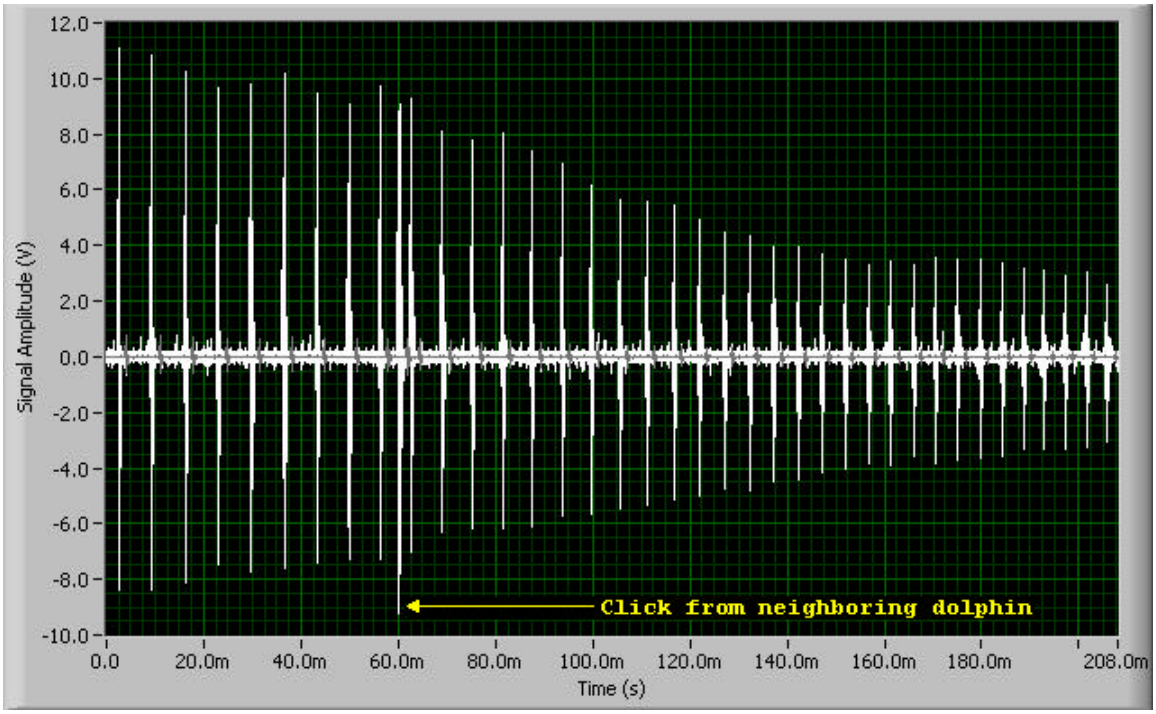

Figure 107. Trial Run 4-2 click train with speculated return signal of each incident echolocation emission.

Plotted transmitting beam patterns for Click 31 (Figures 89 and 104) show significant EFSDLs at frequencies up to 390 kHz. Figure 108 shows the recorded maximum

echolocation click amplitude, the estimated maximum amplitude of the echo and the maximum amplitude of the noise present in the water for Click 31. The maximum amplitude of the noise exceeds the maximum amplitude of the echo signal. The injected broadband noise was limited to below 135 kHz. Even though the dolphin's peak EFSDLs were at 78 kHz throughout the click train, significant EFSDLs transmitted in narrow high frequency beams provide substantial evidence that "Nemo" successfully overcame the low frequency noise by utilizing frequencies higher than 135 kHz.

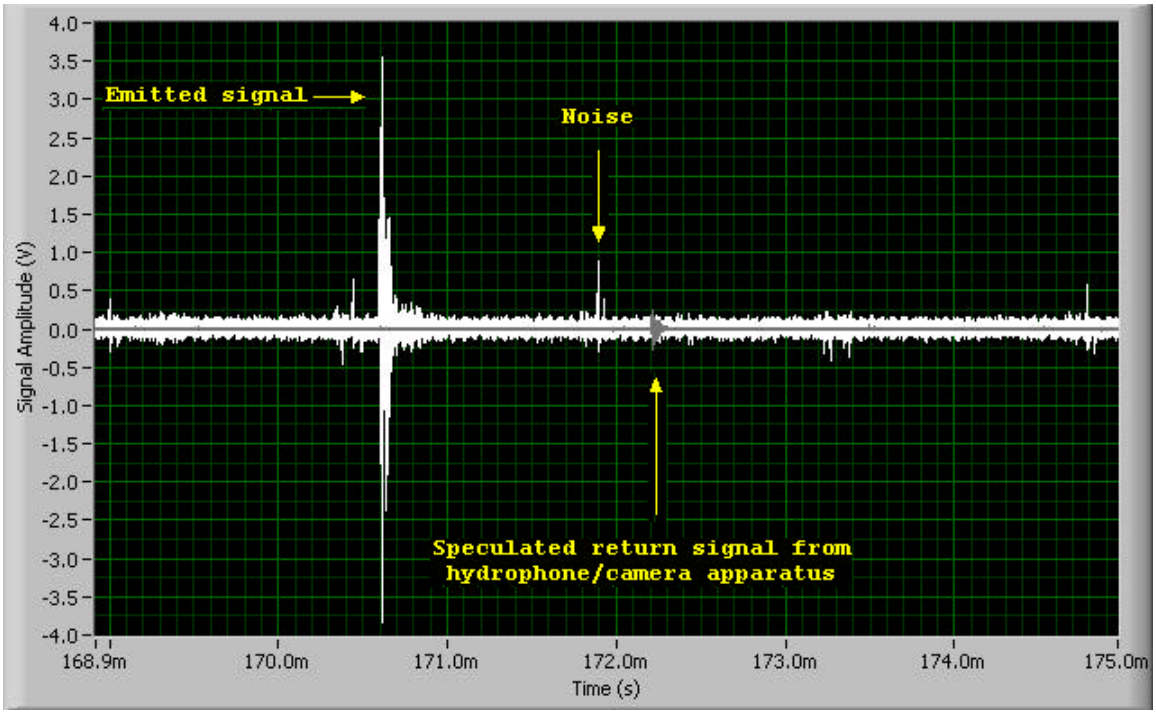

Figure 108. Graphical representation of Click 31's maximum amplitude (received at the hydrophones) and the speculated maximum amplitude of the echo signal.

D. CLICK RATES

Figure 109 shows elapsed time vs. the number of clicks and the clicks per second (cps) for all six trial runs. When “Nemo” did not use high frequencies, he clicked twice as fast as when the high frequency components were present in the echolocation signals. When broadband noise was projected into the water, the dolphin emitted the high frequencies and clicked nearly twice as fast as when he used the high frequencies when no noise was present.

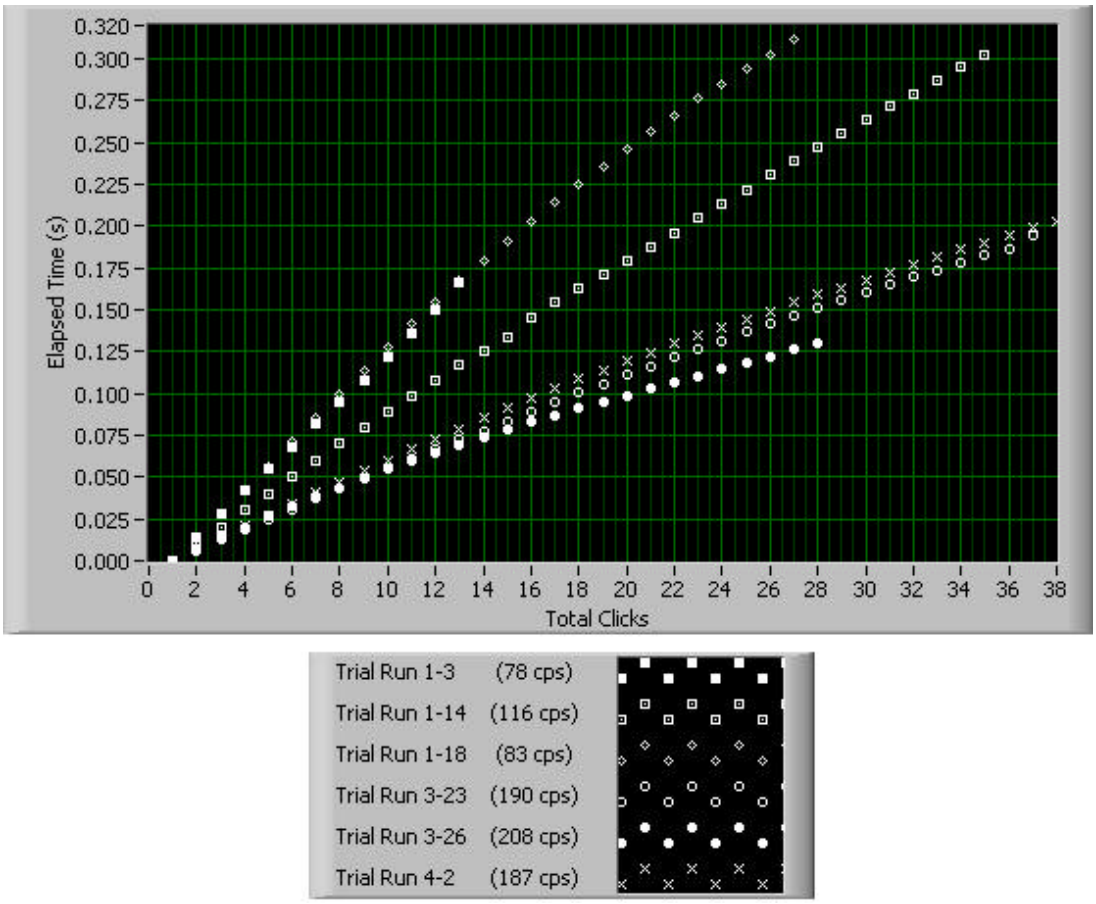

Figure 109. Elapsed time vs. number of clicks and the calculated clicks per second (cps) for all six trial runs.

E. ANALYSIS OF RESULTS

The transmitting beam patterns plotted in the previous section provide comprehensive evidence, not only of the presence of high frequency components in dolphin sonar signals, but also how the dolphin used high frequency signals while actively echolocating targets. When high frequencies are present, the raw data waveforms show that the dolphin emits a different shaped waveform. Additionally, the dolphin adjusted the energy output at different frequencies, as well as steering narrow, focused transmission beams. Previously documented *Tursiops Truncatus* transmitting beam patterns do not include frequencies higher than 130 kHz. Clearly, biosonar signals that exceed 130 kHz play an important role in echolocation. The research presented in this thesis suggests frequencies extending up to 390 kHz should be included in dolphin-based sonar systems, currently being engineered by research scientists.

V. CONCLUSIONS AND RECOMMENDATIONS

A. CONCLUSIONS

The results presented in this thesis clearly show that the bottlenose dolphin not only generates high frequencies, but uses them to echolocate and scan targets. If engineers are going to develop sonar systems based on the capabilities and methods used by marine mammals, then these high frequencies should be incorporated in their biomimetic sonar system designs.

B. RECOMMENDATIONS FOR FUTURE EXPERIMENTS

1. Additional Studies in Dolphin Echolocation

This thesis showed significant differences in dolphin sonar signals when echolocation tasks became routine. In-depth studies should be conducted to compare the energy content during routine echolocation tasks and the energy present when the dolphins work hard to echolocate a target. Frequency masking experiments, where noise is used to test the dolphin's echolocating abilities will give scientists better insight into the capabilities and limitations of *Tursiops Truncatus'* sonar. Additionally, Target Strength experiments, similar to the simple one conducted in this thesis, should be refined and improved. Finally, scientists need a better understanding of the reflected signal the dolphin receives, specifically at the higher frequencies examined in this thesis.

2. Experiment Variation

Dolphins are extremely intelligent animals; after numerous trial runs both dolphins became quite familiar with the target. As shown in Trials 1-3, 1-14 and 1-18, “Nemo” exerted more energy across a broader spectrum when echolocating an unfamiliar target whereas in Trial Runs 3-23 and 3-26, the majority of the energy present in the signal spanned a smaller frequency range, indicating the dolphin did not need to produce the high frequency signals to receive the same fish reward. Trial Run 4-2 challenged the dolphin by flooding the water with low frequency noise. Future experiments should continually challenge the dolphin, compelling the animal to maximize his capabilities.

3. Data Acquisition Equipment

First, the on-axis hydrophone must be better located on the hydrophone array; valuable information was lost due to reflections off the camera lens. Secondly, DAQ and IMAQ boards require a tremendous amount of computing power. Future experiments should utilize the most recent commercial computing technology available to maximize efficiency and minimize wait time as the computer processes and stores large data files. Also, this experiment used a seven-hydrophone array that could be positioned in either the horizontal or vertical planes. Follow on experiments should use more hydrophones to record signals in both planes simultaneously. In addition to increased sonar signal acquisition capability, more underwater cameras

should also be used. A low power laser, mounted in a soft rubber cone, similar to the eyecups used in this experiment, could be placed on the dolphin's rostrum; this would give greater accuracy in determining where the dolphin's head pointed during echolocation. Finally, a better transmitting noise source will allow future experiments to task the dolphin more heavily and test the dolphin’s echolocation capabilities.

THIS PAGE INTENTIONALLY LEFT BLANK

APPENDIX A. ITC-1089D RECEIVE RESPONSE CHARACTERISTICS

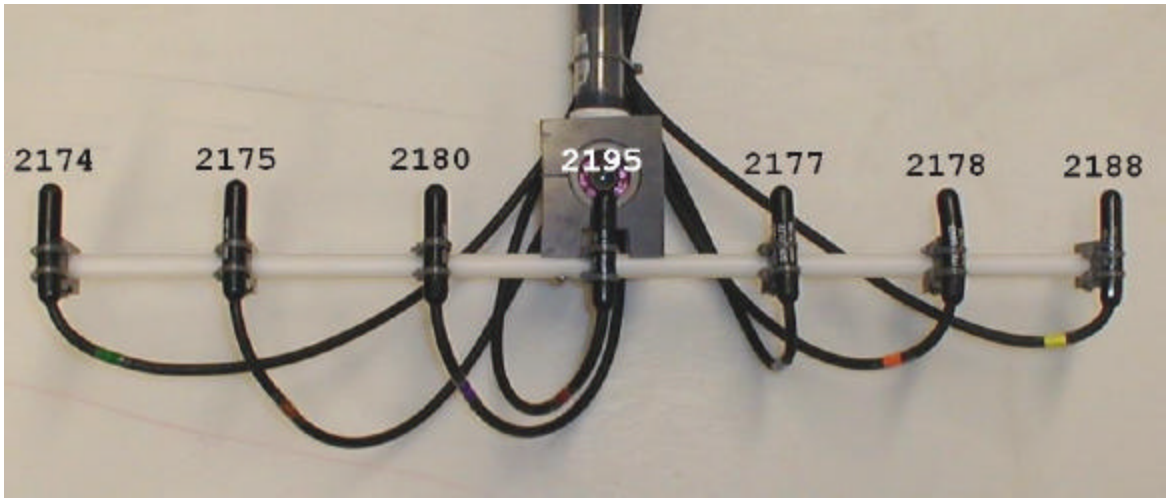

Figure 110. Placement of hydrophones (by serial number).

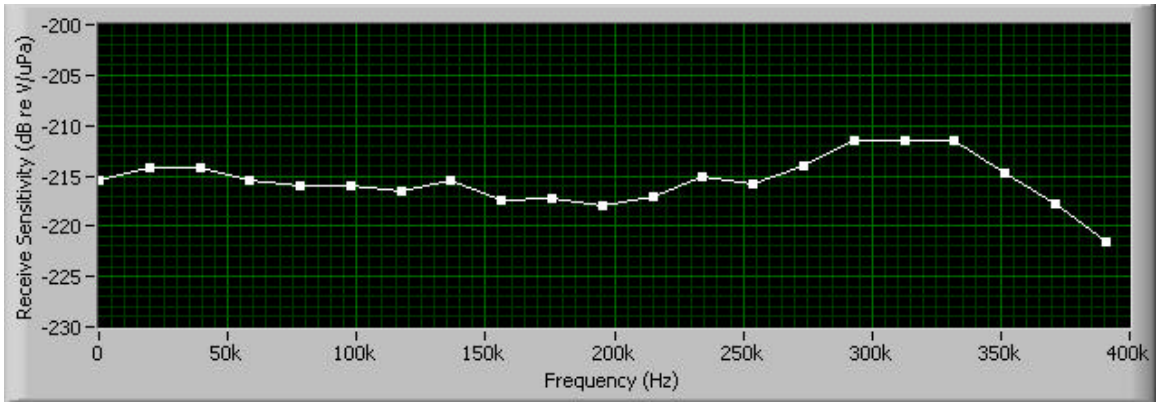

Figure 111. ITC 1089D S/N 2177.

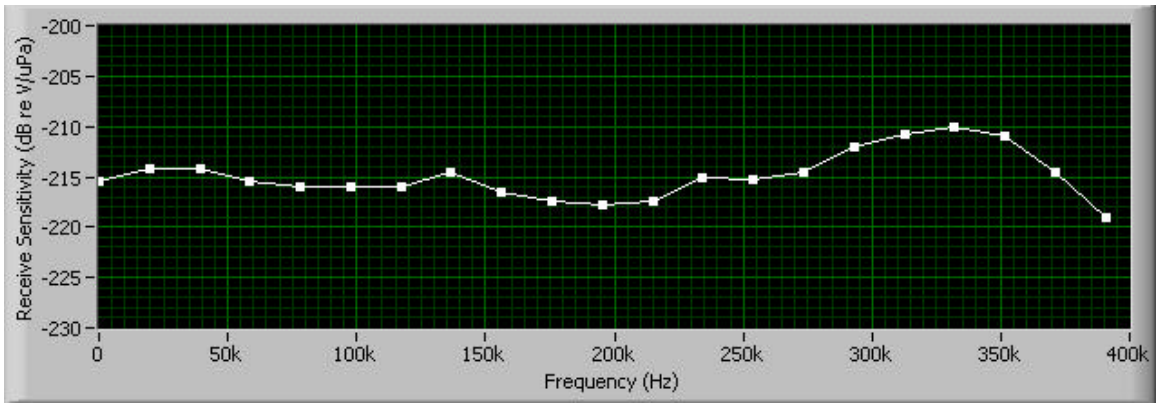

Figure 112. ITC 1089D S/N 2178.

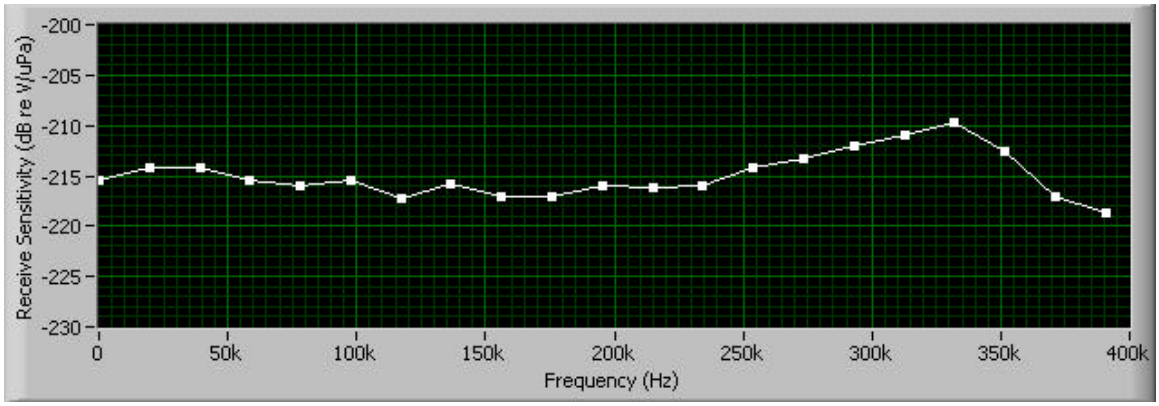

Figure 113. ITC 1089D S/N 2180.

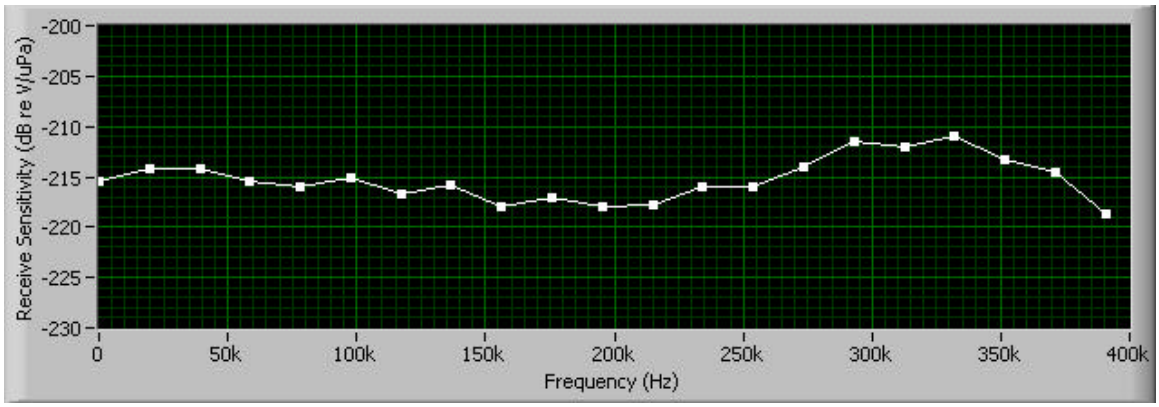

Figure 114. ITC 1089D S/N 2175.

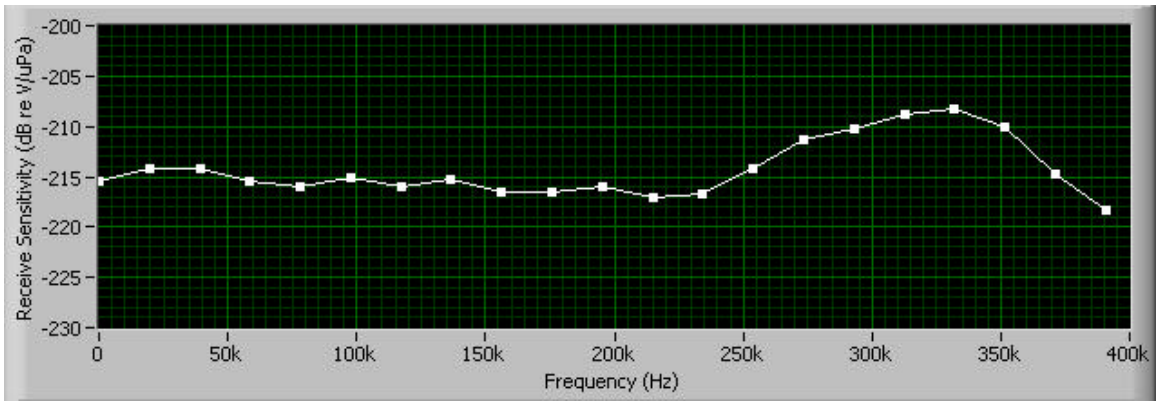

Figure 115. ITC 1089D S/N 2174.

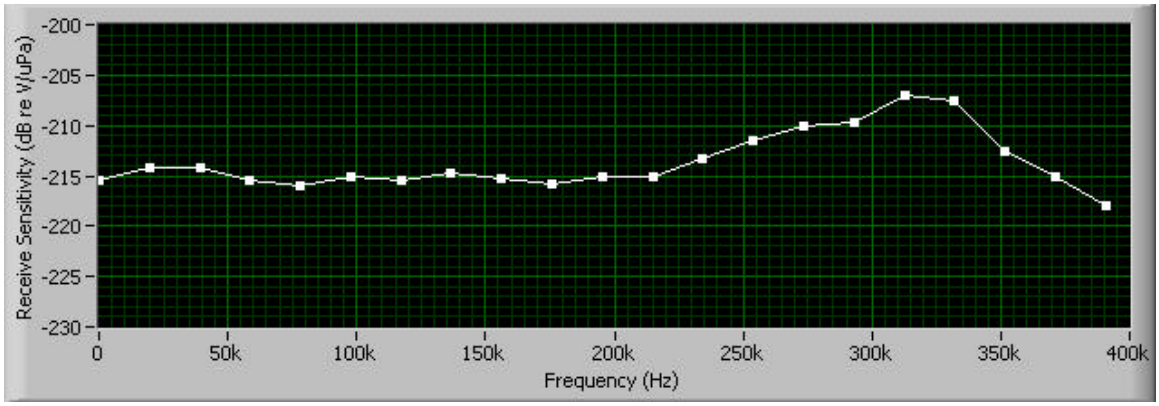

Figure 116. ITC 1089D S/N 2195.

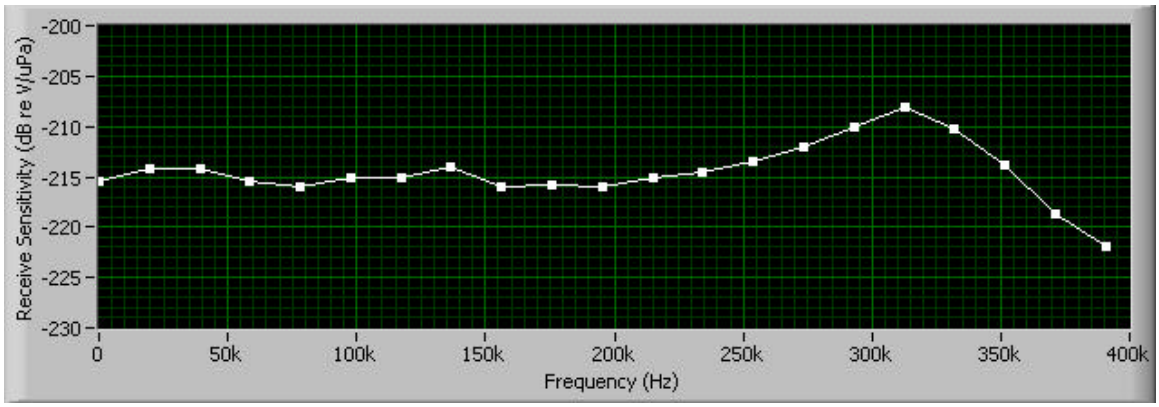

Figure 117. ITC 1089D S/N 2188.

THIS PAGE INTENTIONALLY LEFT BLANK

APPENDIX B. DATA AND IMAGE ACQUISITION LABVIEW WIRING DIAGRAM

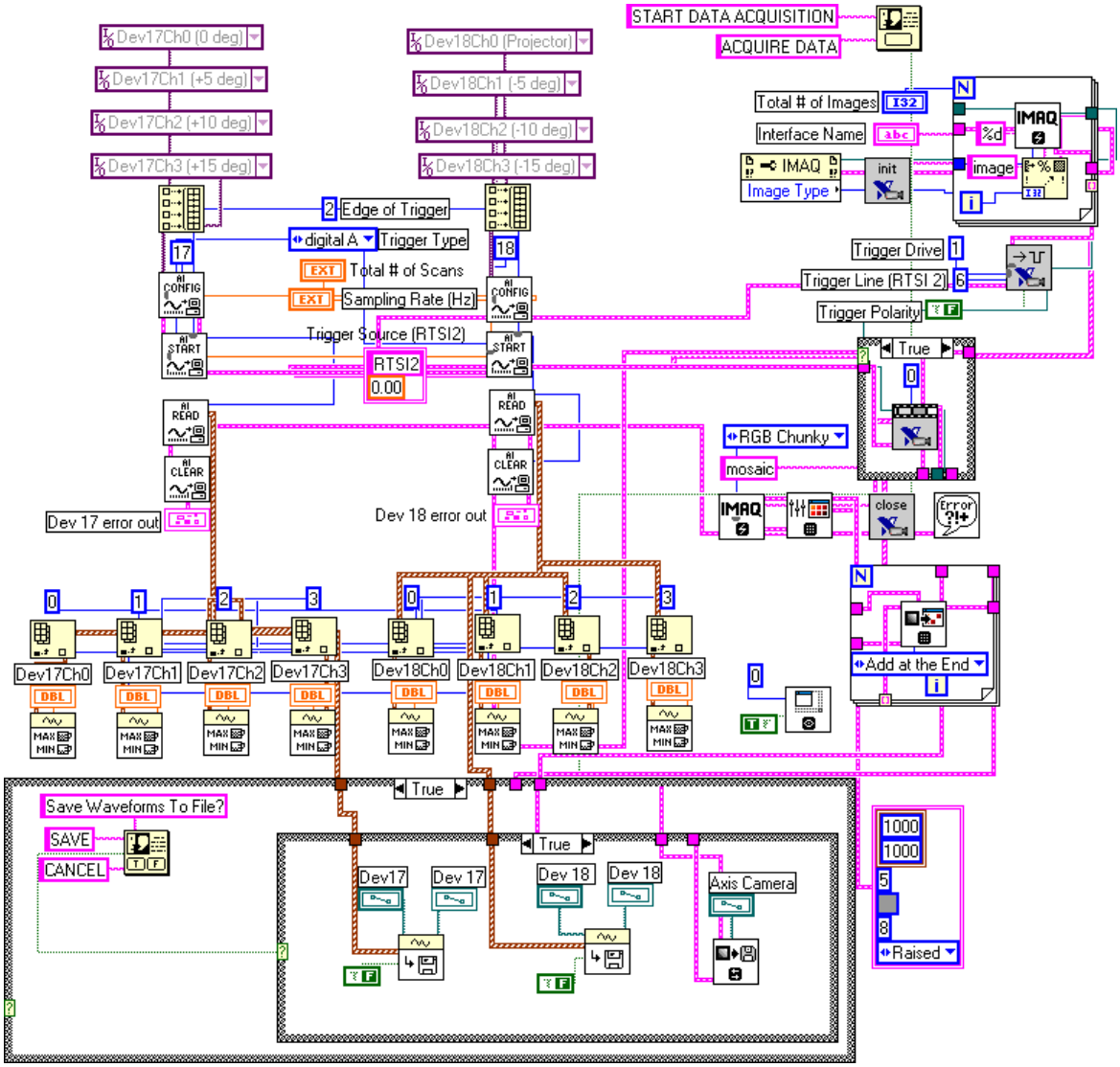

Figure 118. LabVIEW wiring diagram of time synchronized data and video acquisition.

THIS PAGE INTENTIONALLY LEFT BLANK

LIST OF REFERENCES

1. Au, W. W. L., *The Sonar of Dolphins,* Springer-Verlag, New York, 1993.

2. Muir, T., “Role of Nonlinear Acoustics in Biosonar,” Project summary submitted to The Office of Naval Research, 1997.

3. Toland, R., *High Frequency Components in Bottlenose Dolphin Echolocation Signals*, Master's Thesis, Naval Postgraduate School, Monterey, California, September 1998.

4. Dye, D., *High Frequency Components of Normal and Hearing Impaired Dolphins*, Master's Thesis, Naval Postgraduate School, Monterey, California, September 2000.

5. Mitson, R. B., R. J. Morris, “Evidence of High Frequency Acoustic Emissions From The White Beaked Dolphin,” *Journal of the Acoustical Society of America,* Vol. 3:2, pp. 825-826, 1988.

6. Au, W. W. L., D. A. Pawloski, “Cylinder Wall Thickness Difference Discrimination by an Echolocating Dolphin,” (abs.) *Journal of the Acoustical Society of America,* Suppl. 1, Vol. 88, Fall 1990.

7. Jones, H., “Dolphin-Based Sonar,” Physics Colloquium, Naval Postgraduate School, Monterey, CA, 26 April 2002.

8. Au, W. W. L., P. W. B. Moore, D. Pawloski, "Echolocation Transmitting Beam of the Atlantic Bottlenose Dolphin", *Journal of the Acoustical Society of America,* Vol. 80, Number 2, pp. 688-691, August 1986.

9. Ridgway S. H., The Cetacean Central Nervous System,” *Elsevier’s Encyclopedia of Neuroscience, 2nd enlarged and revised ed.*, Elsevier Science, 1999.

10. Ridgway, S. H., "Dolphin Hearing And Sound Production In Health And Illness," *Hearing And Other Senses: Presentations In Honor of E.G. Weaver*, Amphora Press, Groton, 1983.

11. Interview with Dr. Sam Ridgway, Space and Naval Warfare Systems Center-San Diego at Naval Postgraduate School, Monterey, CA, 26 April 2002.

12. Brill, R., “The Effects of Attenuating Returning Echolocation Signals at the Lower Jaw of a Dolphin (*Tursiops Truncatus*)," *Journal of the Acoustical Society of America,* Vol. 89, Number 6, 1991.

13. Drake, E. T. (ed.) *Evolution and Environment*, Yale University Press, New Haven, 1968.

14. Space and Naval Warfare Center-San Diego, “U. S. Navy Marine Mammal Program,” [http://www.spawar.navy.mil/sandiego/technology/mammals]. June 2002.

15. National Instruments, User Manual, Part No. 321759A-01, *PCI-6110E/6111E User Manual*, January 1998.

16. National Instruments, User Manual, Part No. 322811A-01, *IMAQ PCI-PXI 1409 User Manual*, November 2000.

17. National Instruments, User Manual, Part No. 321527E-01, *Getting Started with LabVIEW*, November 2001.

18. Kamminga, C., G. R. Beistsma, "Investigations on Cetacean Sonar IX: Remarks on Dominant Sonar Frequencies from *Tursiops Truncatus*", *Aquatic Mammals*, Vol. 16.1, 1990.

19. National Instruments, "Using Fast Fourier Transforms and Power Spectra in LabVIEW", [http://zone.ni.com/devzone/conceptd.nsf/webmain/CC9733CB28B14EA5862568650060DAA2?opendocument&node=DZ52016_US]. June 2002.

INITIAL DISTRIBUTION LIST

1. Defense Technical Information Center
   Ft. Belvoir, Virginia

2. Dudley Knox Library
   Naval Postgraduate School
   Monterey, California

3. Dr. Teresa McMullen
   Office of Naval Research, Code 342PS
   Arlington, Virginia

4. Dr. Harold Hawkins
   Office of Naval Research, Code342PS
   Arlington, Virginia

5. Dr. Robert Gisiner
   Office of Naval Research, Code 342PS
   Arlington, Virginia

6. Dr. Douglas Todoroff
   Office of Naval Research, Code 321
   Arlington, Virginia

7. Professor Thomas G. Muir, Code PH/Mt
   Naval Postgraduate School
   Monterey, California

8. Professor Steven R. Baker, Code PH/Ba
   Naval Postgraduate School
   Monterey, California

9. Samuel H. Ridgway, DVM
   Space and Naval Warfare Systems Center
   San Diego, California

10. Commanding Officer
    Space and Naval Warfare Systems Center
    San Diego, CA

11. Don Carder
    Space and Naval Warfare Systems Center
    San Diego, California

12. James Finneran
    Space and Naval Warfare Systems Center
    San Diego, California

13. Patrick Moore
    Space and Naval Warfare Systems Center
    San Diego, California

14. Houston Jones
    Space and Naval Warfare Systems Center
    San Diego, California

15. Patricia Kamolnick
    Space and Naval Warfare Systems Center
    San Diego, California

16. Jennifer Jeffress
    Space and Naval Warfare Systems Center
    San Diego, California

17. LT Tobias Lemerande
    Ship Repair Facility
    Yokosuka, Japan

18. Professor William Carey
    Massachusetts Institute of Technology
    Cambridge, Massachusetts

19. Professor Cees Kamminga
    Delft University of Technology
    Delft, The Netherlands